

1 **ENVIRONMENTAL SIGNAL PROPAGATION IN SEDIMENTARY SYSTEMS**
2 **ACROSS TIMESCALES**

3

4 Brian W. Romans¹, Sébastien Castelltort², Jacob A. Covault³, Andrea Fildani⁴, and J.P. Walsh^{5,6}

5 ¹*Department of Geosciences, Virginia Polytechnic Institute and State University, Blacksburg, VA 24061*

6 ²*Section des Sciences de la Terre et de l'Environnement, Université de Genève, 1205 Genève, Suisse*

7 ³*Chevron Energy Technology Company, Houston, TX 77002*

8 ⁴*Statoil RDI, Research Center Austin, TX 78730*

9 ⁵*East Carolina University, Greenville, NC 27858*

10 ⁶*UNC Coastal Studies Institute, Wanchese, NC 27981*

11

12 keywords: source-to-sink; sediment-routing systems; Earth-surface dynamics; stratigraphy; geomorphology; tectonics;
13 paleoclimate

14

15 **Abstract**

16 Earth-surface processes operate across erosionally dominated landscapes and
17 deliver sediment to depositional systems that can be preserved over a range of timescales.
18 The geomorphic and stratigraphic products of this source-to-sink sediment transfer record
19 signals of external environmental forcings, as well as internal, or autogenic, dynamics of
20 the sedimentary system. Here, we evaluate environmental signal propagation across
21 sediment-routing systems with emphasis on sediment supply, Q_s , as the carrier of up-
22 system forcings. We review experimental, numerical, and natural examples of source-to-
23 sink sediment routing and signal propagation during three timescales: (1) Historic, which
24 includes measurement and monitoring of events and processes of landscape change and
25 deposition during decades to centuries; (2) Centuries to several millions of years, referred
26 to as intermediate timescale; and (3) Deep time. We discuss issues related to autogenic

27 dynamics of sediment transport, transient storage, and release that can introduce noise,
28 lags, and/or completely mask signals of external environmental forcings. We provide a
29 set of conceptual and practical tools for evaluating sediment supply within a source-to-
30 sink context, which can inform interpretations of signals from the sedimentary record.
31 These tools include stratigraphic and sediment-routing system characterization, sediment
32 budget determination, geochronology, detrital mineral analysis (e.g., thermochronology),
33 comparative analog approaches, and modeling techniques to measure, calculate, or
34 estimate the magnitude and frequency of external forcings compared to the characteristic
35 response time of the sediment-routing systems.

36

37 **1 Introduction**

38

39 *1.1 What is an 'Environmental Signal'?*

40 From the perspective of sedimentary system analysis, signals are changes in sediment
41 production, transport, or deposition, that originate from perturbations of environmental
42 variables such as precipitation, sea level, rock uplift, subsidence, and human
43 modifications. The origin of the perturbations can be 'natural' when they relate to
44 tectonic and climatic processes that have happened over the course of Earth's history, or
45 'anthropogenic' if they are linked with human actions. Environmental signals occur over
46 many temporal scales, ranging from several hours to millions of years in response to
47 tectonic and climate changes. Signals involve a large range of spatial scales such as
48 localized precipitation affecting small catchments to eustatic sea-level change that affects
49 the globe.

50 An environmental signal can trigger a response of the Earth's surface in the form of
51 erosion, sediment transport, and deposition, and the surface response may be local
52 initially and further afield eventually as it propagates away. A sea-level fall, for example,
53 can create local incision and shoreline regression, but also up-system knickpoint
54 migration and down-system deposition in the deep sea. Similarly, an increase in
55 precipitation can create a wave of incision, alluvial aggradation, and eventually a pulse of
56 sediment discharge to the ocean. The overarching challenge of geomorphology and
57 stratigraphy is to invert the history of environmental signals from landscape and rock
58 records.

59 The transfer, or propagation, of signals is generally examined in the down-system
60 direction, as this is the dominant direction of mass transfer (e.g., [Castelltort and Van Den](#)
61 [Driessche, 2003](#); [Allen, 2008a](#), [Jerolmack and Paola, 2010](#)). However, up-system signal
62 propagation driven by base level change has long been considered in the interpretation of
63 the sedimentary record (e.g., [Fisk, 1944](#)), is important for distributive systems (e.g.,
64 backwater effect in deltas, [Lamb et al., 2012](#)), and is the subject of theoretical work
65 ([Voller et al., 2012](#)).

66 Environmental signals are potentially preserved in the geomorphic expression of
67 landscapes around us, as well as in the stratigraphic record of depositional basins. This
68 review examines how signals propagate within the context of sediment routing systems
69 with emphasis on the nature of sediment supply, or Q_s , as the indicator of up-system
70 forcings (Fig. 1A) ([Allen et al., 2013](#)). We think that reconstructing the rates and
71 magnitudes of signal-generating processes from stratigraphy requires consideration of the
72 nature of system response, and the potential modification of the original signal. It is also

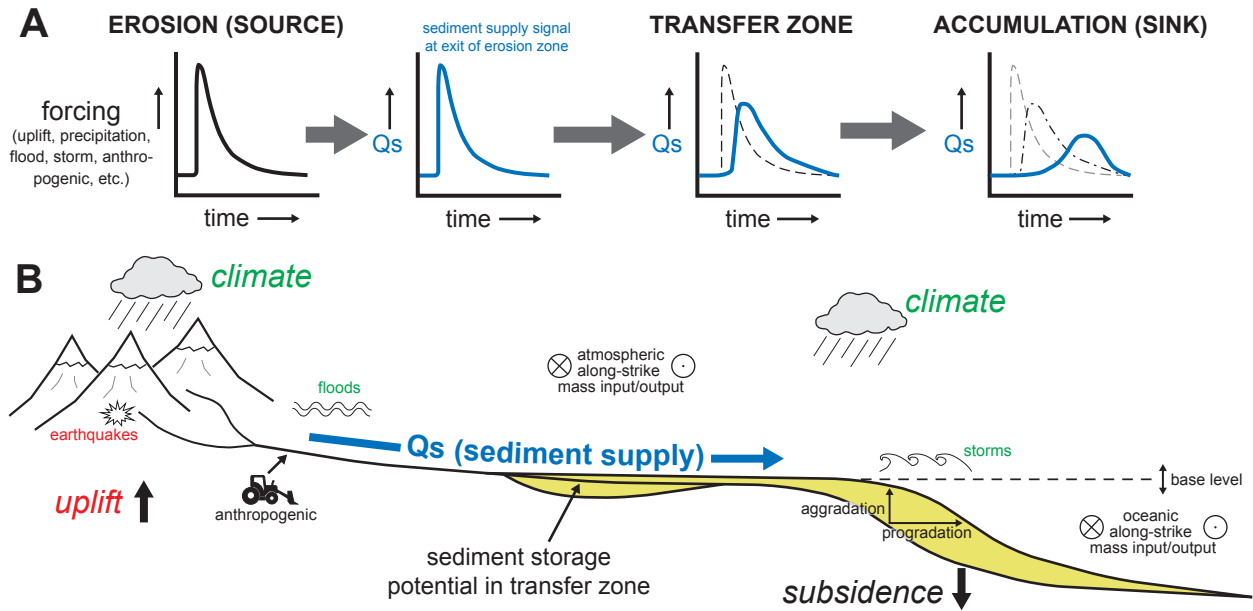


Figure 1: (A) Schematic portrayal of a sediment supply (Q_s) signal from the erosion zone and how that signal propagates through the system. The leftmost Q_s signal represents as measured at the exit of the erosion zone and for simplicity is the same as the original forcing of interest. The transfer zone Q_s signal is measured within the transfer zone at some distance from exit of erosion zone and the rightmost signal represents that which reaches the accumulation zone and is an input for the stratigraphic record. Dashed lines refer to Q_s signal in up-system segment(s) to illustrate that a signal can be modified during propagation. (B) 2-D profile of a generic sediment-routing system emphasizing erosion, transfer, and accumulation zones (potential for intermediate to deep time stratigraphic preservation in yellow) and important controls of tectonics (including earthquakes), climate (including storms), base level, and anthropogenic factors. Part B modified from Castelltort and Van Den Driessche (2003).

Romans et al. -- Figure 1

73 important to recognize that signals can be masked or significantly altered by what can be
74 referred to as ‘noise.’ In the present context, ‘noise’ has the broad meaning of any
75 perturbation of the primary signal of interest, irrespective of its origin, frequency, or
76 magnitude. It is one fundamental goal of stratigraphy to disentangle signal from noise,
77 but what can be considered noise at one timescale may represent a signal at another. One
78 notable type of noise is the result of internal, self-organized, dynamics of a sediment
79 routing system (e.g., [Jerolmack and Paola, 2010](#)), that can potentially ‘shred’
80 environmental signals as a result of their large magnitude and period relative to the
81 primary signal of interest (e.g., [Jerolmack and Paola, 2010](#); [Wang et al., 2011](#)).

82 Deciphering signals has obvious implications for the meaning of the sedimentary
83 record of Earth history: what do sediments and rocks tell us about the past? However,
84 understanding the signal-to-noise character of the sedimentary record is also relevant to
85 the prediction of land-to-sea export and burial of terrestrial organic carbon (e.g., [Kao et](#)
86 [al., 2014](#); [Leithold et al., this volume](#)), landscape resiliency and hazard management (e.g.,
87 [Anthony and Julian, 1999](#)), prediction of depositional systems for natural resource
88 exploration and production ([Bhattacharya et al., this volume](#)), and response of
89 hydrological systems to global climate change (e.g., [Syvitski, 2003](#)). We do not attempt
90 to solve all the outstanding issues related to signal propagation and preservation in this
91 contribution. Our goal is to provide the general Earth scientist a thorough review of the
92 interesting and enigmatic questions and to promote a broader understanding that might
93 attract other researchers to this multidisciplinary field of study.

94

95 *1.2 Importance of Timescale of Investigation*

96 We emphasize the importance of timescale in this review because of its association
97 with the processes of signal generation, propagation, preservation, and analysis. The
98 evaluation of signals requires consideration of the timescale(s) particularly in the context
99 of internally generated ‘noise.’ Also, some signals occur over long durations (e.g., uplift
100 and exhumation of a mountain belt) and, therefore, require a correspondingly long record
101 from which to deduce the signal.

102 How do we put historical (past few centuries) measurements and observations
103 within the framework of landscapes and stratigraphy constructed over timescales $\geq 10^3$
104 yr? Put another way, how do we accurately estimate short-term rates from geologic
105 archives that have longer-term temporal resolution? For example, the < centennial
106 stratigraphic record contains information about short-lived events, such as hurricane
107 deposits, which can be reliably dated. The challenge is to extract meaningful insight from
108 such records in the deeper past.

109 We organize this review of signal propagation and preservation within the context
110 of three important timescales that span a minimum of seven orders of temporal
111 magnitude: (1) Historic, which includes measurement and monitoring of events and
112 processes of landscape change ($< 10^2$ yr); (2) Centennial to several million years, herein
113 referred to as the intermediate timescale (10^2 - 10^6 yr); and (3) Deep time ($\geq 10^7$ yr) (Fig.
114 2). These timescales are discussed in terms of age of the system as well as duration or
115 period of forcing. The timescale of investigation also influences the application of
116 concepts of steady state, response time, and other system dynamics indicators, which will
117 be discussed in detail in the intermediate timescale Section 3.

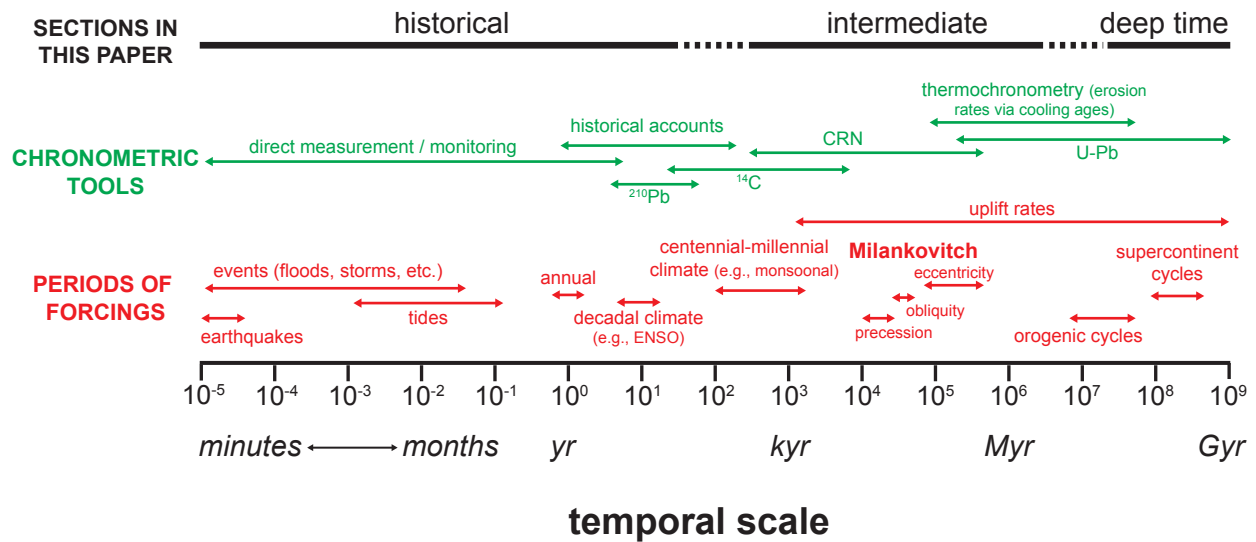


Figure 2: Overview of three timescales of investigation, some of the chronometric tools with which to constrain process rates, and periods of some of the forcings discussed in this review. Dashed lines at the top emphasize the continuum among the timescales. Temporal range of ‘orogenic cycles’ from DeCelles et al. (2009). Effective dating range of chronometric tools from Walker (2005).

Romans et al. -- Figure 2

118

119 *1.3 Sediment Routing Systems*

120 Earth-surface processes operate within erosionally dominated landscapes coupled
121 with depositional systems that can be preserved over a range of timescales. A simple and
122 elegant way to consider an integrated sedimentary system was presented by [Schumm](#)
123 [\(1977\)](#) wherein he subdivided a system into three spatial zones of dominant mass-flux
124 behavior: denudation/erosion, transfer, and accumulation/deposition. Similar to
125 [Castelltort and Van Den Driessche \(2003\)](#) and [Sadler and Jerolmack \(2014\)](#), we depict a
126 generic sediment routing system in cross section and denote the prominent environmental
127 forcings of interest in this review (Fig. 1B). The ‘transfer zone’ is assumed to be the
128 segment of the sedimentary system that is neither net-denudational nor net-accumulative;
129 rather, it is characterized by the balance between sediment removal/remobilization and
130 sediment storage that feeds or starves down-system accumulation zones. Thus, this zone
131 typically does not produce much sediment via bedrock erosion and, over sufficiently long
132 timescales, it will transfer more mass than it produces or accumulates. We consider the
133 morphology and process history of the transfer zone as an indicator of system response to
134 perturbations, which is important for reconstructing paleo-sediment routing systems. A
135 spatial scale is not shown on Figure 1B because the lengths of these zones vary
136 significantly from system to system (e.g., [Somme et al., 2009](#)). For example, small/high-
137 relief sediment routing systems (10-50 km long) typically have very short transfer zones,
138 which results in negligible transient sediment storage, whereas large, continental-scale
139 systems (100-1000 km long) commonly have long transfer zones containing sediment
140 sinks that can store sediment temporarily or permanently given favorable subsidence

141 conditions. The magnitudes and timescales of such mass transfer-and-storage behavior,
142 which can be addressed through the estimation of sediment budgets, are fundamental to
143 the propagation of signals. We focus on the down-system mass transfer of inorganic,
144 dominantly siliciclastic, particulates through water-sediment flows and refer the reader to
145 [Leithold et al. \(this volume\)](#) for a review of organic-carbon dynamics of source-to-sink
146 systems. Additionally, we acknowledge the important and unique sediment-supply
147 characteristics of glaciated systems but do not distinguish them here and refer the reader
148 to [Jaeger and Koppes \(this volume\)](#).

149

150 **2 Sedimentary Process-Response Over Historical (<10² yr) Timescales**

151 Signals at the historical timescale are the result of individual events that last hours to
152 days (e.g., floods, storms, and earthquakes) to longer-lived changes that occur over
153 decades (e.g., watershed deforestation and other land-use alterations) (Fig. 1). The
154 mechanisms involved in the formation and/or propagation of such signals from source to
155 sink include a range of hillslope (e.g., sheetwash, landsliding), glacial, fluvial, volcanic,
156 oceanic (e.g., tides and storm wave) processes and subaqueous mass movements and
157 flows (e.g., turbidity currents). Data from instruments have provided opportunities to
158 measure and quantify sedimentary dynamics, and the stratigraphic record is also
159 examined to link process to product over longer time. The timescale of this section covers
160 what some consider to be the period of significant anthropogenic influence on Earth
161 surface systems (onset of the Industrial Revolution, or ~250 yr before present; [Crutzen](#)
162 [and Stoermer, 2000](#); [Zalasiewicz et al., 2000](#)).

163 We identify four potential challenges to leveraging historic records to understand
164 millennial-scale and deeper-time geology. First, ancient events might have been non-
165 actualistic; i.e., there is no adequate modern analog regarding process ([Myrow and](#)
166 [Southard, 1996](#)). For example, globally distributed strata that were produced by the
167 Cretaceous bolide impact (e.g., [Bralower et al., 1998](#)). Second, although a recent event
168 may have had profound impact on society (e.g., 2005 Hurricane Katrina, 2011
169 Mississippi River flood), the geological record produced might be negligible or non-
170 existent, depending on many factors including spatial variation in supply and erosion
171 ([Turner et al., 2006](#); [Walsh et al., 2006](#); [Goni et al., 2007](#); [McKee and Cherry, 2009](#);
172 [Reed et al., 2009](#); [Allison et al., 2010](#); [Falcini et al., 2012](#); [Kolker et al., 2014](#); [Xu et al.,](#)
173 [2014b](#)). Third, the observation of modern sedimentary processes shows that strata are
174 often destroyed within years after deposition as a result of physical and/or biogenic
175 reworking ([Wheatcroft et al., 2007 and references therein](#)). Finally, there is the problem
176 of discontinuous sedimentation and the likelihood of larger gaps in the record (i.e., time
177 recorded as hiatus) as the time interval of sampling increases ([Sadler, 1981](#); [Sadler and](#)
178 [Jerolmack, 2014](#)), which will be discussed further in Section 4.

179 Erosional landforms provide a rich record of signals in the annual-to-centennial
180 temporal range (e.g., [Viles and Goudie, 2003](#)), but the primary goal of our discussion is
181 to understand signal propagation into the sedimentary record. Many studies at historical
182 timescales are focused on specific processes and segments (e.g., hillslope erosion, shelf
183 sedimentation) and do not strive to directly link source and sink through
184 contemporaneous research. Moreover, simple relationships between event size (e.g.,
185 flood magnitude) and strata thickness may be the exception rather than the norm ([Corbett](#)

186 [et al., 2014 and references therein](#)). As a result, the source-to-sink stratigraphic
187 connection remains a challenge in many studies despite a wealth of data.

188 At the shortest end of the signal transfer spectrum (<1 yr), the potential for direct
189 communication of a sediment supply signal to a sink is greatly limited. To produce a
190 measurable signal in the stratigraphic record of the sink, events that drive sediment
191 redistribution must move a relatively large volume of material over a short time. To
192 understand modern system behavior, we recommend consideration of the source signal
193 relative to the sink size; e.g., volume of event-scale Qs versus volume capacity of a sink.
194 Furthermore, system size can impact the timescale of the signal. For example, a flood or
195 earthquake-driven landslide into a confined mountain lake can be captured quickly (hours
196 to days) and potentially with little post-depositional physical and/or biogenic
197 modification ([Schilleref et al., 2014](#)) compared to a flood of the vast Mississippi River
198 catchment into the Gulf of Mexico, the effects of which can persist for months ([Allison et](#)
199 [al.; 2000](#); [Kolker et al., 2014](#); [Xu et al., 2014b](#)). Resolving events occurring in close
200 succession is challenging because the signals might be truncated, overprinted, or
201 commingled (e.g., hurricanes Katrina and Rita; [Goni et al., 2007](#) or the Morokot
202 earthquake and ensuing flood; [Carter et al., 2012](#)).

203 We first discuss key processes and rates of sediment production and transfer over
204 human timescales. We then address the storage in sedimentary sinks and high-resolution
205 dating typical of historical timescales. Finally, we examine two well-studied modern
206 source-to-sink systems and the specificities of stratal preservation and sediment budgets
207 over centennial timescales.

208

209 *2.1 Sediment Production and Transfer Over Historical Timescales*

210 Sediment production and movement in catchments and river systems is often
211 described in a time-averaged perspective with the timescale of focus related to the
212 measurement tool employed. Annual hillslope erosion rates (in mm/yr or t/ha/yr),
213 sediment loads (t/yr) and yields (t/km²/yr) may be used to compare and contrast systems
214 and help evaluate their overall functioning (Milliman and Syvitski, 1992; Walling and
215 Webb, 1996; Walling, 1999; Syvitski and Saito, 2007; Syvitski and Milliman, 2007;
216 Milliman and Farnsworth, 2011; Covault et al., 2013). Loads and yields are commonly
217 measured with stream gauges (e.g., Milliman and Farnsworth, 2011), which can be used
218 to evaluate catchment erosion rates and/or alluvial storage (e.g., Meade et al., 1990;
219 Walling and Collins, 2008). There are significant challenges to quantifying sediment
220 transfer to the sea by rivers, particularly of large systems because of tidal influence on
221 transport calculations and sediment storage in the lower river (e.g., Milliman et al., 1984;
222 Allison et al., 2012). Historical measurements can be biased as a result of their limited
223 duration or influences of anthropogenic catchment modification, including construction
224 of dams and other land-use activities associated with agriculture, construction, and
225 mining (Wilkinson and McElroy 2007; Milliman and Farnsworth, 2011). Erosion rates
226 also can be measured with cosmogenically derived tracers (e.g., ¹⁰Be; discussed further in
227 Section 3) and radiochemically dated deposits (e.g., ¹⁴C, ¹³⁷Cs or ²¹⁰Pb) from well-
228 defined source areas (e.g., Walling and Collins, 2008). Technological advancements,
229 specifically Light-Detection and Ranging and terrestrial laser scanners, have improved
230 our ability to quantify morphological changes on land. Denudation rates from LiDAR,
231 discharge measurements and ¹⁰Be indicate variability depending on slope and other

232 factors (commonly <0.5 mm/yr, but locally >3 mm/yr) (e.g., [Hovius et al., 1997](#); [Aalto et](#)
233 [al., 2003](#); [Roering et al., 2007](#); [Korup et al., 2014](#)). The contextual and temporal
234 knowledge of precipitation and catchment characteristics usually exceeds what can be
235 measured or inferred in ancient systems, as will be discussed in subsequent sections.

236 Water-driven transport, especially during intense floods, can generate
237 recognizable sedimentary signals in sink areas. Intense rainfall and associated floods can
238 rapidly (hours to days) move large volumes (>5 Mt [million metric tons]) of sediment
239 through small ($<5,000$ km²) catchments to offshore depositional areas (e.g., [Sommerfield](#)
240 [et al., 1999](#); [Hale et al., 2014](#); [Kniskern et al., 2014](#)), and larger catchments ($>50,000$
241 km²) can generate appreciable sediment supply (>10 s Mt) signals to the sea over the
242 course of days to weeks (e.g., [Palinkas et al., 2005](#); [Kolker et al., 2014](#)). Subaerial and
243 submarine landsliding and other mass movements are related to pre-conditioning factors,
244 such as hillslope soil or rock strength, geomorphology, and short-term conditions (e.g.,
245 earthquake and hydrology) ([Dietrich et al., 1995](#); [Roering et al., 2007](#); [Strasser et al.,](#)
246 [2006](#); [Goldfinger et al., 2012](#) and references therein).

247 An earthquake can disturb a catchment by increasing pore pressures and
248 liquefying substrate, among other processes of manipulating gravitational loads on
249 slopes, which can lead to abrupt increases in sediment loads (e.g., [Dadson et al., 2004](#)).
250 Also, earthquake-triggered mass wasting can create conspicuous stratigraphic records in
251 lakes and the deep sea (e.g., [Heezen and Ewing, 1952](#); [Piper and Aksu, 1997](#); [Moernaut](#)
252 [et al., 2007](#)). Much research has explored coastal and marine sedimentary records to
253 evaluate the recurrence interval for earthquakes and associated tsunamis (e.g., [Atwater](#)
254 [and Hemphill-Haley, 1997](#); [Goldfinger et al., 2003](#); [Strasser et al. 2006](#); [Mournaut et al.,](#)

255 2007; Goldfinger et al., 2012; Barnes et al., 2013), including some recent detailed
256 research focused on the Sumatra and Tomoko events (e.g., Szczucinski et al., 2012;
257 Patton et al., 2013). There is still vigorous debate regarding deep-sea turbidite deposits as
258 a reliable paleo-seismometer (e.g., Sumner et al., 2013; Atwater et al., 2014).

259 Over annual to centennial timescales, anthropogenic activities, such as
260 deforestation and pollution, can create signals that become stored in sedimentary sinks
261 (e.g., Paull et al., 2002; Cundy et al., 2003). Many natural and human factors (e.g., land
262 use, dams) have significant influence on sediment yields and loads (Meade et al., 1990;
263 Syvitski et al., 2005; Milliman and Farnsworth, 2011). As a consequence of the potential
264 influence of human activities, Syvitski and Milliman (2007) included an anthropogenic
265 factor in their BQART model that predicts global sediment flux to the oceans. Although
266 intra-system storage might buffer some signals (i.e., low sediment delivery ratios;
267 Phillips, 1991; Walling and Collins; 2008), catchment changes can notably increase Q_s .
268 Damming and leveeing can significantly diminish sediment supply into sink areas
269 (Syvitski et al., 2005; Milliman and Farnsworth, 2011 and references therein), not only
270 precluding new strata development but also yielding land loss in some areas (e.g., Day et
271 al., 2007; Smith and Abdel-Kader, 1988).

272

273 2.2 *Storage in Sedimentary Sinks Over Historical Timescales*

274 To evaluate the presence of signals, including events, in stratigraphic records over
275 historic timescales, ^{210}Pb and ^{137}Cs are commonly used to date deposits or determine
276 sediment accumulation rates (Fig. 2) (e.g., Sommerfield and Nittrouer, 1999).
277 Bathymetric and sub-bottom observations (i.e., seismic reflection) have revealed the

278 geomorphic and stratigraphic complexity of subaqueous environments and such data are
279 helpful to strategically position coring sites to obtain desired records (e.g., [Goldfinger et](#)
280 [al., 2012](#)) or to inform spatial variability for determining sediment budgets (e.g., [Miller](#)
281 [and Kuehl, 2010](#); [Gerber et al., 2010](#)). Recent studies have shown how time-series
282 bathymetric analysis with multibeam may yield new insight into the intermittent nature of
283 fluvial deposition ([Nittrouer et al., 2008](#)) and subaqueous sediment density flows (e.g.,
284 [Smith et al., 2005](#); [Walsh et al., 2006](#); [Paull et al., 2006](#); [Xu et al., 2008](#); [Hughes Clarke](#)
285 [et al., 2012](#)). Additionally, researchers are using innovative methods to track sediment
286 transport and deposition, such as short-lived radiochemical tracers (i.e., ^7Be) for
287 catchment and seaward sediment dispersal (e.g., [Sommerfield et al., 1999](#); [Dail et al.,](#)
288 [2007](#); [Walling, 2013](#)), and mounted acoustic- and light-based sensors for measuring
289 water and sediment movement (e.g., [Xu et al., 2004](#); [Dinehart and Burau, 2005](#);
290 [Cacchione et al., 2006](#)). Deployed systems have provided flow measurements (i.e.,
291 velocity and sediment concentrations), which are essential to modeling sediment
292 transport (e.g., [Traykovski et al., 2007](#); [Moriarty et al., 2014](#)). However, field
293 measurements remain limited especially during extreme and/or rare events when most
294 sediment is moved (e.g., [Ogston et al., 2000](#); [Talling et al., 2013](#); [Hale et al., 2014](#); [Xu et](#)
295 [al., 2014a](#); [Stevens et al., 2014](#)).

296 Sedimentary filling of hollows, ponds, lakes, floodplains, estuaries, and even
297 sinkholes can provide information about individual events or decadal-to-centennial
298 changes in the environment. Evidence for upstream changes includes increased
299 sedimentation rates elevated trace metals, variations in pollen, microfossil organisms
300 and/or assemblages, trace metals, and organic compounds (e.g., estuaries: [Brush et al.,](#)

301 2001; Cooper et al., 2004; lakes: Noren et al., 2002, Girardclos et al., 2007; floodplains:
302 Aalto et al., 2003; coastal deposits: Sorrel et al., 2012; Lane et al., 2011; shelves: Allison
303 et al., 2012; deep sea: Soutar and Crill, 1977). Gilli et al. (2013) and Schillereff et al.
304 (2014) provide reviews of flooding and climate changes from lake records.

305 Continental shelves, slopes, and deeper ocean segments are typically viewed as
306 the ultimate depositional sinks, but their records are variably preserved as a result of post-
307 depositional reworking and can be challenging to unravel (Nittrouer et al., 2007). Theory
308 and modeling emphasize that event-layer preservation is a function of the rate of
309 bioturbation, mixing depth, and layer thickness (Wheatcroft et al., 2007 and references
310 therein). However, time-series coring studies of flood-related deposition on continental
311 shelves offshore the Eel, Po, and Waipaoa sediment-routing systems have shown deep
312 (>5 cm) biological reworking over the span of a few years (Wheatcroft et al., 2007; Tesi
313 et al., 2012; Walsh et al., 2014). Areas of rapid sedimentation and physically reworked
314 areas such as topset and foreset regions of clinoforms might have physical stratification
315 preserved at depth, e.g., Amazon delta front (Kuehl et al., 1996; Sommerfield et al., 1999;
316 Walsh et al., 2004; Rose and Kuehl, 2010). However, the presence of discontinuous,
317 heterolithic bedforms can preclude recognition of event-specific beds (Goff et al., 2002;
318 Walsh et al., 2014). Ocean areas with low or no dissolved oxygen inhospitable to benthic
319 organisms (e.g., Soutar and Crill, 1977) are favorable for signal preservation (Allison et
320 al., 2012). Continental margins and basin-margin deep-sea fans capture event records
321 beyond historical timescales. However, during the sea-level highstand of the past several
322 thousand years, off-shelf sediment transport is reduced in some settings (Posamentier and
323 Vail, 1988; Covault and Graham, 2010), with shelf width serving as an important control

324 (Posamentier et al., 1991; Walsh and Nittrouer, 2003). As a result, limited sediment
325 supply to some deep-sea fans has resulted in condensed sections recording few if any
326 events at historical timescales.

327

328 2.3 Modern Sediment Routing System Examples

329 To further discuss historical ($<10^2$ yr) signal propagation, two differently sized
330 sediment routing systems will be briefly discussed: the Eel River and the Ganges-
331 Brahmaputra-Bengal system. The Eel is a small mountainous river system ($<10^3$ km²)
332 draining northern California, USA that has received intense scrutiny during and since the
333 Office of Naval Research STRATA FORMation on Margins program (STRATAFORM;
334 1995-2004; Nittrouer et al., 2007). Small mountainous rivers are important for
335 understanding sediment flux to the sea because of the minimal onshore sediment storage
336 (Milliman and Syvitski, 1995; Kuehl et al., 2003; Covault et al., 2011). We contrast this
337 work with the much larger Ganges-Brahmaputra-Bengal sediment-routing system, where
338 abundant sediment is stored onshore, on the shelf, and in the canyon today (Kuehl et al.,
339 2005; Walsh et al., 2013). Collectively, large systems provided potentially a third to a
340 half of the sediment to the sea prior to human alterations (Milliman and Farnsworth,
341 2011; Walsh et al., 2013).

342 The Eel River is one of the most comprehensively studied modern sediment routing
343 system over the historical timescale (<500 yr). Its 9,400 km² catchment in a tectonically
344 active setting of outcropping sedimentary rocks is estimated to discharge ~12-16 Mt of
345 sediment to the sea annually (Sommerfield and Nittrouer, 1999; Warrick, 2014;
346 Sommerfield and Nittrouer, 2014) (Fig. 3). Landslides are common in steep portions of
347 the catchment (de la Fuente et al., 2006), but almost 70% of the load comes from the

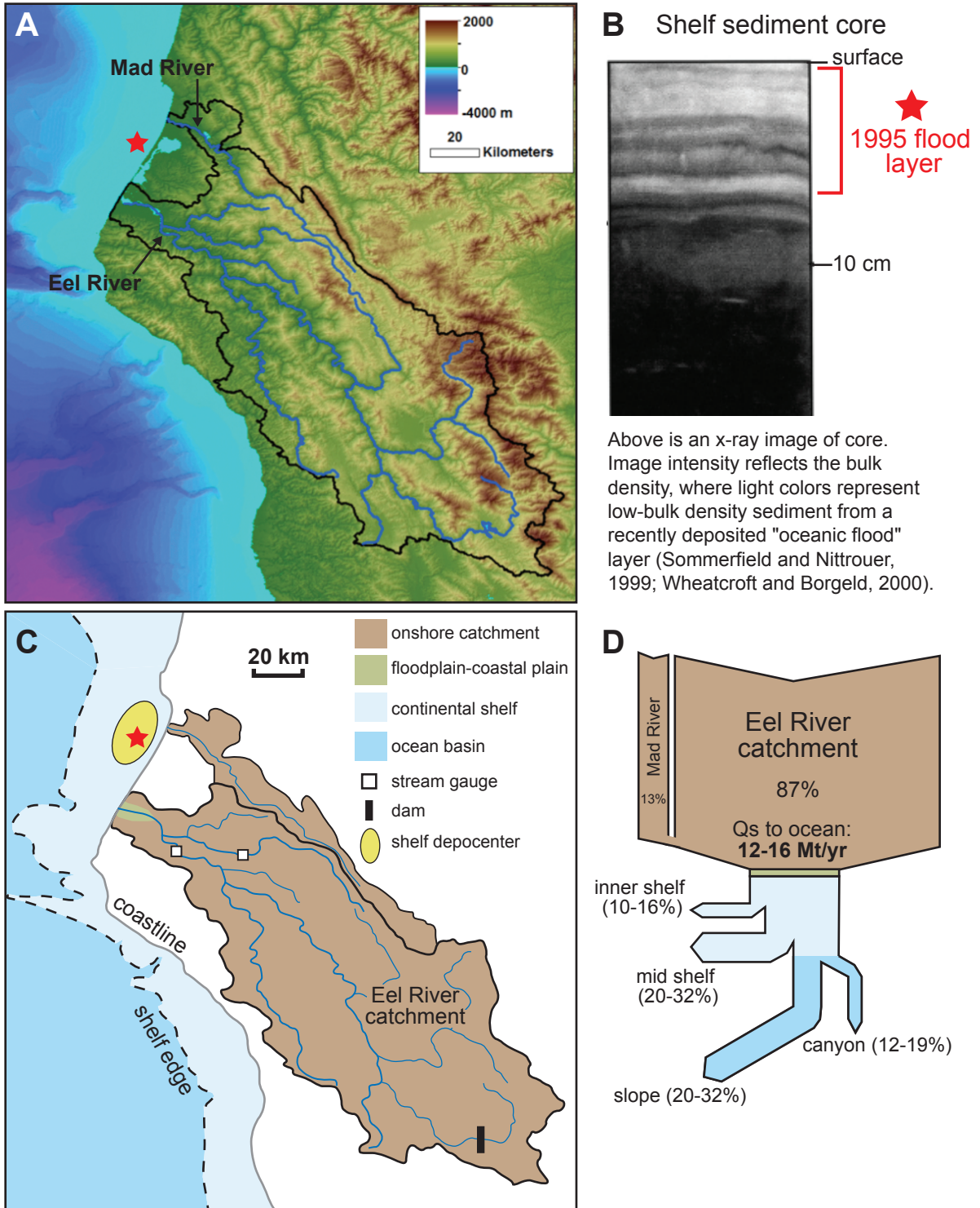


Figure 3: (A) Topography and drainage network of Eel and Mad river catchments, northern California, and bathymetry of the continental margin. Red star denotes location of shelf core x-radiograph shown in (B). (B) X-ray image of shelf reflects bulk density. Light colors (lower bulk density) interpreted as 1995 flood deposit (Sommerfield and Nittrouer, 1999; Wheatcroft and Borgeld, 2000). (C) Map of Eel-Mad sediment-routing system showing catchment area, areal extent of coastal floodplain, and shelf depocenter (yellow). Red star denotes location of shelf core image shown in (B). (D) Historical timescale sediment budget of the Eel-Mad sediment-routing system showing: 1) there is negligible onshore storage, 2) the shelf stores ~30-50% of the budget, and 3) the remainder moves to the canyon and continental slope. Budget estimations from Sommerfield and Nittrouer (1999) and Warrick (2014).

348 central portion of the catchment where mélange outcrops are more erodible ([Brown and](#)
349 [Ritter, 1971](#)). The largest recorded flood event occurred in December 1964, a year during
350 which the Eel River is estimated to have discharged more than 160 Mt of sediment
351 ([Warrick, 2014](#)). This is >13 times the annual average, with most discharge occurring
352 over a few days. In 1995 (January and March) and 1997 (January), three floods occurred,
353 and STRATAFORM scientists documented the deposition of a widespread layer on the
354 shelf (Fig. 3) ([Wheatcroft et al., 1997](#); [Sommerfield and Nittrouer, 1999](#); [Wheatcroft and](#)
355 [Borgeld, 2000](#)). The remarkable similarity between the flood deposits and decadal shelf
356 sedimentation patterns demonstrate how important these events are to shelf construction.
357 However, event and decadal sediment budgets indicate most (>50%) of the sediment is
358 exported beyond the shelf (Fig. 3) giving testimony to the effective transport conditions
359 associated with coherent discharge and energetic ocean conditions ([Wheatcroft and](#)
360 [Borgeld, 2000](#)).

361 Instrument observations made in winter 1996-1997 revealed that a wave-enhanced
362 sediment gravity flow associated with the floods transported an appreciable amount of
363 sediment to the mid-shelf, exceeding other measured events by two orders of magnitude
364 ([Ogston et al., 2000](#); [Traykovski et al., 2000](#)). The widespread and distinctive shelf flood
365 deposit is attributed to this mechanism; however, subsequent examination of the same
366 deposit two years later indicated extensive reworking by physical and biological
367 processes ([Wheatcroft et al., 2007 and references therein](#)). Although some shelf core
368 records have stratigraphic and organic carbon evidence suggestive of older events (e.g.,
369 1964 flood) ([Sommerfield et al., 1999](#); [Leithold et al., 2005](#)), the documentation of post-
370 event reworking indicates that the Eel shelf does not contain a laterally extensive or high-

371 fidelity record of flood signals ([Goff et al., 2002](#); [Wheatcroft et al., 2007](#) and references
372 [therein](#)).

373 Subsequent coring and tripod research in the Eel Canyon documented the possibility
374 of more direct sediment gravity flow to deeper water. Resuspension and transport of
375 sediment via waves also were found to have an important control on this off-shelf export
376 ([Puig et al., 2003](#)). Cores from the canyon indicate sedimentation is spatially and
377 temporal complex, although export to deeper water is apparent ([Mullenbach et al., 2004](#);
378 [Mullenbach and Nittrouer, 2006](#); [Drexler et al., 2006](#)). Nepheloid layers also transport
379 fluvial sediment seaward of the Eel River mouth, allowing hemipelagic sedimentation to
380 accumulate on the slope, but this modest input is easily reworked by the active benthic
381 community precluding event layer formation ([Alexander et al., 1999](#); [Walsh and](#)
382 [Nittrouer, 1999](#)). These studies demonstrate that unravelling signals from Eel margin
383 stratigraphic records is not straightforward, which a similar story for the Waipaoa Rivers
384 of New Zealand ([Kuehl et al., this volume](#)). The apportionment of terrigenous sediment
385 among shelf, slope, and deep-sea segments (Fig. 3D) suggests that shelf records might
386 contain signals of sediment-production events that originated in the catchment, but post-
387 depositional homogenization hampers event-scale determination.

388 The Ganges-Brahmaputra-Bengal is a large (1,656,000 km² catchment) sediment-
389 routing system fed by tectonically active mountains. Sedimentation on the Bengal Fan
390 (>2,000,000 km² depositional area), the ultimate sink for the system, has varied
391 significantly since the Mesozoic because of plate tectonics (i.e., rifting and then collision
392 in the Eocene) and associated sediment production ([Curry, 2014 and references therein](#)).
393 Despite onshore foreland-basin accommodation created by ongoing collisional tectonics,

394 sediments are moving through most of the system over historical timescales, from the
395 Himalayas (>5000 m elevation) to the Bengal Fan (>4000 m water depth) (Fig. 4; [Kuehl](#)
396 [et al., 2005](#)). Sediment production in the Ganges-Brahmaputra catchment (including the
397 Meghna River) corresponds to an average catchment denudation rate of 365 mm/kyr,
398 which is over an order of magnitude larger than the global average of 30 mm/kyr ([Islam](#)
399 [et al., 1999](#)). The sediment load for the integrated catchment is ~1,000 Mt/yr, which
400 equates to a system sediment yield of 556 t/km²/yr. However, sediment yield varies
401 significantly spatially across the catchment. For example, the Brahmaputra River yield is
402 >140% that of the Ganges ([Summerfield and Hulton, 1994](#); [Islam et al., 1999](#)), and most
403 of the Brahmaputra sediment is sourced from a smaller portion of the catchment, the
404 High Himalayas ([Wesson, 2003](#)).

405 Gauging stations for rivers are located about 300 km from the coast, and studies
406 indicate ~30% of the sediment is stored landward of the coastline (Fig. 4) ([Goodbred and](#)
407 [Kuehl, 1999](#)). Sediment sinks include levee, floodplain, and river-bed aggradation, and
408 alluvial accumulation in tectonically subsiding areas ([Allison, 1998](#); [Goodbred and](#)
409 [Kuehl, 1998](#)). Longer timescale records show that since the middle Holocene (~7 ka)
410 slowdown in sea-level rise, some locations have accumulated >20 m of sediment
411 ([Goodbred and Kuehl, 1998](#)), and rates of filling since ~12 ka suggest significant climate
412 forcing on sediment supply ([Goodbred and Kuehl, 2000a](#)). Over historical timescales,
413 floodplain areas of the upper delta plain have linear sediment accumulation rates that
414 generally decrease with distance from the river channel (e.g., from 4 cm/yr to <1 cm/yr,
415 [Allison, 1998](#)). Sediment dynamics in the lower delta plain are influenced by processes
416 that originate in the marine realm such as sea-level rise, waves, tides, and cyclones

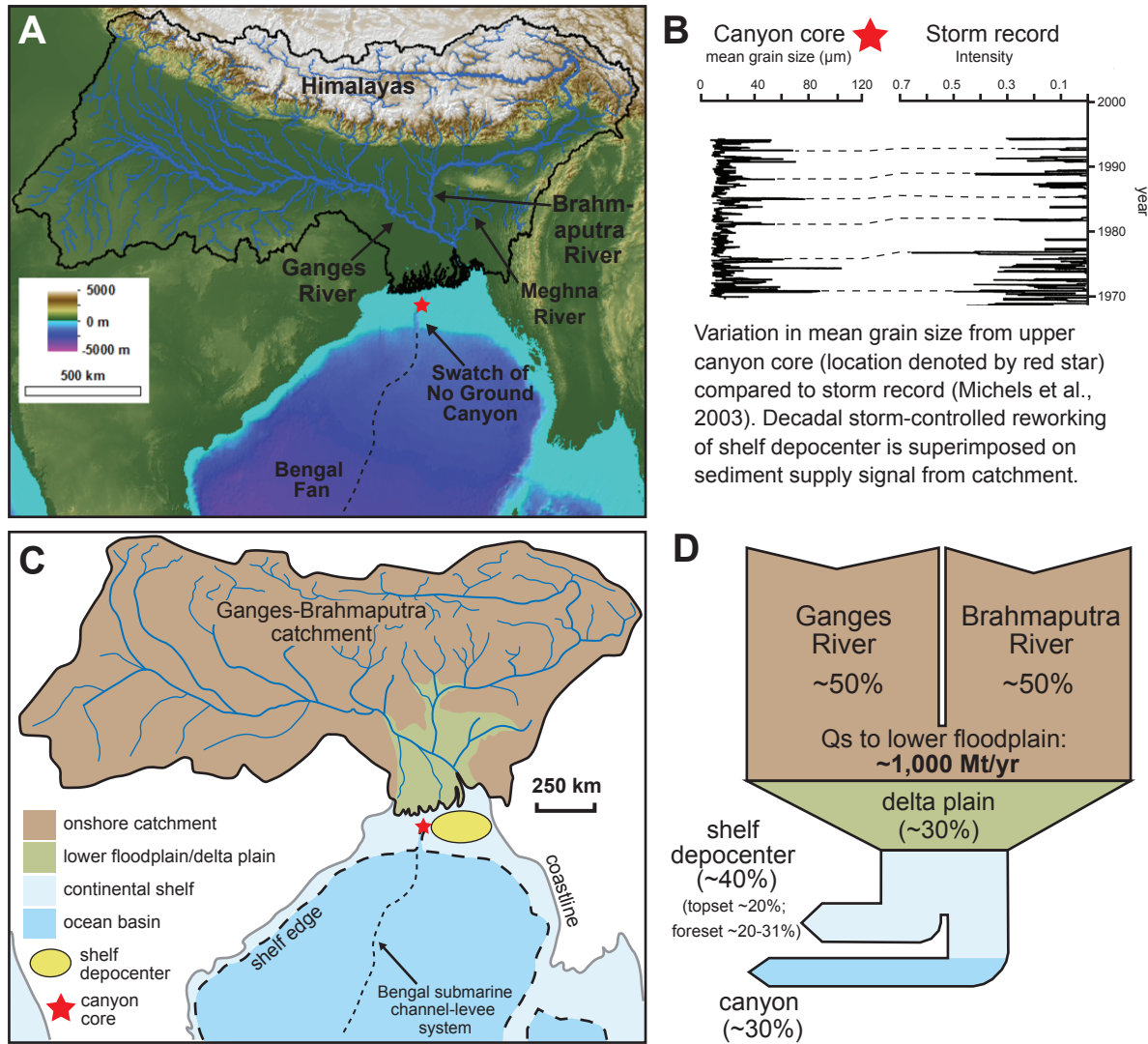


Figure 4: (A) Topography and drainage network of Ganges, Brahmaputra, and Meghna rivers and bathymetry of shelf, Swatch of No Ground submarine canyon, and part of the Bengal submarine fan system. Red star denotes location of core record shown in (B). (B) Core from upper canyon showing variation in mean grain size with time compared to storm record from eastern Bengal shelf. Data is from core 96 KL as reported in Michels et al. (2003). (C) Map of Ganges-Brahmaputra-Bengal sediment-routing system showing catchment area, the large delta plain area, shelf depocenter (yellow) and the Bengal submarine channel-levee system. Red star denotes location of core record shown in (B). (D) Historical timescale sediment budget of Ganges-Brahmaputra-Bengal sediment-routing system showing that almost one-third of the budget is stored on the delta plain, ~40% accumulates in the shelf depocenter, split between the topset and foreset regions, and the remaining ~30% is delivered to the canyon and Bengal submarine fan. Budget estimations from Kuehl et al. (2005) and references therein.

Romans et al. -- Figure 4

417 (Allison and Kepple, 2001; Hanebuth et al., 2013). Shoreline areas show a complex
418 pattern of erosion and accretion (Allison, 1998; Shearman et al., 2013), but radiochemical
419 analyses indicate sediment accumulation generally decreases with distance from the
420 coast, reflecting import of fluvial sediment (Allison and Kepple, 2001).

421 Seismic-reflection profiling has established the presence of a sizable subaqueous
422 delta clinoform on the shelf (Kuehl et al., 1997; Michels et al. 1998). Bathymetric and
423 shoreline changes indicate that ~20% of the fluvial load is building the topset of the
424 clinoform (Fig. 4) (Allison, 1998). Based on core and seismic-reflection data, the foreset
425 region of the clinoform sequesters another 20-31% over historical timescales (Fig. 4)
426 (Michels et al., 1998; Suckow et al., 2001). Transparent layers visible in seismic
427 reflection profiles of the clinoform have been suggested to represent mass flows triggered
428 by earthquakes (Michels et al., 1998). As a result of westward along-shelf currents
429 reworking the delta front, sediment is at present being advected into the head of the
430 Swatch of No Ground submarine canyon and episodically to the Bengal submarine fan
431 (Kuehl et al., 1997; Kuehl et al., 2005). Weber et al. (1997) showed that late Holocene
432 sedimentation occurred on the channel-levee complex (on the middle fan, ~500 km
433 seaward of the shelf), but at a reduced rate compared to latest Pleistocene to early
434 Holocene. Cyclones are hypothesized to be responsible for stratigraphic layering visible
435 on the shelf and in the upper canyon (Fig. 4) (Kudrass et al., 1998; Suckow et al., 2001;
436 Michels et al., 2003). Cyclones also serve as a possible trigger mechanism for episodic
437 mass wasting events (Rogers and Goodbred, 2010). Canyon sedimentation and down-
438 canyon transport, including evidence for turbidite deposition on the Bengal Fan, are
439 hypothesized to account for ~30% of the fluvial load over historical timescales (Fig. 4)

440 (Goodbred and Kuehl, 1999; Kuehl et al., 2005). A terrestrial erosion-zone signal is being
441 driven down this system, but it has been and continues to be significantly modulated by
442 other processes (e.g., cyclones) along the way. As a result, alluvial storage areas might be
443 the best sites for extracting source forcings over the historical timescale.

444 The Ganges-Brahmaputra-Bengal and Eel systems research highlight how historic
445 stratigraphic records, accumulation rates, and sediment budgets can inform system
446 functioning and source-to-sink transfer. This work also demonstrates that, although
447 historical timescale records may be data rich and highly temporally resolved relative to
448 intermediate and deep-time records, evaluation of sediment supply signals generated in
449 upland catchments can be difficult. A more detailed and quantitative documentation of
450 processes, rates, and spatial distribution of sedimentation does not necessarily equate to a
451 better understanding of linkages between system segments. Better preserved and
452 potentially more complete records in proximal storage areas, such as lakes, might allow
453 more detailed records to be captured up system, but the localized nature might not reflect
454 broader system functioning (e.g., Orpin et al., 2010). Combining observations from
455 multiple localities will be essential to defining robust regional or broader, global signals
456 (e.g., Noren et al., 2002). Other insights about catchment sediment production can be
457 provided from the geomorphic record of erosional landforms. The sedimentary signature
458 of events, such as floods, earthquakes, and storms, is likely more easily relatable to its
459 forcing if process and response occur within the same or immediately adjacent
460 segment(s) of the sediment-routing system (e.g., coastal overwash fan deposits from
461 landfalling hurricanes; Boldt et al., 2010). The variability in sediment transport and
462 associated deposits generated at $<10^2$ yr timescales is commonly considered noise over

463 longer timescales as a consequence of combining event-scale and ‘background’
464 sedimentation into a time-averaged rate. However, the findings from historical timescale
465 studies show that there are signals embedded within the noise.

466

467 **3 Sediment Routing at Intermediate (10^2 - 10^6 yr) Timescales**

468 The timescale from just beyond historical (several centuries before present; discussed
469 above) to several millions of years is a critical temporal range in Earth surface dynamics
470 because fundamental climate forcings (i.e., Milankovitch cycles) that control the global
471 climate are prominent over this timescale (Hays et al., 1976). Sustained rates of rock
472 uplift and deformation in tectonically active areas lead to exhumation, sediment
473 production, and morphological change at $\geq 10^5$ yr timescales (Burbank and Anderson,
474 2011). Moreover, it is in this temporal range during which sedimentary deposits can be
475 sufficiently buried to become rock and preserved into the stratigraphic record – durations
476 often referred to as ‘geological timescales’ (e.g., Allen et al., 2013).

477 We first discuss sedimentary system dynamics and associated signal implications
478 based on numerical and physical models. Unlike the short-term timescales during which
479 an integration of direct observation, monitoring, and modeling informs our understanding
480 of source-to-sink signal propagation, modeling and theory become even more critical for
481 intermediate (10^2 - 10^6 yr) timescales. Examples of recent work on paleo-sediment budgets
482 for sediment-routing systems are also discussed.

483

484 *3.1 Model Predictions of Intermediate Timescale Signal Propagation*

485 We review how tectonic or climatic signals with periods of 10^2 – 10^6 yr are propagated
486 through different portions of the sediment routing system (Fig. 2). We emphasize
487 sediment supply (Q_s) as the principal vector for environmental signal propagation and
488 aim to provide a review on the current state of knowledge with respect to the following
489 important questions: (1) Does the erosion zone produce sediment supply signals in
490 response to climate and tectonic perturbations with periods able to generate stratigraphic
491 patterns? (2) Does the transfer zone faithfully transmit signals to the sedimentary basin,
492 or does it modify signals coming from the erosion zone?

493 Signal transfer through a system depends on whether its period is smaller or larger
494 than the response time of the system (Paola, 1992; see also Allen, 1974). Moreover, the
495 action of internal, or autogenic, dynamics in any or all of the mass-flux zones can
496 influence Q_s behavior, which affects signal propagation. We first define and review
497 knowledge of response times for the erosion zone of hillslopes and bedrock channels,
498 then focus on the transfer zone of mixed alluvial and bedrock channels to alluvial
499 channels with floodplains, and its linkage to the accumulation zone in sedimentary basins
500 (Fig. 1).

501

502 *3.1.1 Q_s Signal Generation and Propagation in the Erosion Zone*

503 It is beyond our scope to present a comprehensive review of investigations into
504 how climate and/or tectonic forcings are recorded in net-erosional landscapes (e.g.,
505 Burbank and Anderson, 2011; and references therein). Rather, we emphasize the
506 propagation of those perturbations out of the erosion zone in the form of sediment supply.

507 The concept of steady state as applied to landscape evolution (e.g., [Willet and Brandon,](#)
508 [2002](#)) refers to a state in which Earth's surface elevation relative to a datum is broadly
509 constant as a result of a balance between rock uplift and erosion. Thus, the rate of
510 sediment supply out of an area in steady state is, in the simplest case, also constant when
511 averaged beyond timescales of individual events. A perturbation in the form of varying
512 rates of tectonic movement or precipitation induces a response of the landscape system in
513 the form of varying rates of sediment production. A characteristic equilibrium, or
514 response, time for the system is the time that it takes for this transient landscape to
515 respond to this perturbation and then return to a steady state ([Beaumont et al., 2000](#)) (Fig.
516 5). [Allen \(2008b\)](#) termed landscapes that have a response time shorter than the repeat
517 time of the perturbation as 'reactive' and those with response times longer than
518 perturbation repeat time as 'buffered' landscapes. This equilibrium time is critical to the
519 discussion of signal propagation because it is the *variability* of Q_s out of the erosion zone
520 that can result in recognizable variations in deposit character down system. Here, we
521 focus on the relevance of steady state in terms of denudation because of its close
522 association with sediment production.

523 The physical laboratory experiments of [Bonnet and Crave \(2003\)](#) highlighted the
524 important observation that climate signals, because they can affect the totality of an area
525 at once, can trigger an immediate response of the landscape. In their case, steady state is
526 characterized by a constant mean elevation ([Montgomery, 2001](#); [Willet and Brandon,](#)
527 [2002](#)) and, thus, a response is a change in mean elevation. This contrasts to rock uplift
528 signals, expressed in the form of baselevel changes (see [Schumm, 1993](#)), which
529 propagate as waves of headward incision and diachronously affect the landscape ([Bonnet](#)

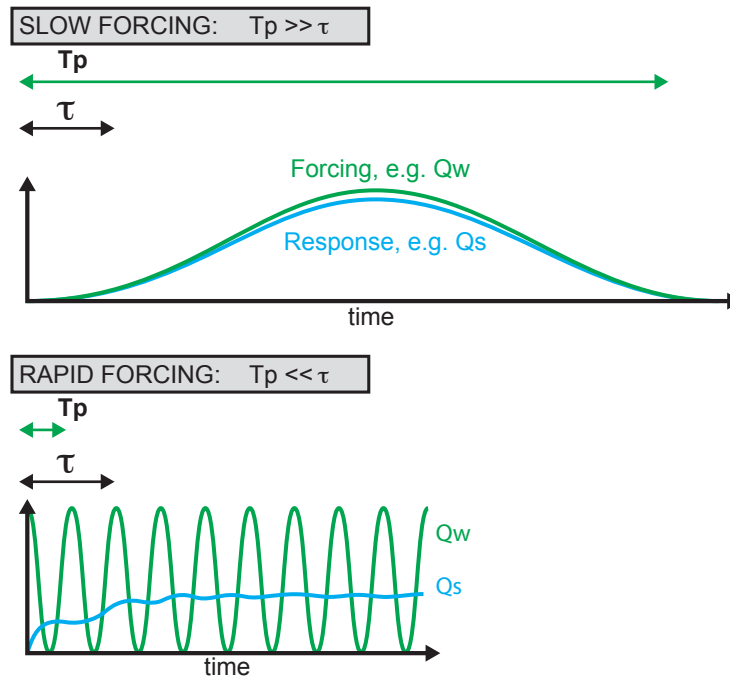


Figure 5: The ratio between the timescale of a perturbation (T_p) and the characteristic equilibrium timescale (τ) of the considered system describes the system response to forcing (after Beaumont et al., 2000; see also Allen, 2008b). A forcing of water discharge (Q_w) and a response of sediment supply (Q_s) are shown for (A) a reactive response when response time is much shorter than timescale of forcing and (B) a buffered response when response time is longer than timescale of perturbation.

Romans et al. -- Figure 5

530 [and Crave, 2003](#)). In a study of the response of bedrock channels to tectonic and climate
531 signals using generic stream-power fluvial incision, [Whipple \(2001\)](#) showed response
532 times ranging from 250 kyr to 2.5 Myr to both tectonics and climate. In this study, the
533 response time is the time required for the landscape to return to a steady state defined as a
534 statistically invariant topography (i.e., constant mean elevation; [Montgomery, 2001](#);
535 [Willet and Brandon, 2002](#)) and constant denudation rate. When climate and tectonics act
536 jointly, the response of a stream-power fluvial landscape may essentially be immediate
537 (i.e., response time tends to zero; [Whipple, 2001](#)). Improvements of the stream-power
538 erosion law produce divergent results as to landscape reactivity. Among these, the
539 consideration of dynamic adjustment of channel width during perturbations induces faster
540 reaction of fluvial landscapes than if channel width is not considered ([Attal et al., 2008](#);
541 [Whittaker et al., 2007](#)). Conversely, a series of stream-power inspired models (e.g.,
542 [Gasparini et al., 2007](#)) including a degree of dependency to saltating bedload tends to
543 suggest longer response times than those predicted by detachment-limited stream power
544 (such as those of [Whipple, 2001](#); see above).

545 Using a nonlinear 1D diffusive model of catchment erosion, [Armitage et al. \(2013\)](#)
546 showed that small (10-20 km long) catchments, such as those draining normal-fault
547 bounded footwalls, are reactive to single-step, sustained changes of precipitation but tend
548 to temporally buffer cyclic precipitation variations with Milankovitch periodicities (i.e.,
549 100 kyr, 400 kyr, 1.2 Myr). Using a 2D model of landscape evolution including diffusive
550 hillslopes and detachment-limited stream-power-governed bedrock incision, [Godard et al.](#)
551 [\(2013\)](#) found that a given landscape possesses a characteristic resonance periodicity for
552 which landscape response to corresponding climatic oscillation is maximized in terms of

553 sediment supply. For more easily erodible lithologies, landscape response to orbitally
554 controlled climate signals could be a significant increase or decrease of the amplitude of
555 sediment supply variations. Thus, some landscapes respond to, might even amplify,
556 climate and tectonic signals. In landscapes dominated by diffusive hillslopes, however,
557 such as in soil-mantled, low-relief settings, diffusion itself might be very efficient at
558 filtering climatic or tectonic oscillations because of slow signal propagation (e.g., [Furbish](#)
559 [and Fagherazzi, 2001](#)).

560

561 ***3.1.2 Qs Signal Generation and Propagation in the Transfer Zone and Preservation*** 562 ***in the Accumulation Zone***

563 In many instances, the terminal depositional sink is not immediately adjacent to the
564 source area but linked to it by a fluvial system. In such cases, it was recognized that the
565 fundamental problem becomes whether climate and tectonic sediment supply signals that
566 originate in the erosion zone are propagated by the transfer system to the sedimentary
567 basin ([Castelltort and Van Den Driessche, 2003](#)). [Paola et al. \(1992\)](#) developed the idea
568 that to understand stratigraphic response to external factors it was fundamental to
569 consider the periodicity of cyclic signals with respect to the characteristic equilibrium, or
570 response, time (T_{eq}) of a sediment-routing system (Fig. 5). They expressed T_{eq} (time unit)
571 for a 1D fluvial profile as a function of characteristic system length (L) and diffusivity
572 (K):

573

$$574 \quad T_{eq} \sim L^2/K$$

575

576 Thus, the larger the system (i.e., the longer the transfer zone), the longer its response time
577 is whereas the more diffusive the transfer zone, the shorter its response time. A prediction
578 of this model is that cyclic perturbations with periods less than T_{eq} are buffered by the
579 system's response time. In contrast, variations of boundary conditions with periodicities
580 greater than T_{eq} produce stratigraphic patterns in the sedimentary basin, but these patterns
581 might be similar for subsidence and sediment supply variation (Paola et al., 1992; see
582 also Marr et al., 2000 and Allen, 2008b).

583 On the basis of a comparison between the modern river sediment discharge of
584 some large Asian rivers and the average sediment discharge deduced from sedimentary
585 basins over the last 2 million years, Métiévier and Gaudemer (1999) suggested that large
586 alluvial systems of Asia behave as diffusive entities buffering the high-frequency climate
587 change known for the late Cenozoic (see also Schaller et al., 2001; and Wittmann et al.,
588 2011). Métiévier and Gaudemer (1999) computed equilibrium times of >1 Myr for such
589 rivers using an expression they proposed for the diffusivity (K) of large rivers as a
590 function of sediment discharge (Q_s), river channel or channel-and-floodplain width (W),
591 and slope (S):

592

$$593 \quad K=Q_s/(W*S)$$

594

595 Following Métiévier and Gaudemer (1999) results, Castellort and Van Den Driessche
596 (2003) calculated the diffusive response time of 93 of the largest modern rivers to
597 investigate the down-system stratigraphic response to high-frequency (10^4 yr) cycles of
598 sediment supply. Castellort and Van Den Driessche (2003) find that the characteristic

599 response times of transfer zones comprising large rivers, which typically include
600 extensive floodplains, are 10^5 - 10^6 yr, exceeding the 10^4 yr climate oscillations. When
601 channel width rather than alluvial valley width is used in this relationship the resulting
602 response times are minimum response times.

603 These diffusion-based investigations suggest that temporary, and in some cases
604 permanent, storage of sediment in catchment and/or transfer-zone sinks (see also [Allen,](#)
605 [2008a](#); [Wittmann et al., 2011](#); [Covault et al., 2013](#); and references therein) can mask the
606 down-system stratigraphic record of external perturbations to the sediment-routing
607 system. In the case of a large, hinterland-river-continental margin sediment-routing
608 system, this transient storage of sediment can result from deposition in floodplains
609 ([Allen, 2008b](#)). Larger catchments can retain sediment for longer periods as a result of
610 more space available for sediment storage and consequent resistance to complete
611 hinterland-to-continental margin sediment transfer in response to short-term, small-
612 magnitude external perturbations, such as local storms and earthquakes ([Allen, 2008a](#)).
613 [Métivier and Gaudemer \(1999\)](#) suggested that rivers and floodplains proportionally adjust
614 to climate changes and upstream denudation in buffered catchments in which sediment
615 loads are approximately balanced over different timescales. That is, if upstream
616 denudation is reduced, the river will incise its floodplain to keep the sediment load at the
617 outlet constant. Conversely, if climate changes force greater upstream denudation, the
618 river is likely to use that increased sediment load to recharge its previously excavated
619 floodplain. In this way, the steady transfer of reworked floodplain sediment to an outlet
620 can be maintained over a range of timescales ([Métivier and Gaudemer, 1999](#); [Phillips,](#)
621 [2003](#); [Phillips and Slattery, 2006](#); [Covault et al., 2013](#); among many others). The

622 ubiquitous alluvial terrace fills that ornate many river systems worldwide are witnesses of
623 the residence time of sediments in the transfer zone.

624 These theoretical results contrast with the sensitivity to Late Quaternary climate
625 change apparently displayed by some large fluvial systems such as the Ganges-
626 Brahmaputra ([Goodbred and Kuehl, 1999; 2000a, 2000b; Goodbred, 2003](#)) and suggest
627 that, although alluvial systems may behave diffusively in response to sediment supply
628 variations, they may be sensitive to perturbations of water discharge, which can increase
629 or decrease diffusivity ([Simpson and Castellort, 2012](#)). Using physical laboratory models
630 of river response to water discharge and sediment supply change, [Van Den Berg Van](#)
631 [Saparoa and Postma \(2008\)](#) show that experimental rivers respond faster to changes of
632 discharge than to perturbations of up-system sediment supply. [Van Den Berg Van](#)
633 [Saparoa and Postma \(2008\)](#) concluded that high-frequency cyclic patterns in marine
634 delta-shelf successions were most likely controlled by high-frequency changes in
635 discharge driven by climate, whereas the low-frequency sequences were likely a result of
636 low-frequency changes in sediment supply driven by tectonic deformation.

637 We recognize that the results of diffusion-based approaches may be dependent on
638 our current ability to estimate parameters of the diffusion laws. [Simpson and Castellort](#)
639 [\(2012\)](#) explored the response of a 1D alluvial river bed to sediment concentration and
640 water discharge pulses using a physically based numerical model of interacting water
641 flow and sediment transport without *a priori* assumption of diffusive behavior. Consistent
642 with the experiments of [Van Den Berg Van Saparoa and Postma \(2008\)](#), in this model
643 the strong coupling between water discharge and river gradient induces amplified
644 sediment supply variations in response to oscillations of water discharge, whereas

645 sediment supply oscillations are dampened because of the negative feedback between
646 sediment concentration and channel gradient. In the future, additional constraints on the
647 behavior of sediment transfer will result from other approaches such as computational
648 fluid dynamics (e.g., [Edmonds and Slingerland, 2007](#)) or cellular automata (e.g., [Murray
649 and Paola, 1997](#)).

650

651 ***3.1.3 Potential Influence of Internal Dynamics on Q_s Signal Recognition***

652 In addition to the buffering of signals linked with the processes reviewed in the
653 previous sub-section, perturbations to sedimentary signal propagation arise from
654 sedimentary processes occurring within the river-floodplain and/or river-coastal plain
655 segments that need not be driven by up-system forcings. Such self-organizing processes,
656 referred to as autogenic dynamics ([Paola et al., 2009](#)), and first emphasized by [Beerbower
657 \(1964\)](#), can create organized depositional architecture (e.g., [Hoyal and Sheets, 2009](#)).
658 Critical to this discussion is the potential for climate or tectonic signals that originated in
659 the catchment to be significantly masked, modified, or ‘shredded’ by such autogenic
660 dynamics ([Jerolmack and Paola, 2010](#)). Variability in sediment transport is a result of the
661 following general autogenic cycle: transient storage of sediment, exceedance of some
662 critical threshold, and release of sediment during relaxation following failure. [Jerolmack
663 and Paola \(2010\)](#) likened the threshold behavior of sediment storage and release to
664 morphodynamic turbulence, analogous to turbulence in fluid flows.

665 Recently, [Ganti et al. \(2014\)](#) developed a quantitative framework to isolate
666 autogenic, morphodynamic processes from external, environmental forcings in the

667 stratigraphic record. They showed that the calculated advection length (l_a) for settling
668 sediment sets bounds on the scale over which autogenic processes operate:

669

$$670 \quad l_a = u h_s / w_s$$

671

672 where u is the flow velocity, h_s is the average sediment settling height, and w_s is the
673 settling velocity. The advection length scale is the horizontal length over which an
674 average particle is transported in the flow before falling to the bed. [Ganti et al. \(2014\)](#)
675 argued that morphodynamic feedbacks, or autogenic ‘shredding,’ can only occur if the
676 length scale of interest, e.g., the system size, is larger than l_a .

677 [Wang et al. \(2011\)](#) recognized the aforementioned work on damping or
678 ‘shredding’ of upstream, external signals by autogenic sediment transport processes, and
679 used numerical and physical experiments, as well as some field data, to gain insight into
680 the timescale of compensational stacking of deposits within a basin. This compensation
681 timescale (T_c) is defined as:

682

$$683 \quad T_c = l/r$$

684

685 where l is a roughness length scale, equal to the amount of topographic ‘mounding’ due
686 to local channel deposition produced between each avulsion, and r is the basin-wide,
687 long-term sediment accumulation rate. This equation suggests that the geometry of
688 deposits carries the signature of stochastic autogenic dynamics during the time necessary
689 to fill a basin to a depth equal to the amount of surface roughness in a sediment-routing

690 system. T_c provides an estimate of temporal scales below which stratigraphers should be
691 cautious about interpreting signals. As a case in point, [Wang et al. \(2011\)](#) calculated T_c
692 for the Lower Mississippi Delta in which they consider that the roughness length scale, l ,
693 was represented by the mean channel depth for the Lower Mississippi River of 30 m and
694 a sediment accumulation rate of 0.26 m/kyr, estimated for the past 8 Myr ([Straub et al.,](#)
695 [2009](#)). T_c is 115 kyr, which is ~ 100 times larger than the ~ 1300 yr recurrence of large
696 avulsions of the Lower Mississippi River ([Aslan et al., 2005](#)). However, subsequent field
697 data from the Lower Mississippi River indicate a rapid response to glacio-eustatic
698 variation since Oxygen Isotope Stage 7 (~ 200 ka) ([Shen et al., 2012](#)). Large amplitude
699 sea-level rise and fall prompted rapid and widespread fluvial aggradation and incision,
700 respectively, the effects of which extended >600 km upstream from the present shoreline
701 ([Shen et al., 2012](#)).

702 The models and experiments discussed above highlight that signal buffering as a
703 result of sediment storage in up-system segments as well as depositional dynamics in the
704 sink can mask the stratigraphic record of external perturbations to the sediment-routing
705 system, although the quantitative expression of this are still being resolved. In summary,
706 signals of a forcing can be passed to a basin and preserved in the stratigraphic record
707 when their period exceeds the characteristic equilibrium time of the sediment-routing
708 system, but this is valid only if their period is also larger than the characteristic timescale
709 of autogenic sediment transport fluctuation and/or when the magnitude of the forcing is
710 larger than the magnitude of internal oscillations (e.g., on the order of the size of
711 catchment and alluvial accommodation) ([Jerolmack and Paola, 2010](#)). In the next section

712 we review sediment budgets of natural sedimentary systems, which allow for accounting
713 of our principal vector of relevance, Qs.

714

715 *3.2 Paleo-Sediment Budgets of Natural Systems and Implications for Signal*

716 *Propagation*

717 In this section we will review work on sediment budgets at 10^2 - 10^5 yr timescales
718 and implications for signal propagation via three sediment-routing systems: (1)
719 tectonically active, small systems of southern California; (2) tectonically quiescent, larger
720 systems of the northwestern Gulf of Mexico; and (3) tectonically active, larger systems of
721 southern Asia. By focusing on sediment delivery from onshore catchments to the deep
722 sea, which is the ultimate sink for coarse-grained terrigenous material, we highlight the
723 role of the shelf as a Qs gateway and filter.

724

725 ***3.2.1 Methods for Paleo-Sediment Budget Reconstruction at Intermediate Timescales***

726 Just as microfossils are the carriers of isotopes used to reconstruct geochemical
727 signals, sediment supply is here considered the carrier of climate and tectonic signals.
728 Thus, determining a paleo-sediment budget, the spatial and temporal partitioning of mass
729 removed, transferred, and deposited within a routing system, is valuable for the
730 interpretation of signal propagation and preservation. For the sake of brevity, we do not
731 present a comprehensive review of the application of sediment budget concepts to
732 timescales beyond direct measurement and instead refer the reader to a recent review by
733 [Hinderer \(2012\)](#). Determining accumulated mass from stratigraphic volumes is
734 straightforward in concept, but can be challenging in practice as a result of lack of

735 appropriate data (e.g., seismic-reflection with proper chronologic control) and/or
736 uncertainties in post-depositional stratal preservation (Sadler and Jerolmack, 2014). The
737 geochemistry and mineralogy of sediment is often used to determine routing pathways as
738 well as the relative contributions and potential residence times of terrigenous versus
739 marine-derived material.

740 Two of the three systems reviewed below combine cosmogenic radionuclide (CRN)
741 analysis for catchment-integrated denudation and radiocarbon dating for continental-
742 margin deposition to reconstruct sediment budgets. Advances in CRN analysis provide
743 catchment-integrated denudation rates and sediment loads at 10^2 – 10^5 yr timescales (von
744 Blanckenburg, 2005), which are comparably similar to the timescales of deposition
745 measured in offshore basins with radiocarbon ages (generally <50 ka; Reimer, 2012).
746 CRNs are produced *in situ* as secondary cosmic rays interact with rocks within meters of
747 Earth's surface; longer exposure to secondary cosmic rays as a result of slower
748 denudation produces more nuclides. Sediment can be liberated from these rocks, mixed in
749 the catchment through hillslope and fluvial transport processes, and ultimately deposited
750 near the catchment outlet. Accordingly, the CRN abundance measured in sediment
751 deposited near the catchment outlet can be used to divulge the catchment-wide
752 denudation rate, which is inversely proportional to nuclide abundance (Brown et al. 1995;
753 Bierman and Steig 1996; Granger et al. 1996).

754 Regardless of the specific tools used, it is of critical importance that all mass inputs
755 and outputs to the system are considered and accounted for. Attempting to close a
756 sediment budget at timescales beyond direct measurement provides an opportunity to

757 evaluate other inputs and outputs that might not be evident with a qualitative
758 interpretation.

759

760 ***3.2.2 Small and Tectonically Active Systems of Southern California***

761 Tectonically active southern California is an ideal setting in which to investigate
762 millennial-scale mass balance as a result of close proximity of sediment-routing
763 components: onshore erosion zones are located adjacent to short alluvial-coastal plain
764 depositional environments and offshore, confined sedimentary basins of the California
765 Continental Borderland (Fig. 6A). The confinement of the offshore basins facilitates
766 complete accounting for detrital mass relative to open-ocean basins, such as the Arabian
767 Gulf and Bay of Bengal (Weber et al., 1997; Curray et al., 2002). Furthermore, many of
768 the submarine canyon and fan systems of the California Continental Borderland are
769 consistently linked to the shoreline and maintain connectivity even during Holocene
770 highstand (Normark et al., 2009).

771 Covault et al. (2011) used CRNs from the Peninsular Ranges of southern California to
772 calculate catchment-integrated denudation rates, which varied from 0.07 to 0.24 mm/yr
773 since 10 ka. These denudation rates were calculated to be 1.9-2.4 Mt/yr and integrated
774 across the total area of drainage basins ($>6 \times 10^3 \text{ km}^2$) delivering sediment to the offshore
775 Oceanside littoral cell and the La Jolla submarine canyon and fan system. Based on
776 radiocarbon-constrained seismic-reflection mapping (Covault et al., 2007) the mass
777 accumulation rate of the La Jolla submarine fan was calculated to be 2.6-3.5 Mt/yr since
778 the Last Glacial Maximum. Although the mass of material denuded from Peninsular
779 Ranges catchments is in close agreement, of the same order of magnitude, as the mass of

780 material deposited in the La Jolla submarine fan, deep-sea deposition exceeds terrestrial
781 denudation by 11%-89%. This additional supply of sediment could be owed to enhanced
782 dispersal of sediment across the shelf caused by sea cliff erosion during postglacial
783 shoreline transgression and initiation of submarine mass wasting.

784 The terrestrial source to deep-sea sink mass balance does not show orders of
785 magnitude inequalities that might be expected in the wake of major sea-level changes
786 since the Last Glacial Maximum. Thus, sediment-routing processes in a globally
787 significant class of small, tectonically active systems might be fundamentally different
788 from those of larger systems that drain entire orogens, in which sediment storage in
789 coastal plains and wide continental shelves can exceed millions of years ([Milliman and](#)
790 [Syvitski, 1992](#)). Furthermore, in such small systems, depositional changes in the deep
791 offshore can reflect onshore changes when viewed over timescales of several thousands
792 of years to more than 10 kyr. For example, [Romans et al. \(2009\)](#) and [Covault et al. \(2010\)](#)
793 examined Holocene deposition of the Hueneme and Newport deep-sea depositional
794 systems offshore of southern California. Integrated datasets of radiocarbon ages from
795 sediment cores and seismic-reflection profiles demonstrated that variability in rates of
796 Holocene deep-sea turbidite deposition is related to complex ocean-atmosphere
797 interactions, including enhanced magnitude and frequency of El Niño-Southern
798 Oscillation (ENSO) cycles, which increased precipitation and fluvial water and sediment
799 discharge in southern California (Fig. 7). Thus, millennial-scale climate forcings are
800 represented as a measureable signal in the stratigraphic record of the deep-sea segment.

801

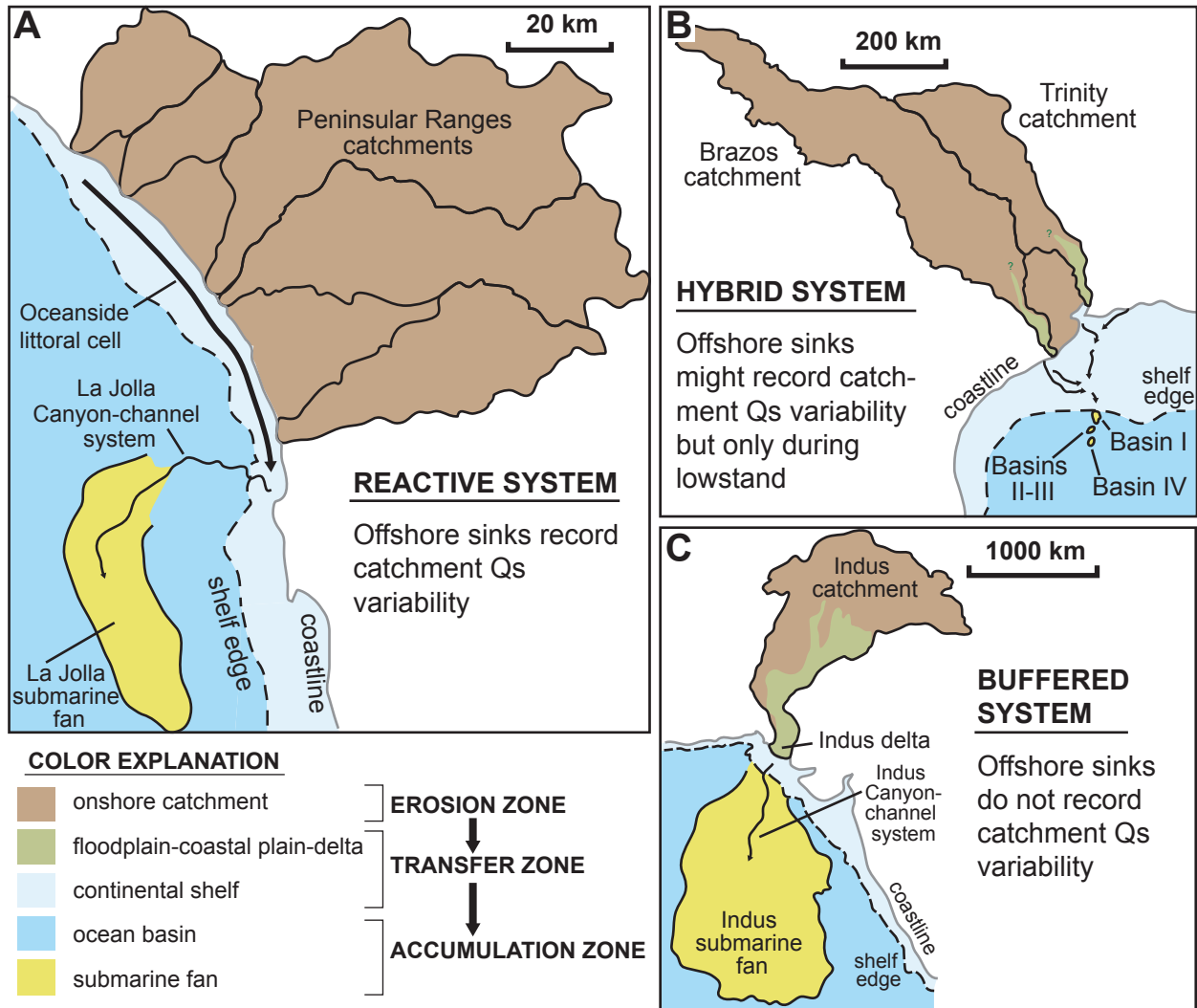


Figure 6: Examples of natural sediment routing systems examined at intermediate timescales. (A) Small and tectonically active system, Peninsular Ranges and Continental Borderland of southern California (Covault et al., 2011); (B) Large and tectonically quiescent system, Texas coastal plain and western Gulf of Mexico (Hidy et al., 2014; Pirmez et al., 2012); (C) Large and tectonically active system, Indus River and Indus submarine fan (Clift et al., 2014). Indus River floodplain extent from Milliman et al. (1984).

Romans et al. -- Figure 6

802 3.2.3 *Large and Tectonically Quiescent Systems of the Western Gulf of Mexico*

803 A sediment budget for the Brazos and Trinity rivers linked to offshore depositional
804 systems in shallow-marine and deep-water environments of the northwestern Gulf of
805 Mexico can be balanced by integrating recent work of [Hidy et al. \(2014\)](#) and [Pirmez et al.](#)
806 [\(2012\)](#). In contrast to the small and tectonically active southern California catchments,
807 the Brazos and Trinity rivers drain a large ($\sim 2 \times 10^5 \text{ km}^2$) tectonically quiescent, non-
808 glaciated, low-relief landscape (Fig. 6B). [Hidy et al. \(2014\)](#) evaluated how denudation
809 rates from CRNs responded to climate change during the last glacial cycle ($\sim 15\text{-}45 \text{ ka}$):
810 Brazos River CRNs yielded a mass load of 5.3 Mt/yr since 35 ka; and Trinity River
811 CRNs yielded a mass load of 2-4 Mt/yr. Furthermore, [Hidy et al. \(2014\)](#) analyzed the
812 CRN ratio of $^{26}\text{Al}/^{10}\text{Be}$ in river sediment to evaluate its transient storage in the catchment
813 in route to its final depositional site (see [Wittmann and von Blanckenburg, 2009](#);
814 [Wittmann et al., 2011](#)). Mass storage on the coastal plain was interpreted to have been
815 greater during glacial periods with lower sea level. Denudation rates and mass loads were
816 calculated to be larger during interglacial periods, which suggest that increased
817 weathering rates associated with warmer climates accelerated landscape erosion.
818 Furthermore, increased mass load measured during warm interglacial periods is
819 interpreted to reflect stronger reworking and delivery of sediment to the river mouth than
820 during cooler glacial periods. An implication of this relationship between temperature
821 and mass load is that global sediment and potentially dissolved load delivery to the ocean
822 from analogous, tectonically quiescent, non-glaciated, low-relief landscapes might have
823 been larger during the warm Pliocene than the cooler Quaternary ([Hidy et al., 2014](#)).
824 However, any transient storage of sediment prior to preservation in terrace deposits

825 would complicate the interpretation of the CRN data as representative of catchment
826 denudation.

827 [Pirmez et al. \(2012\)](#) developed a robust chronostratigraphic framework from Oxygen
828 Isotope Stage 6, ~120 ka, through the Last Glacial Maximum for the sediment deposited
829 in four deep-water, salt-withdrawal slope basins of the northwestern Gulf of Mexico (see
830 also [Prather et al., 2012](#)) (Fig. 6B). The deep-water depositional systems were linked to
831 the Brazos and Trinity river-deltas only during lowstands of sea level, when the shoreline
832 had regressed >100 km from the present-day beach to the shelf edge ([Mallarino et al.,
833 2006; Anderson et al., this volume](#)). Chronostratigraphy was interpreted from an
834 integrated database of 3D seismic-reflection data, age control from analysis of cores from
835 Integrated Ocean Drilling Program Expedition 308, analysis of proprietary cores from
836 Shell Oil Company, and published literature ([Pirmez et al., 2012](#)). The majority of
837 sediment, ~50 km³, was calculated to have been deposited during a period of relatively
838 low sea level, between ~15-24 ka, yielding a mass accumulation rate during this period of
839 5.5 Mt/yr, which is within the same order of magnitude of the CRN-derived mass load of
840 the Brazos and Trinity rivers of 7.3-9.3 Mt/yr ([Hidy et al., 2014](#)) during a similar period,
841 generally <35 ka. The imbalance in rates, with diminished deep-water slope basin mass
842 accumulation, is likely a result of Brazos-Trinity river-delta deposition on the subaerially
843 exposed shelf as the shoreline had regressed to the shelf edge between ~15-24 ka. Indeed,
844 [Pirmez et al. \(2012\)](#) estimate a maximum volume of ~25 km³ of deltaic sediment was
845 deposited between ~15-24 ka, which yields a mass accumulation rate of 2.8 Mt/yr. This
846 mass added to the deep-water basin fill yields a total mass accumulation rate of 8.3 Mt/yr,

847 which is within the range of CRN-derived mass load ([Hidy et al., 2014](#)) of the Brazos and
848 Trinity rivers.

849 In this system, sea level is interpreted to control the delivery of terrigenous sediment
850 to the deep-water slope basins over 10^5 yr timescales: during periods of relatively high
851 sea level, when the shoreline had transgressed, the slope basins were interpreted to
852 receive only hemipelagic, fine-grained sediment. During periods of relatively low sea
853 level and a subaerially exposed shelf, relatively coarse-grained terrigenous sediment was
854 deposited in the slope basins. However, mass accumulation during periods of relatively
855 low sea level was interpreted to have varied between the four slope basins as a result of a
856 complex interaction between river-delta sediment routing and dynamic, salt-withdrawal
857 slope-basin evolution. The complex history of sediment deposition, storage, and
858 remobilization in the zone between the modern coastline and the shelf edge over the past
859 ~ 125 kyr ([Anderson et al., this volume](#)) highlights the role of the shelf as an additional
860 filter of signals generated in the catchment. Therefore, in contrast to the southern
861 California examples, offshore depositional records are hypothesized to primarily reflect
862 sea-level-driven accommodation changes as opposed to Q_s variability from the onshore
863 catchments. However, during glacial periods of terrigenous sediment delivery to deep
864 water, depositional records might reflect Q_s variability from rivers (Fig. 6B). This might
865 be common to other sediment-routing systems, where deep-water canyon heads are
866 stranded at the edges of drowned continental shelves during interglacial periods ([Blum
867 and Hattier-Womack, 2009; Covault and Graham, 2010](#)).

868

869 3.2.4 *Large and Tectonically Active Systems of Southern Asia*

870 Since the Last Glacial Maximum (LGM), the Indus sediment-routing system
871 comprised a steep (total relief of nearly 8 km), tectonically active hinterland and large
872 ($\sim 10^6$ km²) catchment (Milliman and Farnsworth, 2011), a delta located on a wide (~ 120
873 km) shelf, and a submarine canyon that fed the second largest accumulation of
874 terrigenous sediment in the world, the Indus submarine fan (Fig. 6C). Clift et al. (2014)
875 used seismic-reflection data, radiocarbon ages, and analyzed the geochemistry (a suite of
876 major and trace elements, including Zr/Rb, K/Rb, and Nd; Limmer et al., 2012) and
877 mineralogy of sediment of the Pakistani continental margin to investigate sediment
878 routing from the Indus river-delta to the upper submarine canyon (< 1300 m below
879 present sea level) since the LGM. Seismic stratigraphic interpretations of deltaic
880 clinoforms and radiocarbon ages indicate that the majority of Holocene Indus river-delta
881 sediment is stored on the shelf (Giosan et al., 2006; Clift et al., 2014). Clift et al. (2014)
882 interpreted a variety of deltaic clinoform seismic reflections and concluded that sediment
883 used to construct the shelf-edge delta deposits was reworked and dispersed from mid-
884 shelf locations basinward. Neodymium isotopes presented by Limmer et al. (2012)
885 suggests transient storage on the shelf was significant prior to delivery to the canyon and
886 fan system. Neodymium isotope ratios indicate different values compared to those
887 expected from a fluvial source, which points to reworking of marine sediment deposited
888 during the LGM (Clift et al., 2014). Deposition at the head of the Indus Canyon was
889 measured to be rapid during the Holocene, with evidence for annual delivery of Indus
890 river-delta sediment. However, downstream, ~ 1300 m below present sea level, the

891 youngest deposits are greater than approximately 7 ka, and no terrigenous sand has
892 reached the upper submarine fan during the Holocene (Clift et al., 2014).

893 The Indus sedimentary record at the Pakistani continental margin since the LGM
894 indicates reworking and transient storage of sediment on the shelf and within the
895 submarine canyon en route to the deep Arabian Sea. Thus, deep-water deposits of the
896 Indus fan likely do not faithfully record Qs variability related to climatic or tectonic
897 events onshore over timescales of 10^3 - 10^4 years (Clift et al., 2014). This conclusion
898 highlights the role of the shelf segment as a critical process boundary as well as a Qs
899 gateway between land and sea. This is similar to the Brazos-Trinity sediment-routing
900 system (Fig. 6C), where the deep-water depositional record primarily reflects sea-level
901 changes as opposed to Qs variability from the onshore catchments. Moreover, sediment
902 storage in the vast Indus floodplain (Fig. 6C) likely buffers climatic or tectonic signals
903 generated in the up-system headwaters of the Himalayas. Thus, in these large sediment-
904 routing systems (see also the Amazon system, e.g., Wittman et al., 2011), millennial to
905 million-year Qs signals that originated in the erosion zone are potentially recorded in
906 alluvial and floodplain deposits.

907

908 *3.3 Synthesis of Intermediate Timescale Signal Propagation*

909 The theory, models, and natural systems reviewed above inform us about the
910 plausibility of different forcings and how they might generate Qs signals that are then
911 transmitted by the transfer zone to the ultimate depositional sink. These concepts are
912 synthesized in Figure 8, which contains schematic representations of many of the

913 scenarios reviewed in preceding sections, which can also be viewed as hypotheses about
914 sediment-routing system dynamics worthy of further investigation.

915 Tectonic signals (e.g., uplift rates) with periods of >50 kyr are likely to produce
916 Qs signals at the outlet of the erosion zone (Fig. 8A). Such signals may be transmitted to
917 the accumulation zone if the transfer zone is short (<300 km) but will be buffered if the
918 transfer zone is long (>300 km), unless their period exceeds 100 kyr. Tectonic signals
919 with periods of <50 kyr are likely to be already buffered by the dynamics of the erosion
920 zone itself; i.e., before they reach the outlet of the erosion zone (Fig. 8B).

921 Several antithetic results exist with respect to climate signals (e.g., precipitation
922 changes) in the erosion zone. Different models propose that climate signals might be
923 buffered, faithfully transmitted, or even amplified by the erosion zone (Fig. 8C-E). In
924 some natural examples, where sediment budgets have determined the magnitude of
925 sediment supply exiting the erosion zone, there is a relationship between climate (e.g.,
926 variation in precipitation) and Qs signals as recorded in the sink (Covault et al., 2009;
927 Romans et al., 2009; Fig. 7). However, it is challenging to test whether climate signals
928 are amplified since no predictive understanding exists between a given climate change
929 and the corresponding amplitude of catchment response in terms of sediment supply.
930 However, as discussed above, numerical models of sediment transport and deposition
931 offer the opportunity to elucidate the question of climate signal amplification (e.g.,
932 Armitage et al., 2011). Nonetheless, intermediate climate signals in the form of water
933 discharge (Qw) seem to trigger a strong response of the transfer zone in terms of
934 sediment supply and may thus be transmitted faithfully or even amplified to sedimentary
935 basins (Fig. 8C-E) (Godard et al., 2013; Simpson and Castelltort, 2012).

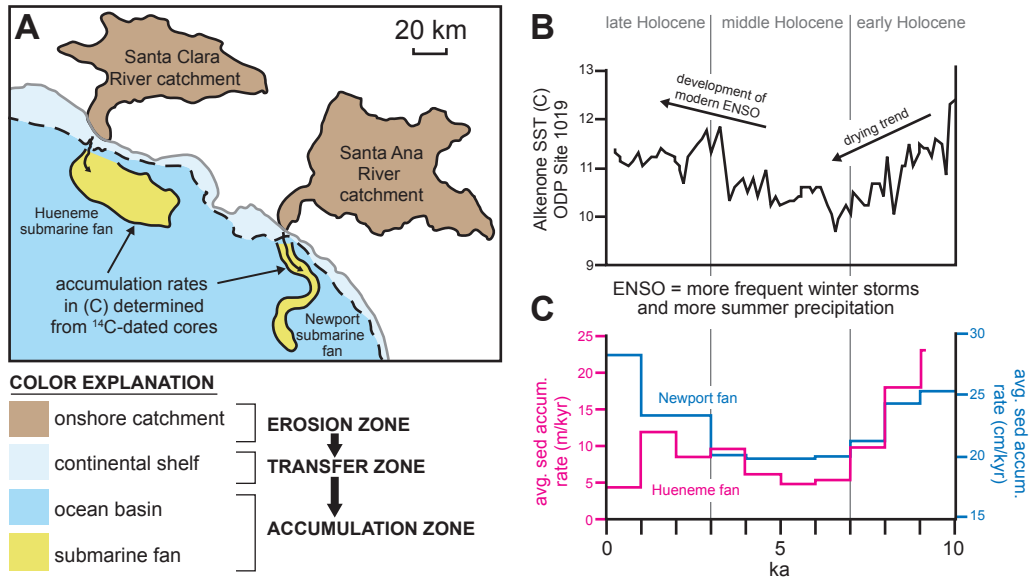


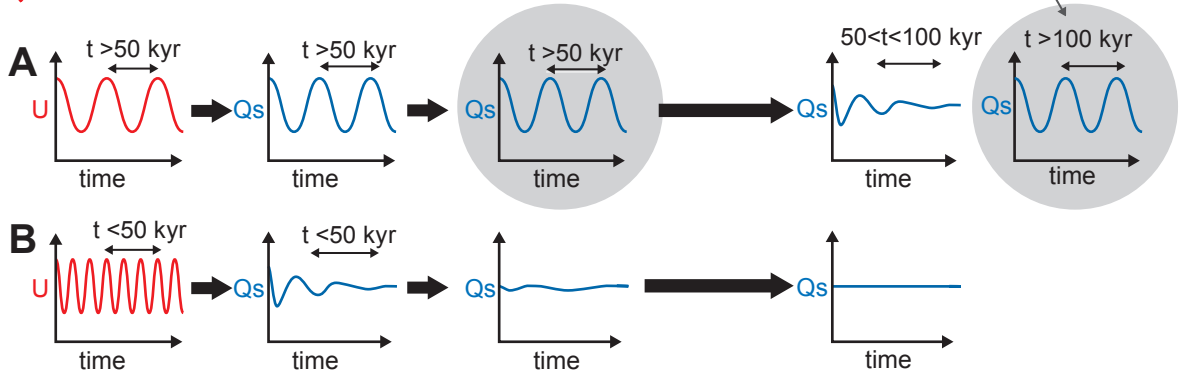
Figure 7: (A) Map showing two southern California sediment-routing systems, each with negligible onshore sediment storage at millennial timescales and correspondingly rapid transfer to offshore submarine fan systems. (B) Alkenone sea surface temperature (SST) proxy for the California coastal region showing a drying trend in the early Holocene followed by the development of the modern El Niño-Southern Oscillation (ENSO), which is known to be sensitive to increased SSTs (Barron et al., 2003). (C) Radiocarbon-constrained weighted-average sediment accumulation rates from Hueneme and Newport submarine fans (Romans et al., 2009; Covault et al., 2011) showing a general correlation of sediment supply to the basin to precipitation regime and, thus, propagation of climatic signal to the stratigraphic record

Romans et al. -- Figure 7



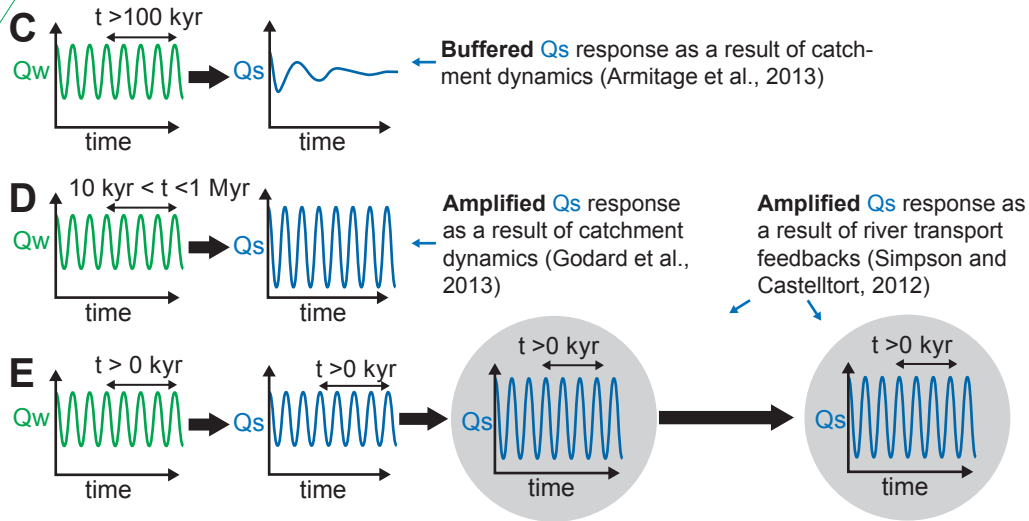
Uplift variations in erosion zone

TECTONICS

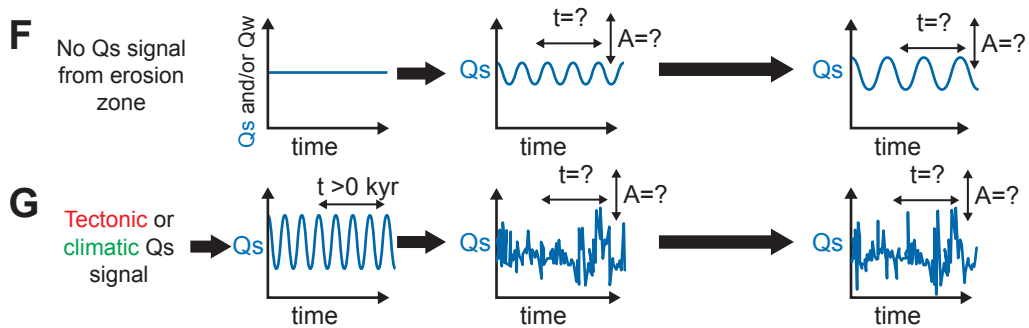


Precipitation change in erosion zone

CLIMATE



Internal dynamics



Romans et al. -- Figure 8 (see caption at end of manuscript text)

936 At the moment, few constraints exist on the characteristic saturation timescales and
937 amplitudes of internally generated Qs fluctuations in natural systems. Current estimates
938 of the typical timescale for channel stacking in large river systems (e.g., [Hajek et al.,](#)
939 [2010](#)) suggest that autogenic dynamics may be able to completely mask or even destroy
940 sedimentary signals with periods of less than 100 kyr.

941

942 **4 Deep-Time ($\geq 10^7$ yr) Sediment Routing**

943

944 *4.1 Challenges and Uncertainties in Deep-Time Signal Propagation Analysis*

945 As sedimentary systems age to tens of millions of years and older, the ability to
946 explicitly measure or calculate source-to-sink sediment supply becomes increasingly
947 challenging because: (1) sediment production areas are poorly preserved or not preserved
948 at all, (2) there is increased uncertainty regarding boundary conditions such as tectonic
949 setting and climate regime, (3) of the diminishing resolution of existing chronological
950 tools, and (4) of the completeness of the stratigraphic record ([Romans and Graham,](#)
951 [2013](#)).

952 Reading the sedimentary record in deep time also requires understanding forcings
953 with long periods. The maximum response times resolvable for erosional and
954 depositional processes in most sedimentary systems is commonly $\sim 10^6$ yr (e.g., [Paola et](#)
955 [al., 1992](#); [Whipple, 2001](#); [Castelltort and Van Den Driessche, 2003](#); [Allen, 2008b](#)). Thus,
956 tectonic and climatic signals with periods of at least several millions of years could
957 induce a measureable equilibrium response of the Earth's surface that is potentially
958 recorded in stratigraphic successions. In other words, long-period stratigraphic archives

959 have more immunity to the internally generated dynamics that plague intermediate
960 timescales. Examples of long-period forcings include the development of orogens and
961 their coupled sedimentary basins ([Dickinson, 1974](#); [DeCelles et al., 2009](#)), Phanerozoic
962 changes of Earth's sea level (e.g., [Miller et al., 2005](#)), and significant shifts in global
963 climate such as the transition from Cretaceous-Eocene greenhouse to Oligocene-present
964 icehouse conditions (e.g., [Zachos et al., 2008](#)).

965 When peering back even further in time ($\geq 10^8$ yr) we lose details about the
966 fundamental boundary conditions of tectonic setting and environmental conditions that
967 are explicitly known for the modern or reliably reconstructed for historical to
968 intermediate timescales. Thus, in many cases, reconstructing those boundary conditions is
969 the primary goal of sedimentary analysis. Linking strata of such old ages to sediment
970 source areas is challenging as a result of major tectonic regime changes (e.g., closing and
971 opening of ocean basins; [Wilson, 1966](#)), poorly understood oceanic and atmospheric
972 conditions, and non-actualistic Earth processes.

973 Our ability to reconstruct deep-time Earth surface conditions is based on rock
974 availability: preserved as intact depositional architecture and/or detrital material
975 representative of long-gone source areas. The following sections briefly review
976 methodologies for characterizing the unpreserved sediment-production zones of ancient
977 systems and potential value for interpreting Qs signal propagation.

978

979 4.2 *Inferring Catchment Characteristics and Sediment Supply From Stratigraphic*
980 *Architecture*

981 Erosion and transfer zones are inherently not preserved in deep time and thus we must
982 rely on preserved stratigraphy to reconstruct their characteristics. In this section we
983 briefly review methods for estimating catchment area from stratigraphic architecture.

984 The dimensions of modern river channels scale to flood, or bankfull, discharge
985 ([Bridge and Demicco, 2008](#); and references therein), which affords estimation of water
986 discharge from preserved fluvial channel stratigraphic architecture (e.g., [Bridge and Tye,](#)
987 [2000](#); [Bhattacharya and Tye, 2004](#); [Adams and Bhattacharya, 2005](#); [Blum et al., 2013](#);
988 [Bhattacharya et al., this volume](#)). Analyses of modern river systems demonstrate a
989 relationship between water discharge and catchment area (e.g., [Hack, 1957](#); [Rodier and](#)
990 [Roche, 1984](#); [Matthai, 1990](#)) and a global empirical model shows that catchment area and
991 relief are first-order controls on sediment supply (BQART model of [Syvitski and](#)
992 [Milliman, 2007](#)). These relationships suggest that an estimate of paleo-catchment area
993 can be determined from stratigraphy with the proviso that the channelized strata
994 measured are truly representative of the alluvial system (see [Blum et al., 2013](#) and
995 [Bhattacharya et al., this volume](#) for discussion of river channel and alluvial valley scaling
996 with respect to sediment delivery dynamics). However, discharge-to-area relationships as
997 well as sediment load-to-area relationships from modern rivers are shown to vary as a
998 function of precipitation and runoff patterns, vegetation, soil type, and geology (e.g.,
999 [Milliman and Farnsworth, 2011](#); [Covault et al., 2013](#) and references therein). Regional
1000 hydraulic curves, which capture such characteristics from modern systems (e.g., [Leopold](#)
1001 [and Maddock, 1953](#)), can be used to further constrain the estimate of catchment area if

1002 some aspects of the paleoclimate can be determined. [Davidson and North \(2009\)](#) provide
1003 a comprehensive discussion of the values and limitations of the regional hydraulic curve
1004 approach, including example applications from the deep-time rock record.

1005 Sediment yield can be approximated with the regional hydraulic curve approach,
1006 providing insight about the paleo-sedimentary system. In practice, however, the
1007 calculation of any mass supply is only as accurate as the chronologic control available;
1008 mass supply averaged over $>10^6$ yr will obviously not capture shorter-period fluctuations.
1009 Furthermore, such paleo-hydrologic methods are burdened with uncertainties that are
1010 challenging to quantify, which limits accuracy to an order of magnitude ([Holbrook and](#)
1011 [Wanas, 2014](#)). These methods are also susceptible to aliasing the record of Qs. For
1012 example, a single, static paleogeographic reconstruction might be used to inform paleo-
1013 hydrology over a large duration of geologic time, which provides average Qs during that
1014 time. However, geologic evolution, and especially Qs, is dynamic and influenced by the
1015 extreme events. Some applications can be satisfactorily addressed with order-of-
1016 magnitude estimates, such as the selection of modern analogs for ancient systems
1017 ([Bhattacharya and Tye, 2004](#); [Bhattacharya et al., this volume](#)). How to better link paleo-
1018 catchment reconstructions with interpretations of signal propagation remains a challenge.
1019 Ultimately, because these methods incorporate information from modern systems, the
1020 reliance on an actualistic approach should be acknowledged.

1021

1022 4.3 *Source Area Signals From Detrital Material Analysis*

1023 Another approach to reconstruct aspects of the erosion zone of deep-time
1024 sediment-routing systems is to characterize the detrital material that is preserved in

1025 sedimentary rocks. Provenance analyses focused on detrital products released from the
1026 erosion zone has long been used to reconstruct and interpret deep-time paleo-drainage
1027 systems and their relationship to tectonic forcings ([Dickinson, 1974](#); [Graham et al., 1986](#);
1028 [McLennan et al., 1983](#); among many others). More recently, radioisotope provenance
1029 studies have been employed to detect sediment supply signals in deep time by identifying
1030 source terranes (Fig. 9) and tracking their evolution through a basin fill (e.g., [Dickinson](#)
1031 [and Gehrels, 2003](#); [Weislogel et al., 2006](#); [Romans et al., 2010](#); [Carrapa, 2010](#); [Blum and](#)
1032 [Pecha, 2014 and references therein](#)). The common pre-conditions for application of such
1033 methods are related to specific characteristic of the source areas, which should be
1034 composed of rocks with different tectonic histories, distinctive crystallization and cooling
1035 ages, and the presence of the unique mineral(s) ([Lawton, 2014](#)).

1036 Combining different thermochronometers on single detrital mineral grains such as
1037 zircon, monazite, white mica, and apatite can be used to determine cooling ages
1038 associated with different closure temperatures (depths) with which to reconstruct tectono-
1039 thermal events ([Rahl et al., 2003](#); [Carrapa et al., 2003](#); [Carrapa, 2010](#); [Lawton, 2014](#)).
1040 This has potential application for the interpretation of the propagation of a tectonic signal
1041 across a paleo-landscape by constraining separate events (e.g., crystallization and
1042 cooling) of a single grain such that durations and rates can be determined. These methods
1043 provide rates for mountain belt emplacement and exhumation, helping to refine timing
1044 and magnitude of tectonic processes.

1045 For example, when zircon U-Pb crystallization ages are coupled with zircon (U-
1046 Th)/He exhumation ages, apatite fission-track (AFT), and/or apatite (U-Th)/He methods,
1047 we gain critical insight into the timing of rock cooling, inferred exhumation, lag times

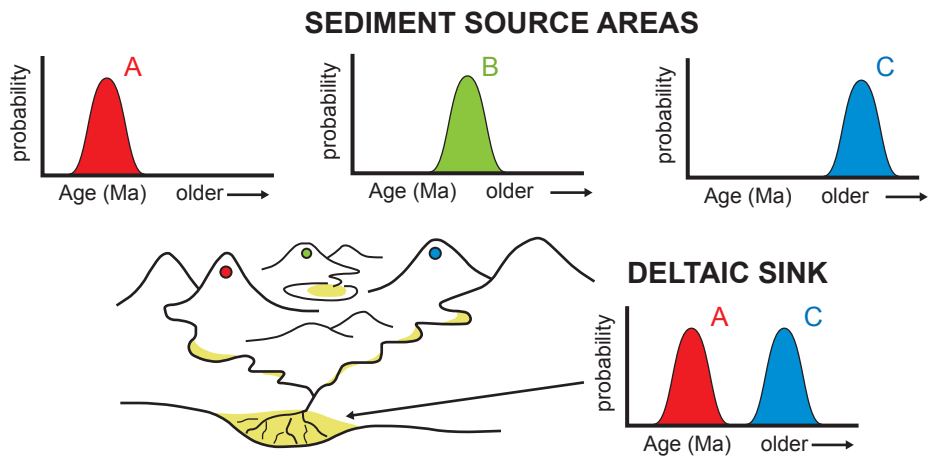


Figure 9: Conceptual diagram of crystallization age of detrital minerals (e.g., zircon U-Pb geochronology) as indicator of sediment-routing system connectivity, which can be used to aid reconstruction of sediment supply history from deep-time stratigraphic archives.

Romans et al. -- Figure 9

1048 between different closure temperature depths, as well as lag times between cooling and
1049 deposition (Fig. 10) (e.g., [Rahl et al., 2003](#); [Reiners and Brandon, 2006](#); [Painter et al.,](#)
1050 [2014](#)). Lag time was originally defined as the difference between the cooling age of a
1051 detrital mineral and the depositional age of its host strata ([Brandon and Vance, 1992](#);
1052 [Garver et al., 1999](#)). According to theoretical modeling, the variability in cooling age-
1053 depositional age lag times through a stratigraphic succession could be used to infer
1054 changing erosion rates in an orogenic belt ([Rahl et al., 2007](#)), which is a potentially
1055 powerful tool to estimate Q_s in deep time (Fig. 10). Most of these studies focus on
1056 synorogenic basins with inferred short transfer zones and correspondingly short duration
1057 of transient storage in order to interpret orogenic signals. Minerals yielded by distinct
1058 source regions could display overlapping crystallization ages related to different volcanic
1059 events but virtually undistinguishable if using a U-Pb dating technique (e.g., [Saylor et al.,](#)
1060 [2012](#)). Coupling these ages with (U-Th)/He ages can help distinguish older exhumed
1061 regions from younger, especially within the context of the omnipresent Grenville U-Pb
1062 age populations of the Appalachian orogenic belt ([Rahl et al., 2003](#)).

1063 Tectonic and/or sedimentary burial can reset thermochronometers, complicating a
1064 simple exhumation to erosion relationship. In some cases, however, orogenic recycling
1065 can be constrained by integrating double dating with time-temperature modeling of burial
1066 history ([Fosdick et al., 2014](#)). These techniques will continue to be used to reconstruct
1067 paleo-drainage system connectivity and evolution, which will help track changes in
1068 sediment supply over $\geq 10^7$ yr timescales ([Carrapa et al., 2003](#)).

1069

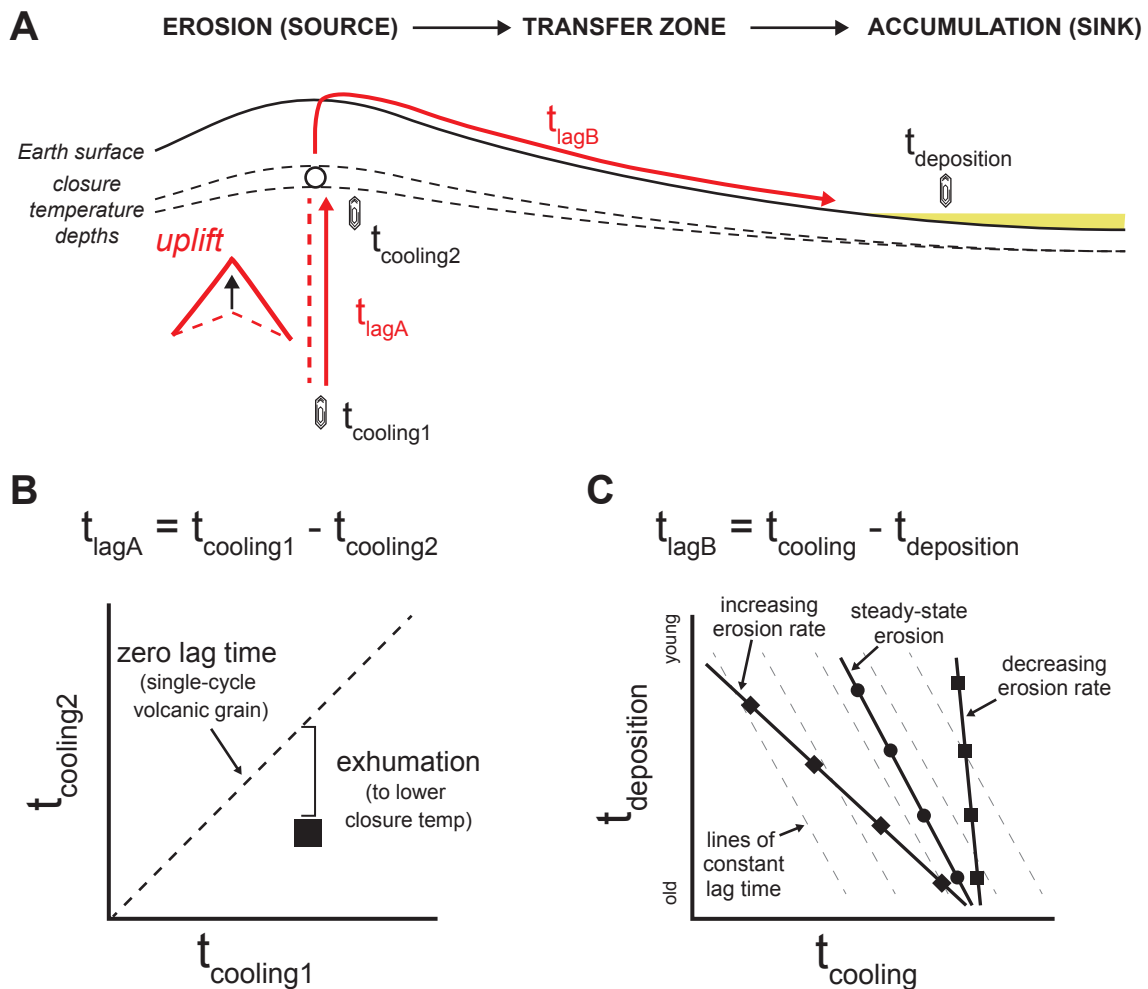


Figure 10: Conceptual diagrams of two different types of lag times to be calculated with combinations of cooling ages and depositional age. (A) Schematic cross section depicting trajectory of a particle through cooling via erosional exhumation followed by transport and deposition. (B) Lag time type A is the difference between higher-temperature cooling age (e.g., crystallization age) and lower-temperature cooling age of a single grain (e.g., zircon) and represents exhumation from depth. (C) Lag time type B is the difference between a cooling age and depositional age and represents the time from closure temperature depth to surface exhumation plus transport (and transient storage) in the sediment-routing system prior to deposition (adapted from Rahl et al., 2007). A consistent Lag time type B calculated through a stratigraphic succession indicates steady erosion whereas departures from that indicate changing erosion rates through time. Note that time within partial annealing/retention zones as well as sedimentary and/or tectonic burial can complicate simple lag time determinations.

Romans et al. -- Figure 10

1070 4.4 *Sedimentary System Mass Balance in Deep Time*

1071 As reviewed in preceding sections, a full accounting of mass supply (and storage)
1072 among erosion, transfer, and accumulation zones of a sediment-routing system can aid
1073 interpretation of signal propagation. For example, transient storage of sediment in
1074 floodplains and coastal plain segments at intermediate timescales can buffer the
1075 transmission of Milankovitch-controlled supply entering the sink (Fig. 6C). These same
1076 concepts can be applied to deep-time systems, but with the significant challenges that
1077 erosion/transfer zones are typically not morphologically preserved and chronology is
1078 more poorly resolved.

1079 Despite these uncertainties, theory and methodologies have been and are being
1080 developed with the goal of characterizing mass-balance in ancient systems. [Paola and](#)
1081 [Martin \(2012\)](#) built on previous work of [Paola and Voller \(2005\)](#) and [Strong et al. \(2005\)](#)
1082 to apply mass-balance concepts to quantitative characterization of sedimentary basin fills.
1083 This and similar studies (e.g., [Whittaker et al., 2011](#); [Carvajal and Steel, 2012](#); [Petter et](#)
1084 [al. 2013](#)) aim to improve the estimation of Q_s from time-averaged stratigraphy. [Sadler](#)
1085 [and Jerolmack \(2014\)](#) point out that well-documented 1D measurement-interval effects
1086 on rates of denudation (e.g., [Gardner et al., 1987](#)) and accumulation (e.g., [Sadler, 1981](#))
1087 are eliminated with full spatial averaging because sediment generation and deposition
1088 must balance. Closing the sediment budget for an ancient system by accounting for all
1089 inputs and outputs is challenging ([Hinderer, 2012](#); [Allen et al., 2013](#)). However, [Sadler](#)
1090 [and Jerolmack \(2014\)](#) make the case that avoiding linear rate measurements (i.e.,
1091 maximizing volumetric analysis) and avoiding rates of any kind derived from the transfer
1092 zone can significantly minimize the measurement-interval bias.

1093 In the same context as box models or other budget diagrams (e.g., [Walling and](#)
1094 [Collins, 2008](#)), [Hay et al. \(1989\)](#) developed a method for generating mass-balanced
1095 paleogeographic maps. These maps aim to depict the source-to-sink redistribution of
1096 mass through time by tracking paleotopographic evolution at $\geq 10^7$ yr timescales.
1097 Similarly, recent efforts by [Meyers and Peters \(2011\)](#) aim to reconstruct stratigraphic
1098 volume and mass distribution through time in relation to long-period ($\geq 10^7$ yr) tectonic
1099 and/or sea-level cycles. The utility of such methods to signal propagation has yet to be
1100 explicitly addressed. Following [Allen et al. \(2013\)](#), wherein the challenge of estimating
1101 sediment supply from strata is termed ‘The Qs problem’, [Michael et al. \(2013\)](#) determine
1102 a sediment budget for Late Eocene (~42-34 Ma) foreland basin strata and use resultant
1103 grain-size partitioning information to reconstruct tectonic subsidence.

1104 The tectonically active region of southern Asia includes high rates of denudation
1105 and mass redistribution, making it an ideal locale to develop longer-term sediment budget
1106 concepts. [Johnson \(1994\)](#) accounted for the volume of sediment deposited in foreland
1107 basins, deltas, and the Indus and Bengal submarine fans forward of the Himalayas to
1108 explore Cenozoic sediment-routing evolution and its relationship to uplift and
1109 exhumation. Using information from literature, [Johnson \(1994\)](#) calculated that the
1110 Himalayan Main Central Thrust, which is interpreted to have been emplaced ~20 Ma, to
1111 be of insufficient volume to balance the depositional systems. Thus, [Johnson \(1994\)](#)
1112 posited that regions outside the Himalaya, including Tibet and the Karakoram, might
1113 have been significant sediment source areas during the Cenozoic, especially prior to the
1114 emplacement of the Himalayan Main Central Thrust.

1115 [Clift et al. \(2001\)](#) used a seismic stratigraphic interpretation to account for the
1116 Cenozoic deposition of the Indus Fan. The erosional record on land was constrained from
1117 provenance analysis using Pb and Nd isotopic compositions and published
1118 thermochronology. Cenozoic land-to-deep sea Indus sediment routing shows a balance of
1119 erosion and deposition, with a greater volume of eroded rock during the Neogene, and
1120 corresponding greater deposition on the Indus submarine fan during the Neogene.
1121 However, the Paleogene was characterized by rapid erosion and coupled accumulation,
1122 with deposition focused in the regions of the Katawaz Basin, the Makran accretionary
1123 wedge, and the Indus foreland. More recently, [Clift et al. \(2008\)](#) compared published
1124 thermochronology from the Himalaya to weathering and climate proxies recorded in
1125 Neogene deposits from the South China Sea, Bay of Bengal, and Arabian Sea. Erosion of
1126 the Himalaya was interpreted to have intensified ~23-10 Ma, and slowed to ~3.5 Ma, but
1127 then began to increase during the Late Pliocene and Pleistocene, which correlates with
1128 monsoon intensity interpreted from climate proxies ([Clift et al., 2008](#)).

1129 In these studies of sediment budgets of Cenozoic sediment routing systems, the
1130 detrital record provides insights into sediment routing evolution, as an indicator of Q_s
1131 variability, and insights into the tectonic and climatic controls on erosion and deposition.
1132 Similar to the use of modern systems to guide the interpretation of transport and
1133 depositional processes from preserved strata, we can use historical-timescale (Figs. 3 and
1134 4) and intermediate-timescale (Fig. 6) sediment-routing systems as analogs of signal-
1135 propagation dynamics for deep-time systems. Studies of Cenozoic systems are of
1136 particular value to better understand deep-time signal propagation because they combine
1137 long-period forcings with relatively well-documented boundary conditions that pre-

1138 Cretaceous systems lack as a result of tectonic reorganization (Romans and Graham,
1139 2013).

1140

1141 **5 Discussion and Research Directions**

1142 External forcings are initially transformed into an Earth-surface signal through the
1143 production of mobile mass that is then redistributed down system as detritus and solutes
1144 (Fig. 1) (Allen et al., 2013). The character of that signal and to what extent a signal is
1145 preserved in sedimentary records are dependent on the magnitude and frequency of the
1146 initial forcing (Fig. 8), on their initial recording or destruction (Wheatcroft et al., 2007),
1147 on the responses of the different segments of the sediment-routing system (Castelltort and
1148 Van Den Driessche, 2003), on their morphology (e.g., for instance promoting buffered
1149 versus reactive sediment and signal transfer) (Covault et al., 2011), and on the ratio of
1150 signal to noise, in particular with respect to autogenic dynamics (Jerolmack and Paola,
1151 2010). In this review, we emphasized the importance of sediment supply (Qs) as the main
1152 carrier of signals that originate in erosion zones. Thus, approaches for determining Qs by
1153 direct observation and measurement (Figs. 3 and 4), calculation from measurement of
1154 related process (e.g., denudation via cosmogenic radionuclides; Fig. 6), or estimation
1155 from stratigraphy and/or detrital minerals (Figs. 9 and 10) that are reviewed in this paper
1156 are critical to understanding how those signals are transmitted through the system.
1157 Furthermore, the development of new computational techniques for numerical modeling
1158 of source-to-sink sediment transport and deposition promise a deeper understanding of
1159 sediment and signal propagation. The benefit of unravelling processes of sediment and
1160 signal propagation is an enhanced understanding of the coupling of Earth surface systems

1161 and improved capability to invert stratigraphic and geomorphic records that relate to
1162 broader Earth dynamics.

1163 The investigation of signal propagation requires a systems approach, which is
1164 provided by the sediment-routing system, or source-to-sink, framework (Allen, 2008a)
1165 (Fig. 1). The concept of sediment mass balance is embedded within such a framework
1166 and variations in system morphology provide insight into signal propagation and
1167 preservation. We emphasized the importance of the transfer zone (Fig. 1) because of its
1168 potential role as a ‘buffer’ (e.g., along-system diffusion and temporary floodplain
1169 deposition) and, correspondingly, the effect on rates and magnitudes of Q_s carried to
1170 down-system segments. Such transfer-zone buffering of up-system signals is highly
1171 relevant to decoding the meaning of coastal and marine stratigraphic archives (Figs. 4 and
1172 6). The transfer-zone concept at historical timescales ($<10^2$ yr) is elusive because
1173 sediment storage can occur across the entire system, including in the erosion zone,
1174 leading to potential buffering over short distances. Reconstructing erosion and transfer
1175 zones in deep time ($\geq 10^7$ yr) is challenging as a result of incomplete or no preservation of
1176 these sediment-routing segments. Characteristics of deep-time sediment production and
1177 transfer areas can be interpreted by employing provenance tools, detrital mineral analysis,
1178 or application of empirical relationships based on modern systems, and tested with
1179 conceptual, analytical, and numerical models.

1180 Implications of signal detection over noise are of paramount importance to
1181 interpreting the stratigraphic record of Q_s variability. Internal, or autogenic, dynamics of
1182 sediment transport, transient storage, and release can introduce noise, lags, and/or
1183 completely mask the signal of interest. Experimental and theoretical work has shown that

1184 a Qs signal can be passed to a basin and preserved in the stratigraphic record when its
1185 period is similar to or exceeds the characteristic response time of the sediment-routing
1186 system, but this is valid only if their periods or magnitudes are also larger than the
1187 characteristic timescale of autogenic sediment transport fluctuations (Jerolmack and
1188 Paola, 2010). Moreover, autogenic ‘shredding’ is potentially more significant if the
1189 length scale of interest, e.g., the system size, is larger than the advection length scale of a
1190 particle of sediment (Ganti et al., 2014). Field studies focused on the coarse-grained
1191 sediment fraction in small, tectonically active sediment-routing systems of southern
1192 California (Fig. 6A) have shown that millennial-scale climate forcings are represented as
1193 a measureable signal in the stratigraphic record of the deep-sea segment (Fig. 7) (Romans
1194 et al., 2009; Covault et al., 2010). These systems are reactive (*sensu* Allen, 2008b) and
1195 comprise sediment-routing segments in close proximity: erosion zones are located
1196 adjacent to short transfer zones and offshore confined basins that make up the
1197 accumulation zone. Noise over historical timescales can be especially problematic as the
1198 observational window is small and the number of signals potentially large (e.g.,
1199 Sommerfield and Wheatcroft, 2007).

1200 Timescale of observation is fundamentally important for signal analysis in
1201 sedimentary systems. Temporal aspects discussed in this review include the duration and
1202 period of forcings, the resolution of chronologic tools with which to evaluate Qs (Fig. 2),
1203 and preservation into the record. At historical timescales the signal of interest is
1204 commonly an individual event, such as an earthquake, flood, or storm. At longer
1205 timescales, shifts in the rate and style of sedimentation in the cumulative record can be
1206 related to longer-period forcings. We devoted much of our treatment of signal

1207 propagation at the intermediate timescale (10^2 - 10^6 yr) because we consider this to be a
1208 critical temporal range in which to understand these dynamics at the scale of entire
1209 sediment-routing systems. The shorter-duration end of this range can be linked to direct
1210 observation and measurement and the longer, million-year end of this range can serve as
1211 a bridge to deep time. The intermediate timescale is the timescale of global climate cycles
1212 and the timescale at which climate and tectonic forcings overlap. Moreover, this is the
1213 timescale at which meso-scale stratigraphic architecture and high-frequency stratigraphic
1214 cycles are created. Our subdivision of timescales in this review is only to aid
1215 communication of dominant aspects within each timescale, but we emphasize that
1216 sedimentary system research strives to integrate across these timescales.

1217 Our review emphasizes the role of sediment supply, yet we acknowledge the role of
1218 accommodation fluctuations in the accumulation zone as an important forcing of
1219 stratigraphic patterns (e.g., [Anderson et al., this volume](#)). Deciphering the relative
1220 contributions of sediment supply versus accommodation changes to the creation of
1221 stratigraphy has been discussed for at least a century (e.g., [Grabau, 1913](#); [Barrell, 1917](#))
1222 and examined via modeling studies for decades (e.g., [Jervy, 1988](#); [Allen and Densmore,](#)
1223 [2000](#); [Paola, 2000](#); [Armitage et al., 2013](#)). The nature of signal generation in the sink and
1224 potential up-system propagation effects (e.g., [Voller et al., 2012](#)) deserve further
1225 attention. Deconvolving the various external forcings from each other and from the
1226 products of internal dynamics encoded in the geologic record remains a prime challenge
1227 in Earth science ([National Research Council, 2010](#)).

1228 This review provides a set of conceptual and practical tools for reaching informed
1229 interpretations of landscape dynamics from the stratigraphic record. These tools include

1230 stratigraphic and sediment-routing system characterization, sediment budget
1231 determination, geochronology, detrital mineral analysis (e.g., thermochronology),
1232 comparative analog approaches, and modeling techniques to measure, calculate, or
1233 estimate the magnitude and frequency of sediment supply signals compared to the
1234 characteristic response time of the sediment-routing systems. However, significant
1235 research challenges remain, which we distill into four research directions:

1236

1237 **1. Improved documentation of sediment production, transfer, and**
1238 **accumulation rates in natural systems.** The propagation of a signal through a
1239 system can be characterized as a phase velocity and, thus, knowledge of time is
1240 required. Research aimed at developing new chronometric techniques and studies
1241 applying existing techniques in novel ways should continue to be a focus in Earth
1242 surface dynamics research. Such work should include the study of and linkage
1243 between erosion, transfer, and accumulation zones across a spectrum of system
1244 sizes and morphologies as well as across a range of timescales. Within this
1245 context, the question of to what degree patterns of stratigraphy (i.e., patterns
1246 documented in the absence of absolute chronology) reflect process rates should be
1247 further explored.

1248

1249 **2. Grain-size partitioning and signal propagation.** What is the size distribution of
1250 sediments exiting the erosion zone as a function of forcings? Our discussion of
1251 how sediment supply signals propagate through a system and how they might be
1252 preserved in the stratigraphic record is simplistic in that only bulk mass balance is

1253 considered. The variability in transit distances of different grain-size classes for a
1254 given forcing might result in the fractionation of catchment-generated signals with
1255 certain grain-sizes temporarily stored along the transfer zone. Attempts to capture
1256 downstream grain-size fining and to invert it to time-averaged grain-size trends in
1257 stratigraphy are promising but still in their embryonic stage (e.g., [Whittaker et al.,](#)
1258 [2011](#); [Michael et al., 2013](#)). The link between forcings in the erosion zone and the
1259 probability density function of the produced grain-size distribution remains a
1260 major unknown and constitutes a fundamental input of Qs propagation models at
1261 all temporal and spatial scales.

1262

1263 **3. Integration of experimental and modeling approaches with natural systems.**

1264 Many of the modeling efforts reviewed here are based on diffusion assumptions
1265 and/or empirical relationships, neither of which truly model sediment transport.
1266 Several approaches are currently tackling sediment transfer more explicitly,
1267 including using increasingly complete physics of water flow and sediment
1268 transport (e.g., Delft3D, broadly labelled Computational Fluid Dynamics, e.g.,
1269 [Lesser et al., 2004](#)); Reduced Complexity Models (such as cellular automata, e.g.
1270 [Murray and Paola, 1997](#); [Liang et al., 2014](#)); and several other modeling
1271 approaches as part of CSDMS (Community Surface Dynamics Modeling System)
1272 ([Syvitski, 2008](#)). These efforts are complementary and promising, but it is
1273 important to maintain a link with natural systems in order to properly assess the
1274 appropriate degree of complexity for which model predictions can be compared to
1275 data from natural systems. Additionally, scaled-down physical experiments are

1276 contributing valuable insights regarding the timescales of dynamics in
1277 depositional landscapes (e.g., autogenic channel avulsion frequency; Paola et al.,
1278 2009). However, how such timescales relate to natural-system timescales remains
1279 an open question. These experimental approaches must continue to strive to
1280 integrate with observation/measurement-based approaches and vice versa.

1281

1282 **4. Integration of particulate transfer dynamics with solute transfer and other**
1283 **geochemical signals.** The denudation of landscapes in erosion zones is the sum of
1284 physical and chemical products that are moved down system. Sedimentary
1285 archives containing chemical precipitates can be reliable recorders continental
1286 weathering as well as atmospheric and oceanic chemistry and have been used to
1287 detect climatic and/or oceanographic signals. However, studies that integrate
1288 geochemical signal analysis with the concepts and tools for signal propagation as
1289 a function of particulate transfer are rare. Additional work combining the
1290 particulate and (bio)geochemical perspectives to examine sedimentary system
1291 response to environmental change (e.g., Foreman et al., 2013) are necessary to
1292 develop a comprehensive understanding of the broader Earth surface system.

1293

1294 **Acknowledgements**

1295 This review of signal propagation concepts in sedimentary system analysis is
1296 purposefully broad in scope and, as a consequence, neither provides a comprehensive
1297 treatment of every relevant issue nor does it refer to all studies that have contributed. We
1298 hope that readers appreciate the challenge of preparing such a review. BWR, JAC, and

1299 AF would like to acknowledge Steve Graham, George Hilley, and Bill Normark for their
1300 mentorship and intellectual guidance. JAC acknowledges intellectual support from
1301 Chevron Energy Technology Company scientists Cristian Carvajal, Ashley Harris, Kristy
1302 Milliken, Marty Perlmutter, Michael Pyrcz, and Tao Sun. AF would like to thank Angela
1303 Hessler and Sam Johnstone for long discussions on deep time. SC acknowledges funding
1304 by the Swiss National Science Foundation grant 200021_146822 and inspiring discussion
1305 with Guy Simpson, Philip Allen, Jean Van Den Driessche, Sean Willett, Philippe Davy
1306 and François Guillocheau. Support for JPW was provided by the National Science
1307 Foundation, Marine Geology & Geophysics Program (OCE-0841092), and JPW
1308 acknowledges research colleagues for their hard work and valuable insights into signal
1309 propagation.

1310

1311 **Figure Captions**

1312

1313 **Figure 1:** (A) Schematic portrayal of a sediment supply (Q_s) signal from the erosion zone
1314 and how that signal propagates through the system. The leftmost Q_s signal represents as
1315 measured at the exit of the erosion zone and for simplicity is the same as the original
1316 forcing of interest. The transfer zone Q_s signal is measured within the transfer zone at
1317 some distance from exit of erosion zone and the rightmost signal represents that which
1318 reaches the accumulation zone and is an input for the stratigraphic record. Dashed lines
1319 refer to Q_s signal in up-system segment(s) to illustrate that a signal can be modified
1320 during propagation. (B) 2-D profile of a generic sediment-routing system emphasizing
1321 erosion, transfer, and accumulation zones (potential for intermediate to deep time

1322 stratigraphic preservation in yellow) and important controls of tectonics (including
1323 earthquakes), climate (including storms), base level, and anthropogenic factors. Part B
1324 modified from [Castelltort and Van Den Driessche \(2003\)](#).

1325

1326 **Figure 2:** Overview of three timescales of investigation, some of the chronometric tools
1327 with which to constrain process rates, and periods of some of the forcings discussed in
1328 this review. Dashed lines at the top emphasize the continuum among the timescales.
1329 Temporal range of ‘orogenic cycles’ from [DeCelles et al. \(2009\)](#). Effective dating range
1330 of chronometric tools from [Walker \(2005\)](#).

1331 **Figure 3:** (A) Topography and drainage network of Eel and Mad river catchments,
1332 northern California, and bathymetry of the continental margin. Red star denotes location
1333 of shelf core x-radiograph shown in (B). (B) X-ray image of shelf reflects bulk density.
1334 Light colors (lower bulk density) interpreted as 1995 flood deposit ([Sommerfield and](#)
1335 [Nittrouer, 1999](#); [Wheatcroft and Borgeld, 2000](#)). (C) Map of Eel-Mad sediment-routing
1336 system showing catchment area, areal extent of coastal floodplain, and shelf depocenter
1337 (yellow). Red star denotes location of shelf core image shown in (B). (D) Historical
1338 timescale sediment budget of the Eel-Mad sediment-routing system showing: 1) there is
1339 negligible onshore storage, 2) the shelf stores ~30-50% of the budget, and 3) the
1340 remainder moves to the canyon and continental slope. Budget estimations from
1341 [Sommerfield and Nittrouer \(1999\)](#) and [Warrick \(2014\)](#).

1342 **Figure 4:** (A) Topography and drainage network of Ganges, Brahmaputra, and Meghna
1343 rivers and bathymetry of shelf, Swatch of No Ground submarine canyon, and part of the

1344 Bengal submarine fan system. Red star denotes location of core record shown in (B). (B)
1345 Core from upper canyon showing variation in mean grain size with time compared to
1346 storm record from eastern Bengal shelf. Data is from core 96 KL as reported in [Michels](#)
1347 [et al. \(2003\)](#). (C) Map of Ganges-Brahmaputra-Bengal sediment-routing system showing
1348 catchment area, the large delta plain area, shelf depocenter (yellow) and the Bengal
1349 submarine channel-levee system. Red star denotes location of core record shown in (B).
1350 (D) Historical timescale sediment budget of Ganges-Brahmaputra-Bengal sediment-
1351 routing system showing that almost one-third of the budget is stored on the delta plain,
1352 ~40% accumulates in the shelf depocenter, split between the topset and foreset regions,
1353 and the remaining ~30% is delivered to the canyon and Bengal submarine fan. Budget
1354 estimations from [Kuehl et al. \(2005\)](#) and references therein.

1355

1356 **Figure 5:** The ratio between the timescale of a perturbation (T_p) and the characteristic
1357 equilibrium timescale (τ) of the considered system describes the system response to
1358 forcing (after [Beaumont et al., 2000](#); see also [Allen, 2008b](#)). A forcing of water discharge
1359 (Q_w) and a response of sediment supply (Q_s) are shown for (A) a reactive response when
1360 response time is much shorter than timescale of forcing and (B) a buffered response when
1361 response time is longer than timescale of perturbation.

1362

1363 **Figure 6:** Examples of natural sediment routing systems examined at intermediate
1364 timescales. (A) Small and tectonically active system, Peninsular Ranges and Continental
1365 Borderland of southern California ([Covault et al., 2011](#)); (B) Large and tectonically
1366 quiescent system, Texas coastal plain and western Gulf of Mexico ([Hidy et al., 2014](#);

1367 [Pirmez et al., 2012](#)); (C) Large and tectonically active system, Indus River and Indus
1368 submarine fan ([Clift et al., 2014](#)). Indus River floodplain extent from [Milliman et al.](#)
1369 [\(1984\)](#).

1370

1371 **Figure 7:** (A) Map showing two southern California sediment-routing systems, each with
1372 negligible onshore sediment storage at millennial timescales and correspondingly rapid
1373 transfer to offshore submarine fan systems. (B) Alkenone sea surface temperature (SST)
1374 proxy for the California coastal region showing a drying trend in the early Holocene
1375 followed by the development of the modern El Niño-Southern Oscillation (ENSO), which
1376 is known to be sensitive to increased SSTs ([Barron et al., 2003](#)). (C) Radiocarbon-
1377 constrained weighted-average sediment accumulation rates from Hueneme and Newport
1378 submarine fans ([Romans et al., 2009](#); [Covault et al., 2011](#)) showing a general correlation
1379 of sediment supply to the basin to precipitation regime and, thus, propagation of climatic
1380 signal to the stratigraphic record.

1381

1382 **Figure 8.** Summary of signal propagation from source to sink at intermediate timescales
1383 (10^2 - 10^6 yr). The figure considers uplift and climate signals in the erosion zone and their
1384 transformation and propagation into sediment supply (Q_s) signals in both the transfer and
1385 accumulation zones. The gray shaded regions indicate the cases in which the original
1386 forcing has been faithfully transmitted to the accumulation zone. (A) An uplift signal
1387 with a period (t) > 50 kyr is transformed into a Q_s signal with same amplitude and period
1388 by the erosion zone and transmitted by a short fluvial segment but buffered by a long
1389 transfer zone unless $t > 100$ kyr (e.g., [Castelltort and Van Den Driessche, 2003](#)). (B) An

1390 uplift signal with $t < 50$ kyr is transformed into a buffered Q_s signal by the diffusive
1391 catchment dynamics in the erosion zone (Allen and Densmore, 2000) and further
1392 buffered by diffusion in the transfer zone (e.g., Castelltort and Van Den Driessche, 2003).
1393 (C) A climate signal of water discharge (Q_w) with $t > 100$ kyr in the erosion zone yields a
1394 buffered Q_s response signal due to catchment dynamics (Armitage et al., 2013). (D) A
1395 climate signal of Q_w with $10 \text{ kyr} < t < 1 \text{ Myr}$ in the erosion zone yields an amplified Q_s
1396 response signal due to catchment dynamics (Godard et al., 2013). (E) Climate signal of
1397 Q_w with $t > 0$ kyr in erosion zone is transferred to the fluvial system where it is
1398 transformed into an amplified Q_s signal by river transport (Simpson and Castelltort,
1399 2012). (F) In the absence of signals coming from the erosion zone, autogenic signals can
1400 emerge out of the transfer zone due to the internal dynamics of the fluvial system (e.g.,
1401 compensational stacking in channelized systems, Hajek et al., 2010), with periodicities
1402 and amplitude poorly constrained. Wang et al. (2011) suggest autogenic periodicities of
1403 the order of 100 kyr for the Mississippi river delta. (G) Regardless of origin, Q_s signal
1404 input to the transfer zone may be ‘shredded’ by the internal dynamics of sediment
1405 transport system when their period and amplitude fall within the range of
1406 ‘morphodynamic turbulence’ (Jerolmack and Paola, 2010).

1407

1408 **Figure 9:** Conceptual diagram of crystallization age of detrital minerals (e.g., zircon U-
1409 Pb geochronology) as indicator of sediment-routing system connectivity, which can be
1410 used to aid reconstruction of sediment supply history from deep-time stratigraphic
1411 archives.

1412

1413 **Figure 10:** Conceptual diagrams of two different types of lag times to be calculated with
1414 combinations of cooling ages and depositional age. (A) Schematic cross section depicting
1415 trajectory of a particle through cooling via erosional exhumation followed by transport
1416 and deposition. (B) Lag time type A is the difference between higher-temperature cooling
1417 age (e.g., crystallization age) and lower-temperature cooling age of a single grain (e.g.,
1418 zircon) and represents exhumation from depth. (C) Lag time type B is the difference
1419 between a cooling age and depositional age and represents the time from closure
1420 temperature depth to surface exhumation plus transport (and transient storage) in the
1421 sediment-routing system prior to deposition (adapted from [Rahl et al., 2007](#)). A
1422 consistent Lag time type B calculated through a stratigraphic succession indicates steady
1423 erosion whereas departures from that indicate changing erosion rates through time. Note
1424 that time within partial annealing/retention zones as well as sedimentary and/or tectonic
1425 burial can complicate simple lag time determinations.

1426

1427 **References**

- 1428 Aalto, R., Maurice-Bourgoin, L., Dunne, T., Montgomery, D. R., Nittrouer, C. A., and Guyot, J.-
1429 L., 2003, Episodic sediment accumulation on Amazonian flood plains influenced by El
1430 Nino/Southern Oscillation: *Nature*, v. 425, no. 6957, p. 493-497.
- 1431 Adams, M.M. and Bhattacharya, J.P., 2005, No change in fluvial style across a sequence
1432 boundary, Cretaceous Blackhawk and Castlegate Formations of central Utah: *Journal of*
1433 *Sedimentary Research*, v., 75, p. 1038-1051.
- 1434 Allen, J. R. L., 1974, Reaction, relaxation and lag in natural sedimentary systems: *General*
1435 *principles, examples and lessons: Earth-Science Reviews*, v. 10, p. 263-342.
- 1436 Allen, P. A., and Densmore, A. L., 2000, Sediment supply from an uplifting fault block: *Basin*
1437 *Research*, v. 12, p. 367-380.
- 1438 Allen, P.A., 2008a, From landscapes into geological history: *Nature*, v. 451, p. 274-276.
- 1439 Allen, P.A., 2008b, Time scales of tectonic landscapes and their sediment routing systems:
1440 *Geological Society London, Special Publication 296*, p. 7-28.
- 1441 Allen, P.A., Armitage, J.J., Carter, A., Duller, R.A., Michael, N.A., Sinclair, H.D., Whitchurch,
1442 A.L., and Whittaker, A.C., 2013, The Qs problem: Sediment volumetric balance of
1443 proximal foreland basin systems: *Sedimentology*, v. 60, p. 102-130.
- 1444 Alexander, C.R. and Simoneau, A.M., 1999, Spatial variability in sedimentary processes on the
1445 Eel continental slope, *Marine Geology*: v. 154, p. 243-254.

- 1446 Allison, M.A., 1998, Historical changes in the Ganges-Brahmaputra delta front, *Journal of Coastal*
1447 *Research*, v.14, p.480–490.
- 1448 Allison, M.A., Kineke, G.C., Gordon, E.S., and Goñi, M.A., 2000, Development and reworking
1449 of a seasonal flood deposit on the inner continental shelf off the Atchafalaya River, *Cont.*
1450 *Shelf Res.*, v. 20, p. 2267-2294.
- 1451 Allison, M.A. and Kepple, E.B., 2001, Modern sediment supply to the lower delta plain of the
1452 Ganges–Brahmaputra River in Bangladesh, *Geo-Marine Letters*, v. 21, 66–74.
- 1453 Allison, M.A., Dellapenna, T.M., Gordon, E.S., Mitra, S., and Petsch, S.T., 2010, Impact of
1454 Hurricane Katrina (2005) on shelf organic carbon burial and deltaic evolution, *Geophys.*
1455 *Res. Lett.*, v. 37, p. - L21605.
- 1456 Allison, M.A., Demas, C.R., Ebersole, B.A., Kleiss, B.A., Little, C.D., Meselhe, E.A., Powell,
1457 N.J., Pratt, T.C., and Vosburg, B.M., 2012, A water and sediment budget for the lower
1458 Mississippi-Atchafalaya River in flood years 2008-2010: Implications for sediment
1459 discharge to the oceans and coastal restoration in Louisiana, *Journal of Hydrology*: v.
1460 432-433, p. 84-97.
- 1461 *Anderson, J.B., Wallace, D.J., Simms, A.R., Rodriguez, A.B., Weight, R.W.R., and Taha, Z.P.,*
1462 *this volume, Recycling sediments between source and sink during a eustatic cycle: Case*
1463 *study of late Quaternary northwestern Gulf of Mexico: Earth-Science Reviews, XXXXX.*
- 1464 Anthony, E.J. and Julian, M., 1999, Source-to-sink sediment transfers, environmental engineering
1465 and hazard mitigation in the steep Var River catchment, French Riviera, southeastern
1466 France: *Geomorphology*, v. 31, p. 337-354.
- 1467 Armitage, J.J., Duller, R.A., Whittaker, A.C., and Allen, P.A., 2011, Transformation of tectonic
1468 and climatic signals from source to sedimentary archive: *Nature Geoscience*, 4, 231-235.
- 1469 Armitage, J.J., Dunkley Jones, T., Duller, R.A., Whittaker, A.C., and Allen, P.A., 2013, Temporal
1470 buffering of climate-driven sediment flux cycles by transient catchment response: *Earth*
1471 *and Planetary Science Letters*, v. 369, p. 200-210.
- 1472 Aslan, A., Autin, W.J., and Blum, M.D., 2005, Causes of river avulsion: Insights from the late
1473 Holocene avulsion of the Mississippi River, USA: *Journal of Sedimentary Research*, v.
1474 75, p 650-664.
- 1475 Attal, M., Tucker, G., Whittaker, A.C., Cowie, P., and Roberts, G.P., 2008, Modeling fluvial
1476 incision and transient landscape evolution: Influence of dynamic channel adjustment:
1477 *Journal of Geophysical Research: Earth Surface*, 113.
- 1478 Atwater, B.F. and Hemphill-Haley, E., 1997, Recurrence intervals for great earthquakes of the
1479 past 3500 years at northeastern Willapa Bay, Washington: U.S. Geological Survey
1480 Professional Paper 1576, 108 p.
- 1481 Atwater, B.F., Carson, B., Griggs, G.B., Johnson, P., and Salmi, M.S., 2014, Rethinking turbidite
1482 paleoseismology along the Cascadia subduction zone, *Geology*: v. 42, p. 827-830.
- 1483 Barnes, P.M., Bostock, H.C., Neil, H.L., Strachan, L.J., and Gosling, M., 2013, A 2300-year
1484 paleoearthquake record of the southern alpine fault and Fiordland subduction zone, New
1485 Zealand, based on stacked turbidites, *Bulletin of the Seismological Society of America*:
1486 v. 103, p. 2424-2446.
- 1487 Barron, J.A., Huesser, L., Herbert, T., and Lyle, M., 2003, High-resolution climatic evolution of
1488 coastal northern California during the past 16,000 years: *Paleoceanography*, 18, 1020.
- 1489 Beerbower, J.R., 1964, Cyclothems and cyclic depositional mechanisms in alluvial plain
1490 sedimentation: Symposium on Cyclic Sedimentation, State Geological Survey of Kansas
1491 Bulletin 169, p. 31-42.
- 1492 Beaumont, C., Kooi, H., and Willett, S., 2000, Coupled tectonic-surface process models with
1493 applications to rifted margins and collisional orogens: In: Summerfield, M.A. (ed.),
1494 *Geomorphology and Global Tectonics*, Wiley, Chichester, pp. 29-55.
- 1495 Barrell, J., 1917, Rhythms and the measurements of geologic time: *Geological Society of*
1496 *America Bulletin*, v. 28, p. 745-904.

- 1497 Bhattacharya, J.P. and Tye, R.S., 2004, Searching for modern Ferron analogs and application to
1498 subsurface interpretation: Regional to wellbore analog for fluvial-deltaic reservoir
1499 modeling: Ferron Sandstone of Utah: AAPG Studies in Geology 50, p 39-57.
- 1500 **Bhattacharya, J.P., Copeland, P., Lawton, T.E., and Holbrook, J., this volume, Estimation of**
1501 **source area, river paleo-discharge, paleoslope, and sediment budgets of linked deep-time**
1502 **depositional systems and implications for hydrocarbon potential: Earth-Science Reviews,**
1503 **XXXXX.**
- 1504 Bierman, P. and Steig, E.J., 1996, Estimating rates of denudation using cosmogenic isotope
1505 abundances in sediment: Earth Surface Processes and Landforms, v. 21, p. 125-139.
- 1506 Blum, M., and Hattier-Womack, J., 2009, Climate change, sea-level change, and fluvial sediment
1507 supply to deepwater depositional systems: External Controls on Deepwater Depositional
1508 Systems: SEPM Special Publication 92, p. 15-39.
- 1509 Blum, M., Martin, J., Milliken, K., and Garvin, M., 2013, Paleovalley systems: Insights from
1510 Quaternary analogs and experiments: Earth-Science Reviews, v. 116, p. 128-169.
- 1511 Blum, M. and Pecha, M., 2014, Mid-Cretaceous to Paleocene North American drainage
1512 reorganization from detrital zircons: Geology, 10.1130/G35513.1.
- 1513 Boldt, K.V., Lane, P., Woodruff, J.D., and Donnelly, J.P., 2010, Calibrating a sedimentary record
1514 of overwash from Southeastern New England using modeled historic hurricane surges:
1515 Marine Geology, v. 275, p. 127-139.
- 1516 Bonnet, S., and Crave, A., 2003, Landscape response to climate change: Insights from
1517 experimental modeling and implications for tectonic versus climatic uplift of topography:
1518 Geology, v. 31, no. 2, p. 123-126.
- 1519 Bralower, T.J., Paull, C.K., and Mark Leckie, R., 1998, The Cretaceous-Tertiary boundary
1520 cocktail: Chicxulub impact triggers margin collapse and extensive sediment gravity
1521 flows, Geology, v. 26, p. 331-334.
- 1522 Brandon, M.T. and Vance, J.A., 1992, Tectonic evolution of the Cenozoic Olympic subduction
1523 complex, Washington State, as deduced from fission track ages for detrital zircons:
1524 American Journal of Science, v. 292, p. 565-636.
- 1525 Bridge, J.S. and Tye, R.S., 2000, Interpreting the dimensions of ancient fluvial channel bars,
1526 channels, and channel belts from wireline-logs and cores: American Association of
1527 Petroleum Geologists Bulletin, v. 84, p. 1205-1228.
- 1528 Bridge, J.S. and Demicco, R., 2008, Earth Surface Processes, Landforms, and Sediment Deposits:
1529 Cambridge University Press.
- 1530 Brown, W.M., III and Ritter, J.R., 1971, Sediment transport and turbidity in the Eel River basin,
1531 California, U.S. Geological Survey Water-Supply Paper 1986.
- 1532 Brown, E.T., Stallard, R.F., Larsen, M.C., Raisbeck, G.M., and Yio, F., 1995, Denudation rates
1533 determined from the accumulation of in situ-produced ¹⁰Be in the Luquillo experimental
1534 forest, Puerto Rico: Earth and Planetary Science Letters, v. 129 p. 193-202.
- 1535 Brush, G.S., 2001, Natural and Anthropogenic Changes in Chesapeake Bay During the Last 1000
1536 Years, Human and Ecological Risk Assessment: An International Journal: v. 7, p. 1283-
1537 1296.
- 1538 Burbank, D.W. and Anderson, R.S., 2011, Tectonic Geomorphology: John Wiley and Sons.
- 1539 Cacchione, D.A., Sternberg, R.W., and Ogston, A.S., 2006, Bottom instrumented tripods:
1540 History, applications, and impacts, Cont. Shelf Res.: v. 26, p. 2319-2334.
- 1541 Carrapa, B., Wijbrans, J., and Bertotti, G., 2003, Episodic exhumation in the Western Alps:
1542 Geology, v. 31, p. 601-604.
- 1543 Carrapa, B., 2010, Resolving tectonic problems by dating detrital minerals: Geology, v. 38, p.
1544 191-192.
- 1545 Carter, L., Milliman, J.D., Talling, P.J., Gavey, R., and Wynn, R.B., 2012, Near-synchronous and
1546 delayed initiation of long run-out submarine sediment flows from a record-breaking river
1547 flood, offshore Taiwan, Geophys. Res. Lett., v. 39, L12603, p. 1-5.

- 1548 Carvajal, C. and Steel, R., 2012, Source-to-sink sediment volumes within a tectono-stratigraphic
1549 model for a Laramide shelf-to-deep-water basin: Methods and results, in: *Tectonics of*
1550 *Sedimentary Basins: Recent Advances*, C. Busby and A. Azor (Eds.). John Wiley &
1551 Sons, Ltd, Chichester, UK, pp. 131-151.
- 1552 Castelltort, S. and Van Den Driessche, J., 2003, How plausible are high-frequency sediment
1553 supply-driven cycles in the stratigraphic record?: *Sedimentary Geology*, v. 157, p. 3-13.
- 1554 Clift, P., Shimizu, N., Layne, G., Blusztajn, J., Gaedicke, C., Schluter, H.-U., Clark, M., and
1555 Amjad, S., 2001, Development of the Indus Fan and its significance for the erosional
1556 history of the Western Himalaya and Karakoram: *Geological Society of America*
1557 *Bulletin*, v. 113, p. 1039-1051.
- 1558 Clift, P.D., Hodges, K.V., Heslop, D., Hannigan, R., Van Long, H., and Calves, G., 2008,
1559 Correlation of Himalayan exhumation rates and Asian monsoon: *Nature Geoscience*, v. 1,
1560 p. 875-880.
- 1561 Clift, P.D. and Giosan, L., 2014, Sediment fluxes and buffering in the post-glacial Indus Basin:
1562 *Basin Research*, v. 26, p. 369-386.
- 1563 Cooper, S.R., McGlothlin, S.K., Madritch, M., and Jones, D.L., 2004, Paleocological evidence
1564 of human impacts on the Neuse and Pamlico estuaries of North Carolina, USA, *Estuaries:*
1565 v. 27, p. 617-633.
- 1566 Corbett, D.R., Walsh, J.P., Harris, C.K., Ogston, A.S, and Orpin, A.R., 2014, Formation and
1567 preservation of sedimentary strata from coastal events: Insights from measurements and
1568 modeling: *Continental Shelf Research*, v. 86, p. 1-5.
- 1569 Covault, J.A., Normark, W.R., Romans, B.W., and Graham, S.A., 2007, Highstand fans in the
1570 California Borderland: The overlooked deep-water depositional system: *Geology*, v. 35,
1571 p. 783-786.
- 1572 Covault, J.A. and Graham, S.A., 2010, Submarine fans at all sea-level stands: Tectono-
1573 morphologic and climatic controls on terrigenous sediment delivery to the deep sea:
1574 *Geology*, v. 38, p. 939-942.
- 1575 Covault, J.A., Romans, B.W., Fildani, A., McGann, M., and Graham, S.A., 2010, Rapid climatic
1576 signal propagation from source to sink in a southern California sediment-routing system:
1577 *The Journal of Geology*, v. 118, p. 247-259.
- 1578 Covault, J.A., Romans, B.W., Graham, S.A., Fildani, A., and Hilley, G.E., 2011, Terrestrial
1579 source to deep-sea sink sediment budgets at high and low sea levels: Insights from
1580 tectonically active southern California: *Geology*, v. 39, p. 619-622.
- 1581 Covault, J.A., Craddock W., Romans, B.W., Fildani, A., and Gosai, M., 2013, Spatial and
1582 temporal variations in landscape evolution: Historic and longer-term sediment flux
1583 through global catchments: *The Journal of Geology*, v. 121, p. 35-56.
- 1584 Crutzen, P.J. and Stoermer, E.F., 2000, The Anthropocene. *Global Change Newsletter*, n. 41, p.
1585 17-18.
- 1586 Cundy, A.B., Croudace, I.W., Cearreta, A., and Irabien, M.J., 2003, Reconstructing historical
1587 trends in metal input in heavily-disturbed, contaminated estuaries: Studies from Bilbao,
1588 Southampton Water and Sicily, *Appl. Geochem.*: v. 18, p. 311-325.
- 1589 Curray, J.R., Emmel, F.J., and Moore, D.G., 2002, The Bengal Fan: Morphology, geometry,
1590 stratigraphy, history, and processes: *Marine and Petroleum Geology*, v. 19, p. 1191-1223.
- 1591 Curray, J.R., 2014, The Bengal Depositional System: From rift to orogeny, *Mar. Geol.*: v. 352, p.
1592 59-69.
- 1593 Dadson, S.J., Hovius, N., Chen, H., Dade, W.B., Lin, J., Hsu, M., Lin, C., Horng, M., Chen, T.,
1594 Milliman, J., and Stark, C.P., 2004, Earthquake-triggered increase in sediment delivery
1595 from an active mountain belt, *Geology*: v. 32, p. 733-736.
- 1596 Dail, M.B., Reide Corbett, D., and Walsh, J.P., 2007, Assessing the importance of tropical
1597 cyclones on continental margin sedimentation in the Mississippi delta region, *Cont. Shelf*
1598 *Res.*: v. 27, p. 1857-1874.

- 1599 Davidson, S.K. and North, C.P., 2009, Geomorphological regional curves for prediction of
1600 drainage area and screening modern analogues for rivers in the rock record: *Journal of*
1601 *Sedimentary Research*, v. 79, p. 773-792.
- 1602 Day Jr., J.W., Boesch, D.F., Clairain, E.J., Kemp, G.P., Laska, S.D., Mitsch, W.J., Orth, K.,
1603 Mashriqui, H., Reed, D.J., Shabman, L., Simenstad, C.A., Streever, B.J., Twilley, R.R.,
1604 Watson, C.C., Wells, J.T., and Whigham, D.F., 2007, Restoration of the Mississippi
1605 Delta: Lessons from Hurricanes Katrina and Rita, *Science*: v. 315, p. 1679-1684.
- 1606 de la Fuente, J., Miller, A., Elder, D., Faust, R., and Snavely, W., 2006, Landslide sediment
1607 production rates in the middle fork and upper Eel River basins, northern California,
1608 *Proceedings of the Eighth Federal Interagency Sedimentation Conference (8thFISC)*,
1609 April 2-6, 2006, Reno, NV, USA.
- 1610 DeCelles, P.G., Ducea, M.N., Kapp, P., and Zandt, G., 2009, Cyclicity in Cordilleran orogenic
1611 systems: *Nature Geoscience*, v. 2, p. 251-257.
- 1612 Dickinson, W.R., 1974, Plate tectonics and sedimentation: *SEPM Special Publication 22*.
- 1613 Dickinson, W.R. and Gehrels, G.E., 2003, U-Pb ages of detrital zircons from Permian and
1614 Jurassic eolian sandstones of the Colorado Plateau, USA: *Paleogeographic implications*:
1615 *Sedimentary Geology*, v. 163, p. 29-66.
- 1616 Dinehart, R.L. and Burau, J.R., 2005, Repeated surveys by acoustic Doppler current profiler for
1617 flow and sediment dynamics in a tidal river, *Journal of Hydrology*: v. 314, p. 1-21.
- 1618 Drexler, T.M., Nittrouer, C.A., and Mullenbach, B.L., 2006, Impact for local morphology on
1619 sedimentation in a submarine canyon, ROV studies in Eel Canyon, Northern California,
1620 U.S.A, *Journal of Sedimentary Research*: v. 76, p. 839-853.
- 1621 Edmonds, D. and Slingerland, R., 2007, Mechanics of river mouth bar formation: Implications for
1622 the morphodynamics of delta distributary networks: *Journal of Geophysical Research –*
1623 *Earth Surface* 112.
- 1624 Falcini, F., Khan, N.S., Macelloni, L., Horton, B.P., Lutken, C.B., Mckee, K.L., Santoleri, R.,
1625 Colella, S., Li, C., Volpe, G., D'emidio, M., Salusti, A., and Jerolmack, D.J., 2012,
1626 Linking the historic 2011 Mississippi River flood to coastal wetland sedimentation,
1627 *Nature Geoscience*, v. 5, p. 803-807.
- 1628 Fisk, H.N., 1944, Geological investigation of the alluvial valley of the lower Mississippi River:
1629 *Mississippi River Commission*, Vicksburg, Mississippi, p. 1-78.
- 1630 Fosdick, J.C., Grove, M., Graham, S.A., Hourigan, J.K., Lovera, O., and Romans, B.W., 2014,
1631 Detrital thermochronologic record of burial heating and sediment recycling in the
1632 Magallanes foreland basin, Patagonian Andes: *Basin Research*, 10.1111/bre.12088.
- 1633 Furbish, D.J. and Fagherazzi, S., 2001, Stability of creeping soil and implications for hillslope
1634 evolution: *Water Resources Research*, v. 37, p. 2607-2618.
- 1635 Ganti, V., Lamb, M.P., and McElroy, B., 2014, Quantitative bounds on morphodynamics and
1636 implications for reading the sedimentary record: *Nature Communications*, v. 5:3298,
1637 10.1038/ncomms4298.
- 1638 Gardner, T.W., Jorgensen, D.W., Shuman, C., and Lemieux, C.R., 1987, Geomorphic and
1639 tectonic process rates: Effects of measured time interval: *Geology*, v. 15, p. 259-261.
- 1640 Garver, J.I., Brandon, M.T., Roden-Tice, M., and Kamp, P.J., 1999, Exhumation history of
1641 orogenic highlands determined by detrital fission-track thermochronology: *Geological*
1642 *Society London Special Publication 154*, p. 283-304.
- 1643 Gasparini, N.M., Whipple, K.X., and Bras, R.L., 2007, Predictions of steady state and transient
1644 landscape morphology using sediment-flux-dependent river incision models: *Journal of*
1645 *Geophysical Research – Earth Surface*, 112.
- 1646 Gerber, T.P., Pratson, L.F., Kuehl, S., Walsh, J.P., Alexander, C., and Palmer, A., 2010, The
1647 influence of sea level and tectonics on Late Pleistocene through Holocene sediment
1648 storage along the high-sediment supply Waipaoa continental shelf, *Mar. Geol.*: v. 270, p.
1649 139-159.

- 1650 Gilli, A., Anselmetti, F., Glur, L., Wirth, S., 2013. Lake Sediments as Archives of Recurrence
1651 Rates and Intensities of Past Flood Events, in: Schneuwly-Bollschweiler, M., Stoffel, M.,
1652 Rudolf-Miklau, F. (Eds.). Springer Netherlands, pp. 225-242.
- 1653 Giosan, L., Constantinescu, S., Clift, P.D., Tabrez, A.R., Danish, M., and Inam, A., 2006, Recent
1654 morphodynamics of the Indus delta shore and shelf: *Continental Shelf Research*, v. 26, p.
1655 1668-1684.
- 1656 Girardclos, S., Schmidt, O.T., Sturm, M., Ariztegui, D., Pugin, A., and Anselmetti, F.S., 2007,
1657 The 1996 AD delta collapse and large turbidite in Lake Brienz, *Mar. Geol.*: v. 241, p.
1658 137-154.
- 1659 Godard, V., Tucker, G. E., Burch Fisher, G., Burbank, D. W., and Bookhagen, B., 2013,
1660 Frequency-dependent landscape response to climatic forcing: *Geophysical Research*
1661 *Letters*, v. 40, no. 5, p. 859-863.
- 1662 Goff, J.A., Wheatcroft, R.A., Lee, H., Drake, D.E., Swift, D.J.P., and Fan, S., 2002, Spatial
1663 variability of shelf sediments in the STRATAFORM natural laboratory, Northern
1664 California, *Cont. Shelf Res.*: v. 22, p. 1199-1223.
- 1665 Goldfinger, C., Nelson, C.H., and Johnson, J.E., 2003, Holocene earthquake records from the
1666 Cascadia subduction zone and northern San Andreas fault based on precise dating of
1667 offshore turbidites, *Annu. Rev. Earth Planet. Sci.*: v. 31, p. 555-577.
- 1668 Goldfinger, C., Nelson, C.H. , Morey, A.E. , Johnson, J.E., Patton, J., Karabanov, E., Gutiérrez-
1669 Pastor, J., Eriksson, A.T., Gràcia, E., Dunhill, G. , Enkin, R.J. , Dallimore, A., and
1670 Vallier, T., 2012, Turbidite event history — methods and implications for Holocene
1671 paleoseismicity of the Cascadia subduction zone, U.S. Geological Survey Professional
1672 Paper 1661-F.
- 1673 Goni, M.A., Alleau, Y., Corbett, D., Walsh, J.P., Mallinson, D., Allison, M.A., Gordon, E.,
1674 Petsch, S., and Dellapena, T.M., 2007, The effects of Hurricanes Katrina and Rita on the
1675 seabed of the Louisiana shelf, *The Sedimentary Record*, v. 5, p. 5-9.
- 1676 Goodbred, S.L. and Kuehl, S.A., 1998, Floodplain processes in the Bengal Basin and the storage
1677 of Ganges-Brahmaputra river sediment: an accretion study using Cs- 137 and Pb-210
1678 geochronology, *Sediment. Geol.*: v. 121, p. 239-258.
- 1679 Goodbred Jr, S.L. and Kuehl, S.A., 1999, Holocene and modern sediment budgets for the
1680 Ganges-Brahmaputra river system: Evidence for highstand dispersal to floodplain, shelf,
1681 and deep-sea depocenters: *Geology*, v. 27, p. 559-562.
- 1682 Goodbred, S.J. and Kuehl, S.A., 2000a, Enormous Ganges-Brahmaputra sediment discharge
1683 during strengthened early Holocene monsoon, *Geology*: v. 28, p. 1083-1086.
- 1684 Goodbred Jr, S.L. and Kuehl, S.A., 2000b, The significance of large sediment supply, active
1685 tectonism, and eustasy on margin sequence development: Late Quaternary stratigraphy
1686 and evolution of the Ganges-Brahmaputra delta: *Sedimentary Geology*, v. 133, p. 227-
1687 248.
- 1688 Goodbred Jr, S. L., 2003, Response of the Ganges dispersal system to climate change: a source-
1689 to-sink view since the last interstade: *Sedimentary Geology*, v. 162, no. 1–2, p. 83-104.
- 1690 Grabau, A.W., 1913, *Principles of Stratigraphy*: A.G. Seiler and Company, New York.
- 1691 Graham, S.A., Tolson, R., DeCelles, P., Ingersoll, R., Bargar, E., Caldwell, L., Cavazza, W.,
1692 Edwards, D., Follo, M., and Handschy, J., 1986, Provenance modeling as technique for
1693 analyzing source terrane evolution and controls on foreland sedimentation: *Foreland*
1694 *Basins*, Blackwell Publishing, p. 425-436.
- 1695 Granger, D.E., Kirchner, J.W., and Finkel, R., 1996, Spatially averaged long-term erosion rates
1696 measured from in situ-produced cosmogenic nuclides in alluvial sediment: *The Journal of*
1697 *Geology*, p. 249-257.
- 1698 Hack, J.T., 1957, *Studies of longitudinal stream profiles in Virginia and Maryland*: United States
1699 Geological Survey Professional Paper 294-B.

- 1700 Hajek, E.A., Heller, P.L., and Sheets, B.A., 2010, Significance of channel-belt clustering in
1701 alluvial basins: *Geology*, v. 38, p. 535-538.
- 1702 Hale, R.P., Ogston, A.S., Walsh, J.P., and Orpin, A.R., 2014, Sediment transport and event
1703 deposition on the Waipaoa River Shelf, New Zealand, *Cont. Shelf Res.*: v. 86, p. 52-65.
- 1704 Hanebuth, T.J.J., Kudrass, H.R., Linstadter, J., Islam, B., and Zander, A.M., 2013, Rapid coastal
1705 subsidence in the central Ganges-Brahmaputra delta (Bangladesh) since the 17th century
1706 deduced from submerged salt producing kilns, *Geology*: v. 41, p. 987-990.
- 1707 Hays, J.D., Imbrie, J., and Shackleton, N.J., 1976, Variations in the Earth's orbit: Pacemaker of
1708 the ice ages: *Science*, v. 194, p. 1121-1132.
- 1709 Hay, W.W., Wold, C.N., and Shaw, C.A., 1989, Mass-balanced paleogeographic maps:
1710 Background and input requirements: *Quantitative Dynamic Stratigraphy*, Prentice Hall, p.
1711 261-275.
- 1712 Heezen, B. C. and Ewing, M., 1952, Turbidity currents and submarine slumps, and the 1929
1713 Grand Banks earthquake, *Am. J. Sci.*, 250, 849-873.
- 1714 Hidy, A.J., Gosse, J.C., Blum, M.D., and Gibling, M.R., 2014, Glacial-interglacial variation in
1715 denudation rates from interior Texas, USA, established with cosmogenic nuclides: *Earth
1716 and Planetary Science Letters*, v. 390, p. 209-221.
- 1717 Hinderer, M., 2012, From gullies to mountain belts: A review of sediment budgets at various
1718 scales: *Sedimentary Geology*, v. 280, p. 21-59.
- 1719 Holbrook, J. and Wanas, H., 2014, A fulcrum approach to assessing source-to-sink mass balance
1720 using channel paleohydrologic parameters derivable from common fluvial data sets with
1721 an example from the Cretaceous of Egypt: *Journal of Sedimentary Research*, v. 84, p.
1722 349-372.
- 1723 Hovius, N., Stark, C.P., and Allen, P.A., 1997, Sediment flux from a mountain belt derived by
1724 landslide mapping, *Geology*: v. 25, p. 231-234.
- 1725 Hoyal, D. and Sheets, B., 2009, Morphodynamic evolution of experimental cohesive deltas:
1726 *Journal of Geophysical Research – Earth Surface*, 114.
- 1727 Hughes Clarke, J.E., Brucker, S., Muggah, J., Church, I., Cartwright, D., Kuus, P., Hamilton, T.,
1728 Pratomo, D., and Eisan, B., 2012, The Squamish ProDelta: Monitoring Active Landslides
1729 and Turbidity Currents: Canadian Hydrographic Conference 2012, Proceedings, 15pp.
- 1730 **Jaeger, J.M. and Koppes, M., this volume, The role of the cryosphere in source to sink systems:**
1731 **Earth-Science Reviews, XXXXX.**
- 1732 Jerolmack, D.J. and Paola, C., 2010, Shredding of environmental signals by sediment transport:
1733 *Geophysical Research Letters*, v. 37, L19401.
- 1734 Jervey, M.T., 1988, Quantitative geological modeling of siliciclastic rock sequences and their
1735 seismic expression, in: Wilgus, Hastings, Kendall, Posamentier, Ross, Van Wagoner,
1736 eds., *Sea Level Changes – an Integrated Approach*.
- 1737 Johnson, M., 1994, Volume balance of erosional loss and sediment deposition related to
1738 Himalayan uplifts: *Journal of the Geological Society*, v. 151, p. 217-220.
- 1739 Kao, S.-J., Hilton, R.G., Selvaraj, K., Dai, M., Zehetner, F., Huang, J.-C., Hsu, S.-C., Sparkes, R.,
1740 Liu, J.T., Lee, T.-Y., Yang, J.-Y.T., Galy, A., Xu, X., and Hovius, N., 2014, Preservation
1741 of terrestrial organic carbon in marine sediments offshore Taiwan: Mountain building and
1742 atmospheric carbon dioxide sequestration: *Earth Surface Dynamics*, v. 2, p. 127-139.
- 1743 Kniskern, T.A., Mitra, S., Orpin, A.R., Harris, C.K., Walsh, J.P., and Corbett, D.R., 2014,
1744 Characterization of a flood-associated deposit on the Waipaoa River shelf using
1745 radioisotopes and terrigenous organic matter abundance and composition, *Cont. Shelf
1746 Res.*: v. 86, p. 66-84.
- 1747 Kolker, A.S., Li, C., Walker, N.D., Pilley, C., Ameen, A.D., Boxer, G., Ramatchandirane, C.,
1748 Ullah, M., and Williams, K.A., 2014, The impacts of the great Mississippi/Atchafalaya
1749 River flood on the oceanography of the Atchafalaya Shelf, *Cont. Shelf Res.*, v. 86, p. 17-
1750 33.

- 1751 Korup, O., Hayakawa, Y., Codilean, A.T., Matsushi, Y., Saito, H., Oguchi, T., and Matsuzaki, H.,
 1752 2014, Japan's sediment flux to the Pacific Ocean revisited, *Earth-Sci. Rev.*: v. 135, p. 1-
 1753 16.
- 1754 Kuehl, S.A., Nittrouer, C.A., Allison, M.A., Faria, L.E.C., Dukat, D.A., Jaeger, J.M., Pacioni,
 1755 T.D., Figueiredo, A.G., and Underkoffler, E.C., 1996, Sediment deposition,
 1756 accumulation, and seabed dynamics in an energetic fine-grained coastal environment,
 1757 *Cont. Shelf Res.*: v. 16, p. 787-815.
- 1758 Kuehl, S.A., Levy, B.M., Moore, W.S., and Allison, M.A., 1997, Subaqueous delta of the
 1759 Ganges-Brahmaputra river system, *Mar. Geol.*: v. 144, p. 81-96.
- 1760 Kuehl, S.A., Carter, L., Gomez, B. and Trustrum, N., 2003, Holistic approach offers potential to
 1761 quantify mass fluxes across continental margins, *Eos*, v. 84, 379/388.
- 1762 Kuehl, S.A., Allison, M.A., Goodbred, S.L. and Kudrass, H., 2005, The Ganges-Brahmaputra
 1763 Delta, in: Giosan, L. and Bhattacharya, J., eds., *River Deltas - Concepts, Models, and*
 1764 *Examples*, SEPM Special Publication No. 83, p. 413-434.
- 1765 Kuehl, S.A., Alexander, C.R., Blair, N.E., Harris, C.K., Marsaglia, K.M., Ogston, A.S., Orpin, A.
 1766 R., Roering, J., Bever, A., Bilderback, E.L., Carter, L., Cerovski-Darriau, C., Childress,
 1767 L.B., Corbett, R., Hale, R., Leithold, E.L., Litchfield, N., Moriarty, J.M., Page, M.J.,
 1768 Pierce, L.E., Upton, P., and Walsh, J.P., this volume, *A source to sink perspective of the*
 1769 *Waipaoa River margin: Earth-Science Reviews, XXXXX.*
- 1770 Lamb, M.P., Nittrouer, J.A., Mohrig, D., and Shaw, J., 2012, Backwater and river plume controls
 1771 on scour upstream of river mouths: Implications for fluvio-deltaic morphodynamics:
 1772 *Journal of Geophysical Research*, 117, F01002.
- 1773 Lawton, T.F., 2014, Small grains, big rivers, continental concepts: *Geology*, v. 42, p. 639-640.
- 1774 Leithold, E.L., Perkey, D.W., Blair, N.E., and Creamer, T.N., 2005, Sedimentation and carbon
 1775 burial on the northern California continental shelf: the signatures of land-use change,
 1776 *Cont. Shelf Res.*: v. 25, p. 349-371.
- 1777 Leithold, E.L., Blair, N.E., and Wegmann, K.W., this volume, *Source to sink sedimentary*
 1778 *systems and the global C-cycle: A river runs through it: Earth-Science Reviews,*
 1779 *XXXXX.*
- 1780 Leopold, L.B. and Maddock, T., 1953, The hydraulic geometry of stream channels and some
 1781 physiographic implications: United States Geological Survey Professional Paper 252.
- 1782 Lesser, G.R., Roelvink, J.A., van Kester, J.A.T.M., and Stelling, G., 2004, Development and
 1783 validation of a three-dimensional morphological model: *Journal of Coastal Engineering*,
 1784 v. 51, p. 883-915.
- 1785 Liang, M., Voller, V.R., and Paola, C., 2014, A reduced-complexity model for river delta
 1786 formation – Part 1: Modeling deltas with channel dynamics: *Earth Surface Dynamics*
 1787 *Discussions*, v. 2, p. 823-869.
- 1788 Limmer, D.R., Kohler, C.M., Hillier, S., Moreton, S.G., Tabrez, A.R., and Clift, P.D., 2012,
 1789 Chemical weathering and provenance evolution of Holocene-Recent sediments from the
 1790 Western Indus Shelf, Northern Arabian Sea, inferred from physical and mineralogical
 1791 properties: *Marine Geology*, v. 326, p. 101-115.
- 1792 Mallarino, G., Beaubouef, R.T., Droxler, A.W., Abreu, V., and Labeyrie, L., 2006, Sea level
 1793 influence on the nature and timing of a minibasin sedimentary fill (northwestern slope of
 1794 the Gulf of Mexico): *AAPG Bulletin*, v. 90, p. 1089-1119.
- 1795 Marr, J.G., Swenson, J.B., Paola, C., and Voller, R., 2002, A two-diffusion model of fluvial
 1796 stratigraphy in close depositional basins: *Basin Research*, 12, p. 381-398..
- 1797 Matthai, H., 1990, *Floods: Surface Water Hydrology*, Geological Society of America, Boulder,
 1798 Colorado, p. 97-120.
- 1799 McKee, K.L. and Cherry, J.A., 2009, Hurricane Katrina Sediment Slowed Elevation Loss in
 1800 Subsiding Brackish Marshes of the Mississippi River Delta, *Wetlands*, v. 29, p. 2-15.

- 1801 McLennan, S.M., Taylor, S., and Eriksson, K.A., 1983, Geochemistry of Archean shales from the
1802 Pilbara Supergroup, western Australia: *Geochimica et Cosmochimica Acta*, v. 47, p.
1803 1211-1222.
- 1804 Meade, R.H, Yuzyk, T.R., and Day, T.J., 1990, Movement and storage of sediment in rivers of
1805 the United States and Canada. in: M.G. Wolman and H.C. Riggs, eds., *The Geology of*
1806 *North America*, vol. 1, Surface Water Hydrology: Boulder, Geol. Soc. America, p. 255-
1807 280.
- 1808 Métivier, F. and Gaudemer, Y., 1999, Stability of output fluxes of large rivers in South and East
1809 Asia during the last 2 million years: Implications on floodplain processes: *Basin*
1810 *Research*, v. 11, p. 293-303.
- 1811 Meyers, S.R. and Peters, S.E., 2011, A 56 million-year rhythm in North American sedimentation
1812 during the Phanerozoic: *Earth and Planetary Science Letters*, v. 303, p. 174-180.
- 1813 Michael, N.A., Whittaker, A.C., and Allen, P.A., 2013, The functioning of sediment routing
1814 systems using a mass balance approach: Example from the Eocene of the southern
1815 Pyrenees: *The Journal of Geology*, v. 121, p. 581-606.
- 1816 Michels, K.H., Kudrass, H.R., Hübscher, C., Suckow, A., and Wiedicke, M., 1998, The
1817 submarine delta of the Ganges–Brahmaputra: cyclone-dominated sedimentation patterns,
1818 *Mar. Geol.*: v. 149, p. 133-154.
- 1819 Michels, K.H., Suckow, A., Breitzke, M., Kudrass, H.R., and Kottke, B., 2003, Sediment
1820 transport in the shelf canyon “Swatch of No Ground” (Bay of Bengal), *Deep Sea*
1821 *Research Part II: Topical Studies in Oceanography*: v. 50, p. 1003-1022. Miller, K.G.,
1822 Kominz, M.A., Browning, J.V., Wright, J.D., Mountain, G.S., Katz, M.E., Sugarman,
1823 P.J., Cramer, B.S., Christie-Blick, N., and Pekar, S.F., 2005, The Phanerozoic record of
1824 global sea-level change: *Science*, v. 310, p. 1293-1298.
- 1825 Miller, K.G., Kominz, M.A., Browning, J.V., Wright, J.D., Mountain, G.S., Katz, M.E.,
1826 Sugarman, P.J., Cramer, B.S., Christie-Blick, N., and Pekar, S.F., 2005, The Phanerozoic
1827 record of global sea-level change: *Science*, 310, 1293-1298.
- 1828 Miller, A.J. and Kuehl, S.A., 2010, Shelf sedimentation on a tectonically active margin: A
1829 modern sediment budget for Poverty continental shelf, New Zealand, *Mar. Geol.*: v. 270,
1830 p. 175-187. Milliman, J.D. and Syvitski, J.P., 1992, Geomorphic/tectonic control of
1831 sediment discharge to the ocean: The importance of small mountainous rivers: *The*
1832 *Journal of Geology*, v. 100, p. 525-544.
- 1833 Milliman, J.D., Quraishie, G.S., and Beg, M.A.A., 1984, Sediment discharge from the Indus
1834 River to the ocean: Past, present, and future: *Marine Geology and Oceanography of the*
1835 *Arabian Sea and Coastal Pakistan*, p. 65-70.
- 1836 Milliman, J.D. and Syvitski, J.P.M., 1992, Geomorphic/tectonic control of sediment discharge to
1837 the ocean: The importance of small mountainous rivers: *The Journal of Geology*, 100,
1838 525-544.
- 1839 Milliman, J.D. and Farnsworth, K.L., 2011, *River discharge to the coastal ocean: A global*
1840 *synthesis*: Cambridge University Press, 392 p.
- 1841 Moernaut, J., De Batist, M., Charlet, F., Heirman, K., Chapron, E., Pino, M., Brummer, R., and
1842 Urrutia, R., 2007, Giant earthquakes in South-Central Chile revealed by Holocene mass-
1843 wasting events in Lake Puyehue, *Sediment. Geol.*: v. 195, p. 239-256.
- 1844 Montgomery, D.R., 2001, Slope distributions, threshold hillslopes, and steady-state topography:
1845 *American Journal of Science*, v. 301, p. 432-454.
- 1846 Moriarty, J.M., Harris, C.K., and Hadfield, M.G., 2014, A hydrodynamic and sediment transport
1847 model for the Waipaoa Shelf, New Zealand: Sensitivity of fluxes to spatially varying
1848 erodibility and model nesting: *J. Mar. Sci. Eng.*, 2, 336-369.
- 1849 Mullenbach, B.L., Nittrouer, C.A., Puig, P., and Orange, D.L., 2004, Sediment deposition in a
1850 modern submarine canyon: eel canyon, northern California, *Mar. Geol.*: v. 211, p. 101-
1851 119.

- 1852 Mullenbach, B.L. and Nittrouer, C.A., 2006, Decadal record of sediment export to the deep sea
1853 via Eel Canyon, *Cont. Shelf Res.*: v. 26, p. 2157-2177.
- 1854 Murray, A.B. and Paola, C., 1997, Properties of cellular braided-stream model: *Earth Surface*
1855 *Processes and Landforms*, v. 22, p. 1001-1025.
- 1856 Myrow, P.M. and Southard, J.B., 1996, Tempestite deposition, *Journal of Sedimentary Research*,
1857 v. 66, p. 875-887.
- 1858 National Research Council, 2010, *Landscapes on the Edge: New Horizons for Research on*
1859 *Earth's Surface. Committee on Challenges and Opportunities in Earth Surface Processes*,
1860 National Research Council. ISBN: 0-309-14205-0, 180 p.
- 1861 Nittrouer, C.A., Austin, J.A., Field, M.E., Kravitz, J.H., Syvitski, J.P.M., and P.L. Wiberg. 2007.
1862 *Continental margin sedimentation: from sediment transport to sequence stratigraphy*.
1863 Malden, MA: Blackwell Pub. for the International Association of Sedimentologists. 549
1864 pgs.
- 1865 Nittrouer, J.A., Allison, M.A., and Campanella, R., 2008, Bedform transport rates for the
1866 lowermost Mississippi River, *Journal of Geophysical Research F: Earth Surface*: v. 113.
1867 F03004, p. 1-16.
- 1868 Noren, A.J., Biennan, P.R., Steig, E.J., Lini, A., and Southon, J., 2002, Millennial-scale
1869 storminess variability in the northeastern United States during the Holocene epoch,
1870 *Nature*: v. 419, p. 821-824.
- 1871 Normark, W.R., Piper, D.J., Romans, B.W., Covault, J.A., Dartnell, P., and Sliter, R.W., 2009,
1872 Submarine canyon and fan systems of the California Continental Borderland: *Geological*
1873 *Society of America Special Paper 454*, p. 141-168.
- 1874 Ogston, A.S., Cacchione, D.A., Sternberg, R.W., and Kineke, G.C., 2000, Observations of storm
1875 and river flood-driven sediment transport on the northern California continental shelf,
1876 *Cont. Shelf Res.*: v. 20, p. 2141-2162.
- 1877 Painter, C.S., Carrapa, B., DeCelles, P.G., Gehrels, G.E., and Thomson, S.N., 2014, Exhumation
1878 of the North American Cordillera revealed by multi-dating of Upper Jurassic-Upper
1879 Cretaceous foreland basin deposits: *Geological Society of America Bulletin*,
1880 10.1130/B30999.1.
- 1881 Palinkas, C.M., Nittrouer, C.A., Wheatcroft, R.A., and Langone, L., 2005, The use of ⁷Be to
1882 identify event and seasonal sedimentation near the Po River delta, *Adriatic Sea, Mar.*
1883 *Geol.*: v. 222–223, p. 95-112.
- 1884 Paola, C., Heller, P.L., Angevine, C.L., 1992, The large-scale dynamics of grain-size variation in
1885 alluvial basins, 1: Theory: *Basin Research*, v. 4, p. 73–90.
- 1886 Paola, C., 2000, Quantitative models of sedimentary basin filling: *Sedimentology*, 47, 121-178.
- 1887 Paola, C., Straub, K., Mohrig, D., and Reinhardt, L., 2009, The “unreasonable effectiveness” of
1888 stratigraphic and geomorphic experiments: *Earth-Science Reviews*, v. 97, p. 1-43.
- 1889 Paola, C. and Voller, V., 2005, A generalized Exner equation for sediment mass balance: *Journal*
1890 *of Geophysical Research – Earth Surface*, v. 110.
- 1891 Paola, C. and Martin, J.M., 2012, Mass-balance effects in depositional systems: *Journal of*
1892 *Sedimentary Research*, v. 82, p. 435-450.
- 1893 Patton, J.R., Goldfinger, C., Morey, A.E., Romsos, C., Black, B., Djadjadihardja, Y., and
1894 Udrekth., 2013, Seismoturbidite record as preserved at core sites at the Cascadia and
1895 Sumatra-Andaman subduction zones, *Natural Hazards and Earth System Science*: v. 13,
1896 p. 833-867.
- 1897 Paull, C., Greene, H., Ussler, W., and Mitts, P., 2002, Pesticides as tracers of sediment transport
1898 through Monterey Canyon: *Geo-Marine Letters*, 22, pp. 121-126.
- 1899 Petter, A.L., Steel, R.J., Mohrig, D., Kim, W., and Carvajal, C., 2013, Estimation of the paleoflux
1900 of terrestrial-derived solids across ancient basin margins using the stratigraphic record:
1901 *Geological Society of America Bulletin*, v. 125, p. 578-593.

- 1902 Phillips, J.D., 1991, Fluvial sediment delivery to a Coastal Plain estuary in the Atlantic Drainage
1903 of the United States, *Mar. Geol.*: v. 98, p. 121-134.
- 1904 Phillips, J.D., 2003, Sources of nonlinearity and complexity in geomorphic systems: Progress in
1905 Physical Geography, v. 27, p. 1-23.
- 1906 Phillips, J.D. and Slattery, M.C., 2006, Sediment storage, sea level, and sediment delivery to the
1907 ocean by coastal plain rivers: Progress in Physical Geography, v. 30, p. 513-530.
- 1908 Piper, D.W. and Aksu, A., 1987, The source and origin of the 1929 grand banks turbidity current
1909 inferred from sediment budgets, *Geo-Mar. Lett.*: v. 7, p. 177-182.
- 1910 Posamentier, H.W. and Vail, P.R., 1988, Eustatic controls on clastic deposition II9d/sequence and
1911 systems tract models, *Sea-Level Changes: An Integrated Approach*: p. 125-154.
- 1912 Posamentier, H.W., Erskine, R.D., and Mitchum, R.M, Jr., 1991, Submarine fan deposition
1913 within a sequence stratigraphic framework: *Seismic Facies and Sedimentary Processes of*
1914 *Submarine Fans and Turbidite Systems*: Springer-Verlag, p. 127-136..
- 1915 Pirmez, C., Prather, B., Mallarino, G., O'Hayer, W., Droxler, A., and Winker, C., 2012,
1916 Chronostratigraphy of the Brazos-Trinity depositional system, western Gulf of Mexico:
1917 Implications for deepwater depositional models: Application of the Principles of Seismic
1918 Geomorphology to Continental-slope and Base-of-Slope Systems: Case Studies from
1919 Seafloor and Near Seafloor Analogues, *SEPM Special Publication 99*, p. 111-143.
- 1920 Prather, B., Pirmez, C., and Winker, C., 2012, Stratigraphy of linked intraslope basins: Brazos-
1921 Trinity system, western Gulf of Mexico: Application of the Principles of Seismic
1922 Geomorphology to Continental-slope and Base-of-Slope Systems: Case Studies from
1923 Seafloor and Near Seafloor Analogues, *SEPM Special Publication 99*, p. 83-109.
- 1924 Puig, P., Ogston, A.S., Mullenbach, B.L., Nittrouer, C.A., and Sternberg, R.W., 2003, Shelf-to-
1925 canyon sediment-transport processes on the Eel continental margin (northern California),
1926 *Mar. Geol.*: v. 193, p. 129-149.
- 1927 Rahl, J.M., Reiners, P.W., Campbell, I.H., Nicolescu, S., and Allen, C.M., 2003, Combined
1928 single-grain (U-Th)/He and U/Pb dating of detrital zircons from the Navajo Sandstone,
1929 Utah: *Geology*, v. 31, p. 761-764.
- 1930 Rahl, J.M., Ehlers, T.A., and van der Pluijm, B.A., 2007, Quantifying transient erosion of orogens
1931 with detrital thermochronology from syntectonic basin deposits: *Earth and Planetary*
1932 *Science Letters*, v. 256, p. 147-161.
- 1933 Reed, D.J., Commagere, A.M., and Hester, M.W., 2009, Marsh Elevation Response to Hurricanes
1934 Katrina and Rita and the Effect of Altered Nutrient Regimes, *J. Coast. Res.*, p. 166-173.
- 1935 Reimer, P.J., 2012, Refining the radiocarbon time scale: *Science*, v. 338, p. 337-338.
- 1936 Reiners, P.W. and Brandon, M.T., 2006, Using thermochronology to understand orogenic
1937 erosion: *Annual Reviews of Earth and Planetary Science*, v. 34, p. 419-466.
- 1938 Rodier, J. and Roche, M., 1984, World catalogue of maximum observed floods: *IAHS*
1939 *Publication no. 143*.
- 1940 Roering, J.J., Perron, J.T., and Kirchner, J.W., 2007, Functional relationships between denudation
1941 and hillslope form and relief, *Earth Planet. Sci. Lett.*: v. 264, p. 245-258.
- 1942 Rogers, K.G. and Goodbred Jr., S.L., 2010, Mass failures associated with the passage of a large
1943 tropical cyclone over the Swath of No Ground submarine canyon (Bay of Bengal),
1944 *Geology*: v. 38, p. 1051-1054.
- 1945 Romans, B.W., Normark, W.R., McGann, M.M., Covault, J.A., and Graham, S.A., 2009, Coarse-
1946 grained sediment delivery and distribution in the Holocene Santa Monica Basin,
1947 California: Implications for evaluating source-to-sink flux at millennial timescales:
1948 *Geological Society of America Bulletin*, v. 121, p. 1394-1408.
- 1949 Romans, B.W., Fildani, A., Graham, S.A., Hubbard, S.M., and Covault, J.A., 2010, Importance of
1950 predecessor basin history on sedimentary fill of a retroarc foreland basin: Provenance
1951 analysis of the Cretaceous Magallanes basin, Chile (50-52S): *Basin Research*, v. 22, p.
1952 640-658.

- 1953 Romans, B.W. and Graham, S.A., 2013, A deep-time perspective of land-ocean linkages in the
1954 sedimentary record: *Annual Reviews of Marine Science*, v. 5, p. 69-94.
- 1955 Rose, L.E. and Kuehl, S.A., 2010, Recent sedimentation patterns and facies distribution on the
1956 Poverty Shelf, New Zealand, *Mar. Geol.*: v. 270, p. 160-174.
- 1957 Sadler, P.M., 1981, Sediment accumulation rates and the completeness of stratigraphic sections:
1958 *The Journal of Geology*, v. 89, p. 569-584.
- 1959 Sadler, P.M. and Jerolmack, D.J., 2014, Scaling laws for aggradation, denudation, and
1960 progradation rates: The case for time-scale invariance at sediment sources and sinks:
1961 *Geological Society London Special Publication* 404.
- 1962 Saylor, J.E., Stockli, D.F., Horton, B.K., Nie, J., and Mora, A., 2012, Discriminating rapid
1963 exhumation from syndepositional volcanism using detrital zircon double dating:
1964 Implications for the tectonic history of the Eastern Cordillera, Colombia: *Geological*
1965 *Society of America Bulletin*, v. 124, p. 762-779.
- 1966 Schaller, M., von Blanckenburg, F., Hovius, N., and Kubik, P., 2001, Large-scale erosion rates
1967 from in situ-produced cosmogenic nuclides in European river sediments: *Earth and*
1968 *Planetary Science Letters*, v. 188, p. 441-458.
- 1969 Schumm, 1977, *The Fluvial System*, New York, John Wiley & Sons, 338 p.
- 1970 Schumm, S., 1993, River response to baselevel change: Implications for sequence stratigraphy:
1971 *The Journal of Geology*, v. 101, p. 279-294.
- 1972 Schillereff, D.N., Chiverrell, R.C., Macdonald, N., and Hooke, J.M., 2014, Flood stratigraphies in
1973 lake sediments: A review, *Earth-Sci. Rev.*, v. 135, p. 17-37.
- 1974 Shearman, P., Bryan, J., and Walsh, J.P., 2013, Trends in Deltaic Change over Three Decades in
1975 the Asia-Pacific Region, *J. Coast. Res.*: p. 1169-1183.
- 1976 Shen, Z., Tornqvist, T.E., Autin, W.J., Mateo, Z.R.P., Straub, K.M., and Mauz, B., 2012, Rapid
1977 and widespread response of the Lower Mississippi River to eustatic forcing during last
1978 glacial-interglacial cycle: *Geological Society of America Bulletin*, v. 124, p. 690-704.
- 1979 Simpson, G., Castellort, S., 2012. Model shows that rivers transmit high-frequency climate
1980 cycles to the sedimentary record: *Geology*, v. 40, p. 1131–1134. doi:10.1130/G33451.1
- 1981 Smith, S.E. and Abdel-Kader, A., 1988, Coastal Erosion along the Egyptian Delta, *J. Coast. Res.*:
1982 v. 4, p. 245-255.
- 1983 Smith, D.P., Ruiz, G., Kvitek, R., and Iampietro, P.J., 2005, Semiannual patterns of erosion and
1984 deposition in upper Monterey Canyon from serial multibeam bathymetry: *GSA Bulletin* ,
1985 v. 117, 1123–1133; doi: 10.1130/B25510.1
- 1986 Stevens, T., Paull, C.K., Ussler, W., III, McGann, M., Buylaert, J-P., and Lundsten, E., 2014, The
1987 timing of sediment transport down the Monterey Canyon. *Geological Society of America*
1988 *Bulletin*, v. 126, p. 103-121
- 1989 Straub, K.M., Paola, C., Mohrig, D., Wolinsky, M.A., and George, T., 2009, Compensational
1990 stacking of channelized sedimentary deposits: *Journal of Sedimentary Research*, v. 79, p.
1991 673-688.
- 1992 Strong, N., Sheets, B., Hickson, T., and Paola, C., 2005, A mass-balance framework for
1993 quantifying downstream changes in fluvial architecture: *Fluvial Sedimentology VII*,
1994 *Special Publication* 35, p. 243-253.
- 1995 Sømme, T.O., Helland-Hansen, W., Martinsen, O.J., and Thurmond, J.B., 2009, Relationships
1996 between morphological and sedimentological parameters in source-to-sink systems: A
1997 basis for predicting semi-quantitative characteristics in subsurface systems: *Basin*
1998 *Research*, v. 21, p. 361-387.
- 1999 Sommerfield, C.K. and Nittrouer, C.A., 1999, Modern accumulation rates and a sediment budget
2000 for the Eel shelf: A flood-dominated depositional environment: *Marine Geology*, 154,
2001 227-241.

- 2002 Sommerfield, C.K., Nittrouer, C.A., and Alexander, C.R., 1999, ^{7}Be as a tracer of flood
2003 sedimentation on the northern Californian continental margin: *Continental Shelf*
2004 *Research*, 19, 335-361.
- 2005 Sommerfield, C.K. and Wheatcroft, R.A., 2007, Late Holocene sediment accumulation on the
2006 northern California shelf: Oceanic, fluvial, and anthropogenic influences, *Bull. Geol. Soc.*
2007 *Am.*: v. 119, p. 1120-1134.
- 2008 Sommerfield, C.K. and Nittrouer, C.A., 2014, Comment on “Eel River margin source-to-sink
2009 sediment budgets: Revisited” by J.A. Warrick [*Marine Geology* 351 (2014) 25–37], *Mar.*
2010 *Geol.*
- 2011 Sorrel, P., Debret, M., Billeaud, I., Jaccard, S.L., McManus, J.F., and Tessier, B., 2012, Persistent
2012 non-solar forcing of Holocene storm dynamics in coastal sedimentary archives, *Nature*
2013 *Geoscience*: v. 5, p. 892-896.
- 2014 Soutar, A. and Crill, P.A., 1977, Sedimentation and climatic patterns in the Santa Barbara Basin
2015 during the 19th and 20th centuries., *Geol. Soc. Am. Bull.*, 88, 1161-1172.
- 2016 Strasser, M., Anselmetti, F.S., Fah, D., Giardini, D., and Schnellmann, M., 2006, Magnitudes and
2017 source areas of large prehistoric northern Alpine earthquakes revealed by slope failures in
2018 lakes, *Geology*: v. 34, p. 1005-1008.
- 2019 Suckow, A., Morgenstern, U., and Kudrass, H.R., 2001, Absolute dating of recent sediments in
2020 the cyclone-influenced shelf area off Bangladesh: comparison of gamma spectrometric
2021 (^{137}Cs , ^{210}Pb , ^{228}Ra), radiocarbon, and ^{32}Si ages, *Radiocarbon*, v. 43, 917- 927.
- 2022 Sumner, E.J., Siti, M.I., McNeill, L.C., Talling, P.J., Henstock, T.J., Wynn, R.B., Djajadihardja,
2023 Y.S., and Permana, H., 2013, Can turbidites be used to reconstruct a paleoearthquake
2024 record for the central Sumatran margin? *Geology*: v. 41, p. 763-766.
- 2025 Szczucinski, W., Kokocinski, M., Rzeszewski, M., Chague-Goff, C., Cachao, M., Goto, K., and
2026 Sugawara, D., 2012, Sediment sources and sedimentation processes of 2011 Tohoku-oki
2027 tsunami deposits on the Sendai Plain, Japan - Insights from diatoms, nannoliths and grain
2028 size distribution, *Sediment. Geol.*: v. 282, p. 40-56
- 2029 Syvitski, J.P., 2003, Supply and flux of sediment along hydrological pathways: Research for the
2030 21st Century: *Global and Planetary Change*, v. 39, p. 1-11.
- 2031 Syvitski, J.P., 2008, Predictive modeling in sediment transport and stratigraphy: *Computers and*
2032 *Geoscience*, 10.1016/j.cageo.2008.02.001.
- 2033 Syvitski, J.P.M., Vorosmarty, C.J., Kettner, A.J., and Green, P., 2005, Impact of humans on the
2034 flux of terrestrial sediment to the global coastal ocean, *Science*, v. 308, p. 376-380.
- 2035 Syvitski, J.P.M. and Milliman, J.D., 2007, Geology, geography, and humans battle for dominance
2036 over the delivery of fluvial sediment to the coastal ocean, *J. Geol.*, v. 115, p. 1-19.
- 2037 Syvitski, J.P.M. and Saito, Y., 2007, Morphodynamics of deltas under the influence of humans,
2038 *Global Planet. Change*, v. 57, p. 261-282.
- 2039 Talling, P.J., Paull, C.K., and Piper, D.J.W., 2013, How are subaqueous sediment density flows
2040 triggered, what is their internal structure and how does it evolve? Direct observations
2041 from monitoring of active flows, *Earth-Sci. Rev.*: v. 125, p. 244-287.
- 2042 Tesi, T., Langone, L., Goñi, M.A., Wheatcroft, R.A., Miserocchi, S., and Bertotti, L., 2012, Early
2043 diagenesis of recently deposited organic matter: A 9-yr time-series study of a flood
2044 deposit, *Geochim. Cosmochim. Acta*: v. 83, p. 19-36.
- 2045 Traykovski, P., Geyer, W.R., Irish, J.D., and Lynch, J.F., 2000, The role of wave-induced
2046 density-driven fluid mud flows for cross-shelf transport on the Eel River continental
2047 shelf, *Cont. Shelf Res.*: v. 20, p. 2113-2140.
- 2048 Traykovski, P., Wiberg, P.L., and Geyer, W.R., 2007, Observations and modeling of wave-
2049 supported sediment gravity flows on the Po prodelta and comparison to prior
2050 observations from the Eel shelf, *Cont. Shelf Res.*: v. 27, p. 375-399.
- 2051 Turner, R.E., Baustian, J.J., Swenson, E.M., and Spicer, J.S., 2006, Wetland sedimentation from
2052 hurricanes Katrina and Rita, *Science*, v. 314, p. 449-452.

- 2053 Van den Berg van Saparoea, A.-P. and Postma, G., 2008, Control of climate change on the yield
2054 of river systems: Recent Advances in Models of Siliciclastic Shallow-Marine
2055 Stratigraphy: SEPM Special Publication 90, p. 15-33.
- 2056 Viles, H.A. and Goudie, A.S., 2003, Interannual, decadal and multidecadal scale climatic
2057 variability and geomorphology, *Earth-Sci. Rev.*, v. 61, p. 105-131.
- 2058 Voller, V.R., Ganti, V., Paola, C., and Fofoula-Georgiou, E., 2012, Does the flow of information
2059 in a landscape have direction?: *Geophysical Research Letters*, 39.
- 2060 Von Blanckenburg, F., 2005, The control mechanisms of erosion and weathering at basin scale
2061 from cosmogenic nuclides in river sediment: *Earth and Planetary Science Letters*, v. 237,
2062 p. 462-479.
- 2063 Walling, D.E. and Webb, B.W., 1996, Erosion and sediment yield: a global overview, IAHS
2064 Publication: v. 236, p. 3-19.
- 2065 Walling, D.E., 1999, Linking land use, erosion and sediment yields in river basins,
2066 *Hydrobiologia*: v. 410, p. 223-240.
- 2067 Walling, D.E. and Collins, A.L., 2008, The catchment sediment budget as a management tool,
2068 *Environ. Sci. & Policy*: v. 11, p. 136-143.
- 2069 Walling, D.E., 2013, The evolution of sediment source fingerprinting investigations in fluvial
2070 systems, *Journal of Soils and Sediments*: v. 13, p. 1658-1675.
- 2071 Walker, M., 2005, Quaternary dating methods: John Wiley & Sons, 286 p.
- 2072 Walsh, J.P. and Nittrouer, C.A., 1999, Observations of sediment flux to the Eel continental slope,
2073 northern California, *Mar. Geol.*: v. 154, p. 55-68.
- 2074 Walsh, J.P. and Nittrouer, C.A., 2003, Contrasting styles of off-shelf sediment accumulation in
2075 New Guinea, *Mar. Geol.*: v. 196, p. 105-125.
- 2076 Walsh, J.P., Nittrouer, C.A., Palinkas, C.M., Ogston, A.S., Sternberg, R.W., and Brunskill, G.J.,
2077 2004, Clinoform mechanics in the Gulf of Papua, New Guinea, *Cont. Shelf Res.*: v. 24, p.
2078 2487-2510.
- 2079 Walsh, J.P., Corbett, R., Mallinson, D., Goni, M., Dail, M., Loewy, C., Marciniak, K., Ryan, K.,
2080 Smith, C., Stevens, A., Summers, B., and Tesi, T., 2006, Mississippi delta mudflow
2081 activity and 2005 Gulf hurricanes, *EOS Trans. Am. Geophys. Union*: v. 87, p. 477-479.
- 2082 Walsh, J.P., Corbett, D.R., Ogston, A.S., Nittrouer, C., Kuehl, S.A., Allison, M.A., and
2083 Goodbred, S.L. Jr., 2013, Shelf and slope sedimentation associated with large deltaic
2084 systems: In: *Biogeochemical Dynamics at Major River-Coastal Interfaces: Linkages with*
2085 *Global Change*, editors: T.S. Bianchi, M.A. Allison, and W.Cai. Cambridge University
2086 Press, New York, NY, p. 86-117.
- 2087 Walsh, J.P., Corbett, D.R., Kiker, J.M., Orpin, A.R., Hale, R.P., and Ogston, A.S., 2014, Spatial
2088 and temporal variability in sediment deposition and seabed character on the Waipaoa
2089 River margin, New Zealand, *Cont. Shelf Res.*: v. 86, p. 85-102.
- 2090 Wang, Y., Straub, K.M., and Hajek, E.A., 2011, Scale-dependent compensational stacking: An
2091 estimate of autogenic time scales in channelized sedimentary deposits: *Geology*, v. 39, p.
2092 811-814.
- 2093 Warrick, J.A., 2014, Eel River margin source-to-sink sediment budgets: Revisited, *Mar. Geol.*: v.
2094 351, p. 25-37.
- 2095 Weislogel, A.L., Graham, S.A., Chang, E.Z., Wooden, J.L., Gehrels, G.E., and Yang, H., 2006,
2096 Detrital zircon provenance of the Late Triassic Songpan-Ganzi complex: Sedimentary
2097 record of collision of the North and South China Blocks: *Geology*, v. 34, p. 97-100.
- 2098 Weber, M.E., Wiedicke, M.H., Kudrass, H.R., Hubscher, C., and Erlenkeuser, H., 1997, Active
2099 growth of the Bengal Fan during sea-level rise and highstand: *Geology*, v. 25, p. 315-318.
- 2100 Wheatcroft, R.A., Sommerfield, C.K., Drake, D.E., Borgeld, J.C., and Nittrouer, C.A., 1997,
2101 Rapid and widespread dispersal of flood sediment on the northern California margin,
2102 *Geology*: v. 25, p. 163-166.

2103 Wheatcroft, R.A. and Borgeld, J.C., 2000, Oceanic flood deposits on the northern California
2104 shelf: Large-scale distribution and small-scale physical properties, *Cont. Shelf Res.*: v.
2105 20, p. 2163-2190.

2106 Wheatcroft, R.A., Wiberg, P.L., Alexander, C.R., S.J. Bentley, D.E. Drake, C.K. Harris and A.S.
2107 Ogston, 2007, in: Nittrouer, C.A., Austin, J.A., Field, M.E., Kravitz, J.H., Syvitski,
2108 J.P.M., and P.L. Wiberg, eds., *Continental margin sedimentation: from sediment*
2109 *transport to sequence stratigraphy*. Malden, MA: Blackwell Pub. for the International
2110 Association of Sedimentologists. p. 101-155.

2111 Whipple, K. X., 2001, Fluvial landscape response time: how plausible is steady-state
2112 denudation?: *American Journal of Science*, v. 301, p. 313-325.

2113 Whittaker, A.C., Cowie, P.A., Attal, M., Tucker, G.E., and Roberts, G.P., 2007, Bedrock channel
2114 adjustment to tectonic forcing: Implications for predicting river incision rates: *Geology*,
2115 v. 35, p. 103-106.

2116 Whittaker, A.C., Duller, R.A., Springett, J., Smithells, R.A., Whitchurch, A.L., and Allen, P.A.,
2117 2011, Decoding downstream trends in stratigraphic grain size as a function of tectonic
2118 subsidence and sediment supply: *Geological Society of America Bulletin*, v. 123, p.
2119 1363-1382.

2120 Willett, S.D. and Brandon, M.T., 2002, On steady state in mountain belts: *Geology*, v. 30, p 175-
2121 178.

2122 Wilkinson, B.H. and McElroy, B.J., 2007, The impact of humans on continental erosion and
2123 sedimentation, *Bull. Geol. Soc. Am.*: v. 119, p. 140-156.

2124 Wilson, J.T., 1966, Did the Atlantic close and then re-open?: *Nature*, v. 211, p. 676-681.

2125 Wittmann, H. and Von Blanckenburg, F., 2009, Cosmogenic nuclide budgeting of floodplain
2126 sediment transfer: *Geomorphology*, v. 109, p. 246-256.

2127 Wittmann, H., Von Blanckenburg, F., Maurice, L., Guyot, J.-L., and Kubik, P., 2011, Recycling
2128 of Amazon floodplain sediment quantified by cosmogenic ²⁶Al and ¹⁰Be: *Geology*, v.
2129 39, p. 467-470.

2130 Xu, J.P., Sequeiros, O.E., and Noble, M.A., 2014a, Sediment concentrations, flow conditions, and
2131 downstream evolution of two turbidity currents, Monterey Canyon, USA, *Deep-Sea*
2132 *Research Part I: Oceanographic Research Papers*: v. 89, p. 11-34.

2133 Xu, J.P., Wong, F.L., Kvittek, R., Smith, D.P., and Paull, C.K., 2008, Sandwave migration in
2134 Monterey Submarine Canyon, Central California, *Mar. Geol.*: v. 248, p. 193-212.

2135 Xu, J.P., Noble, M.A., and Rosenfeld, L.K., 2004, In-situ measurements of velocity structure
2136 within turbidity currents, *Geophys. Res. Lett.*: v. 31, p. L09311 1-4.

2137 Xu, K., Corbett, D.R., Walsh, J.P., Young, D., Briggs, K.B., Cartwright, G.M., Friedrichs, C.T.,
2138 Harris, C.K., Mickey, R.C., and Mitra, S., 2014b, Seabed erodibility variations on the
2139 Louisiana continental shelf before and after the 2011 Mississippi River flood, *Estuar.*
2140 *Coast. Shelf Sci.*, v. 149, p. 283-293.

2141 Zachos, J.C., Dickens, G.R., and Zeebe, R.E., 2008, An early Cenozoic perspective on
2142 greenhouse warming and carbon-cycle dynamics: *Nature*, v. 451, p 279-283.

2143 Zalasiewicz, J., Williams, M., Smith, A., T. L. Barry, A. L. Coe, P. R. Bown, P. Brenchley, D.
2144 Cantrill, A. Gale, P. Gibbard, F. J. Gregory, M. W. Hounslow, A. C. Kerr, P. Pearson, R.
2145 Knox, J. Powell, C. Waters, J. Marshall, M. Oates, P. Rawson, and P. Stone. 2008. Are
2146 we now living in the Anthropocene? *GSA Today* 18:4-8.

2147
2148